Preparari de filme nanostructurate prin metoda arcului termoionic in vid

Cristian P. Lungu

Institutul National pentru Fizica Laserilor, Plasmei si Radiatiei din Magurele

NATIONAL INSTITUTE FOR LASERS, PLASMA AND RADIATION PHYSICS, BUCHAREST, ROMANIA

Group: *"Elementary Processes in Plasma and Applications"*

Contact person: **Cristian P. LUNGU**

E-mail: cristian.lungu@inflpr.ro; Web: www.inflpr.ro

Group members (20): 1 Professor, 5 PhD Researchers, 4 Researchers, 2 Assist. Res., 5 Technical staff, 4 Students

Team : 1. Dr. Lungu P. Cristian, 2. Dr. Mustata Ion, 3. Prof. Dr. Popa Gheorghe, 4. Dr. Surdu Bob Cristina, 5. Dr. Ticos Catalin, 6. Phys. Lungu Ana Mihaela, 7. Eng. Phys. Chiru Petrica, 8. Eng. Phys. Anghel Alexandru, 9. Phys. Pompilian Oana, 10. Dr. Georgescu Claudiu, 11. Eng. Iacob Cristian, 12. Techn. Zaroschi Valer, 13. Techn. Dragusin Vasile, 14. Techn. Balint Mihaela, 15. Techn. Mihai Vlad, 16. Techn. Toinac Maria, 17. Student Funieru Bogdan, 18. Master student Badulescu Marius, 19. Student Porosnicu Cornel, 20. Student Ionut Jepu

1. Introduction: TVA principle

2. High-temperature oxidation resistant coatings

3. Tribological coatings

4. Nanostructured diamond like carbon (DLC) films preparation

5. Giant Magnetoresistive (GMR) films.

6. Coatings for fusion technology

Plasma processing

- Nano-materials → part of everyday life (PC's, mobile phones, Satellite navigation)
- Growth conditions → Film properties
- Independent control of ion energy and flux → greater flexibility in tailoring film structure and properties
- Increasing need for mastering plasma capabilities

Thermoionic Vacuum Arc (TVA)

- Creation of vapour phase species → Electron bombardment
- Transport from source to substrate → Without collisions
- Nucleation → ionic and neutral species

TVA Experimental Setup

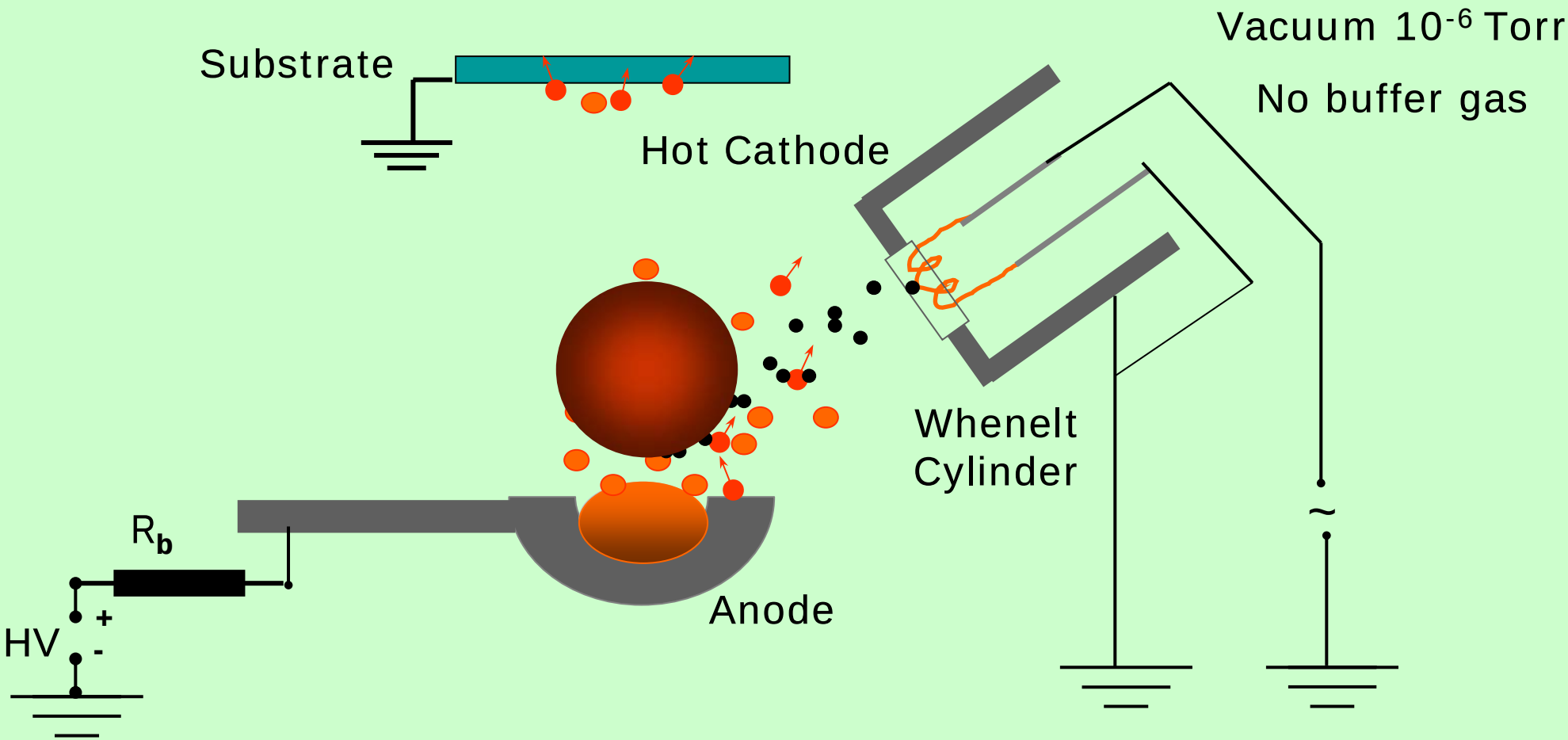

Ignition of the TVA plasma

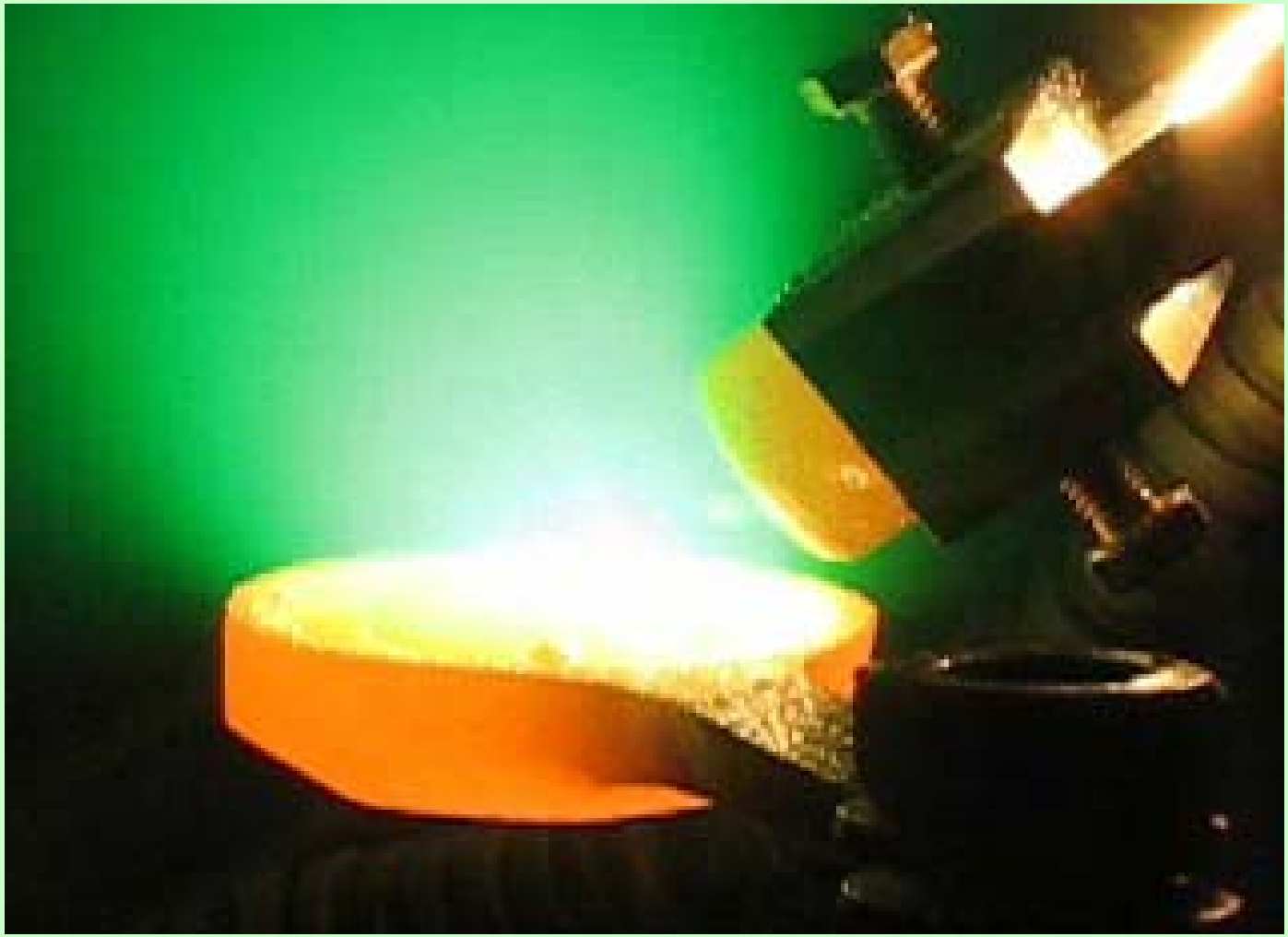

I-V characteristic

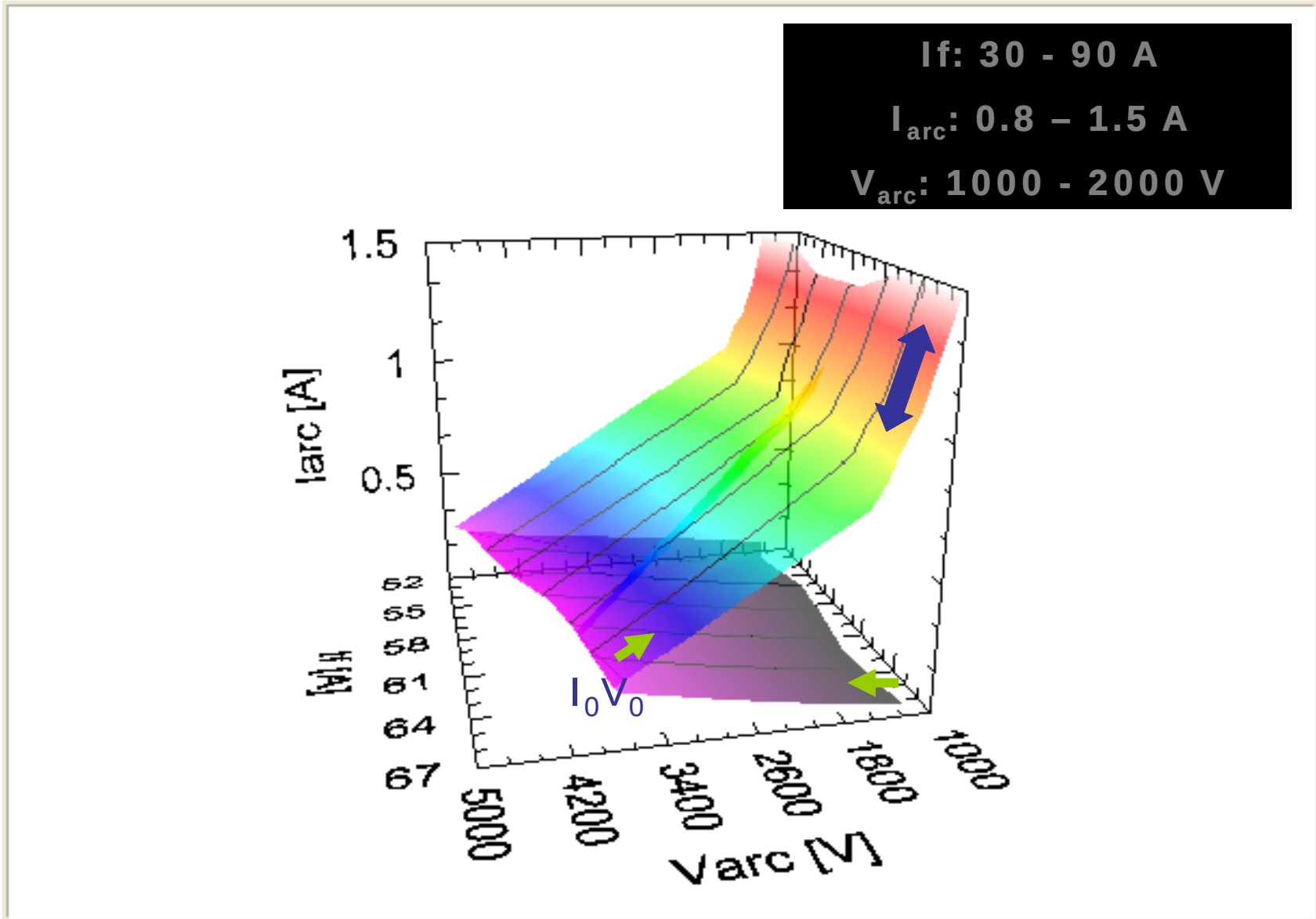

3D

TVA plasma ignition stages

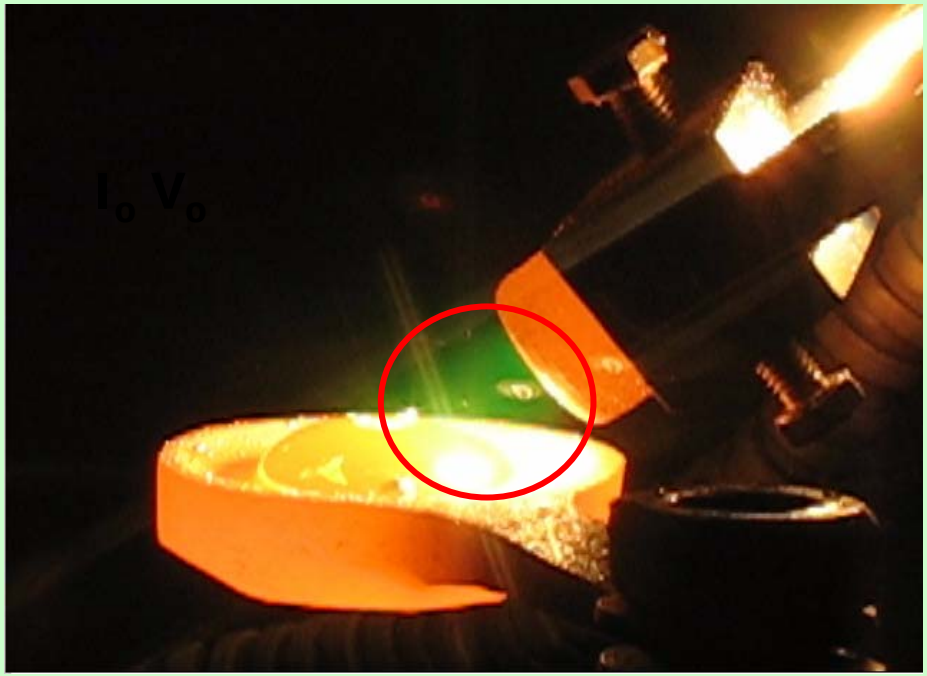

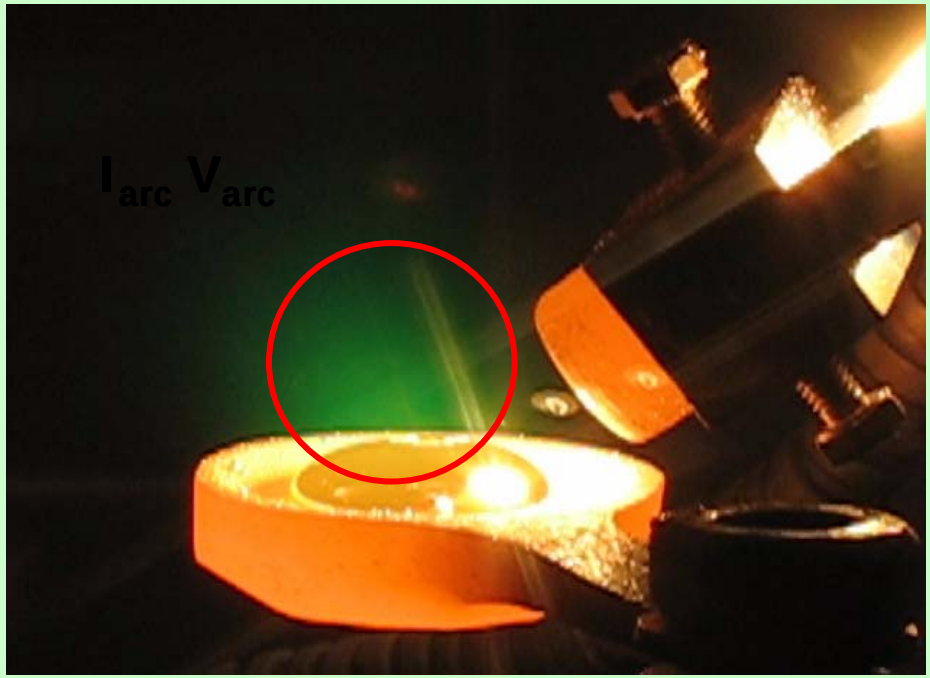

$$V_p = V - (Io*Vo)/I$$

$$E_{ion} = eV_p$$

New setup of the TVA

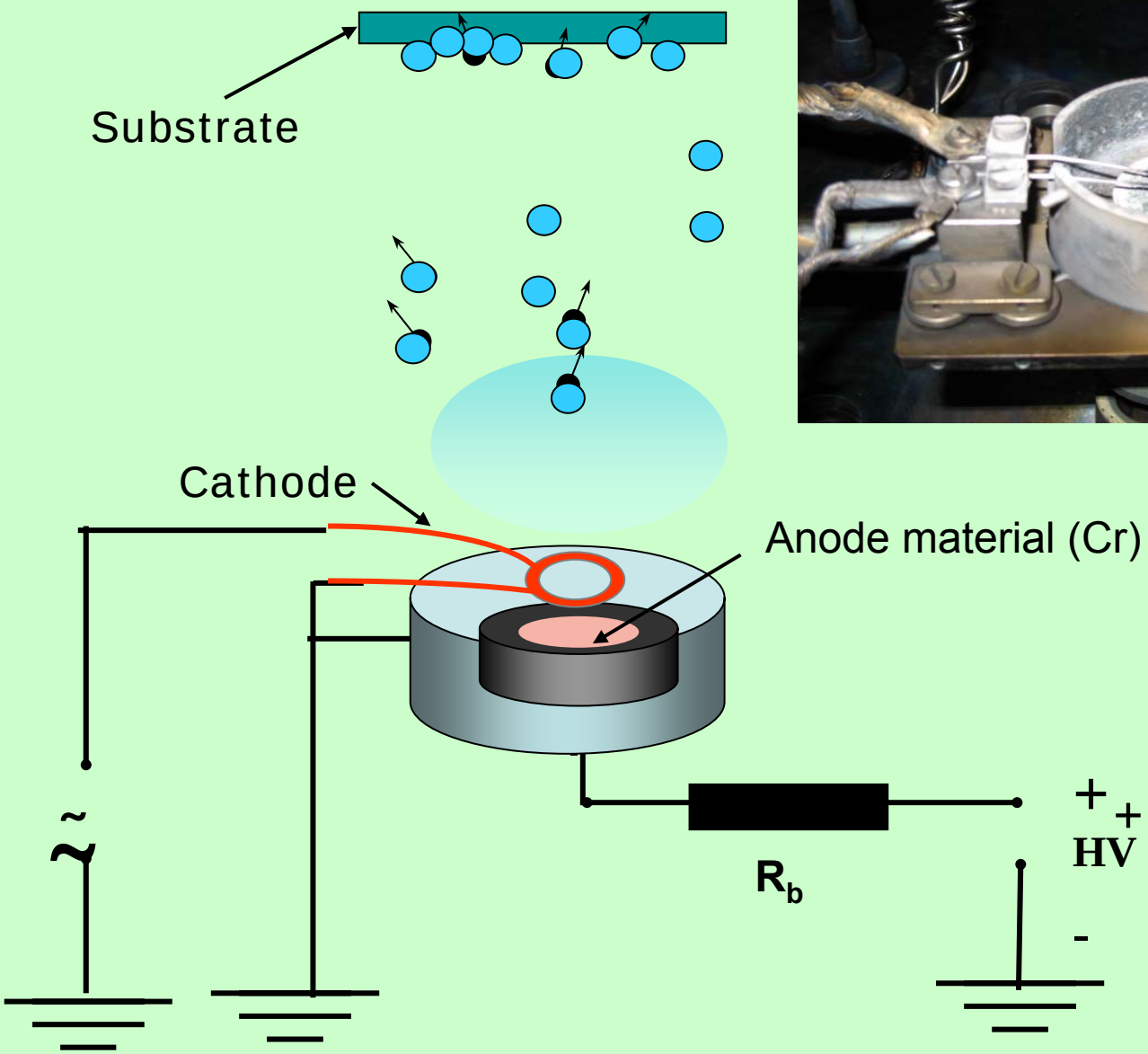

Power input = 1550 W

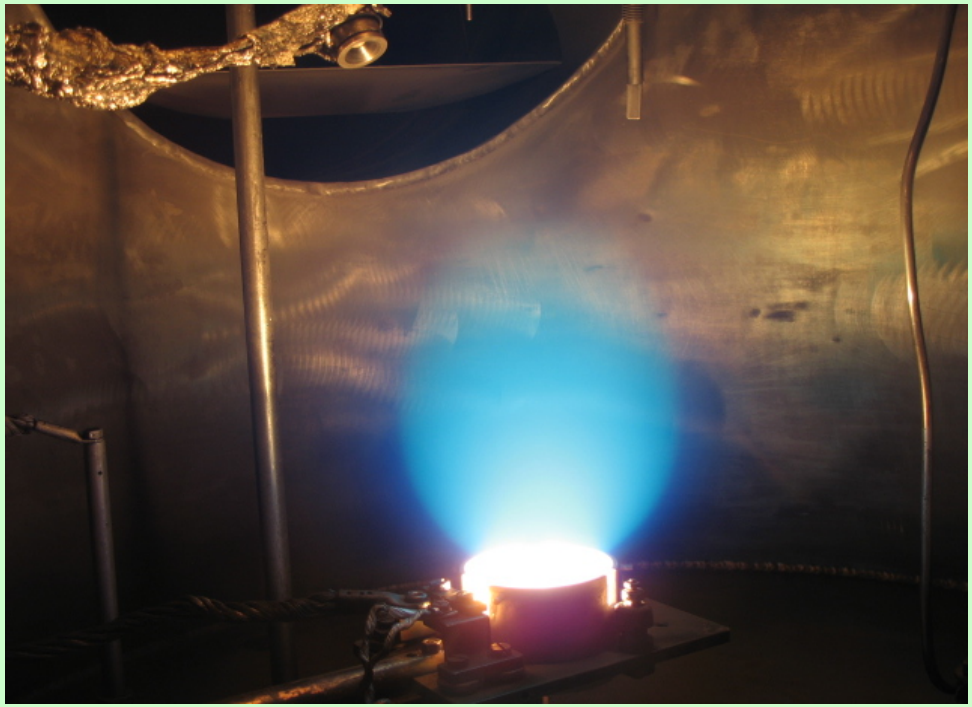

Power input = 1800 W

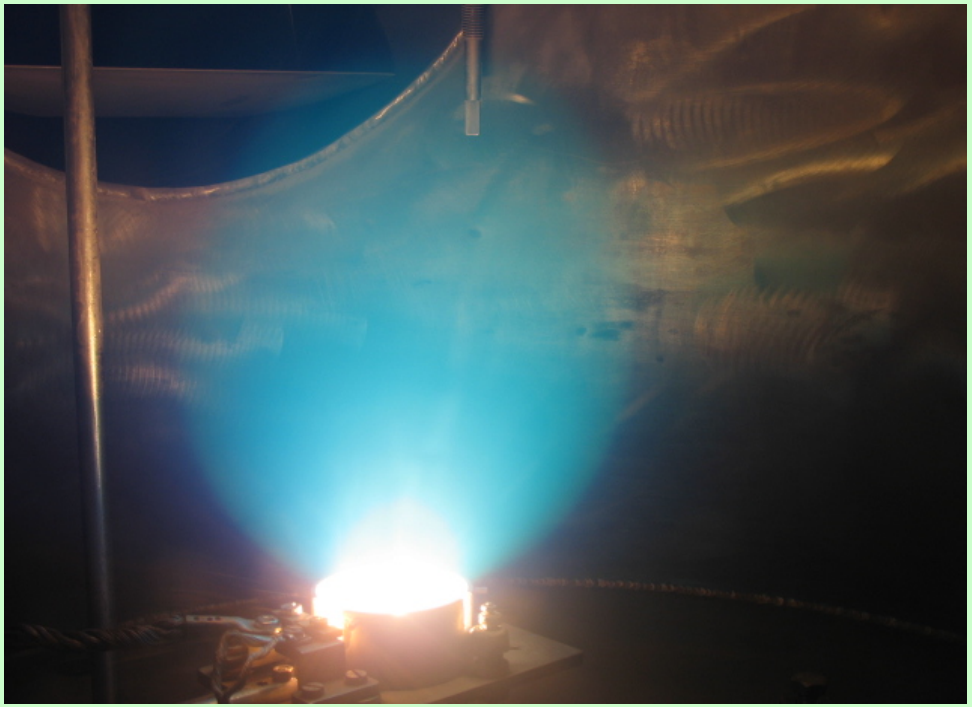

Optical emission spectrum of the Chromium TVA plasma

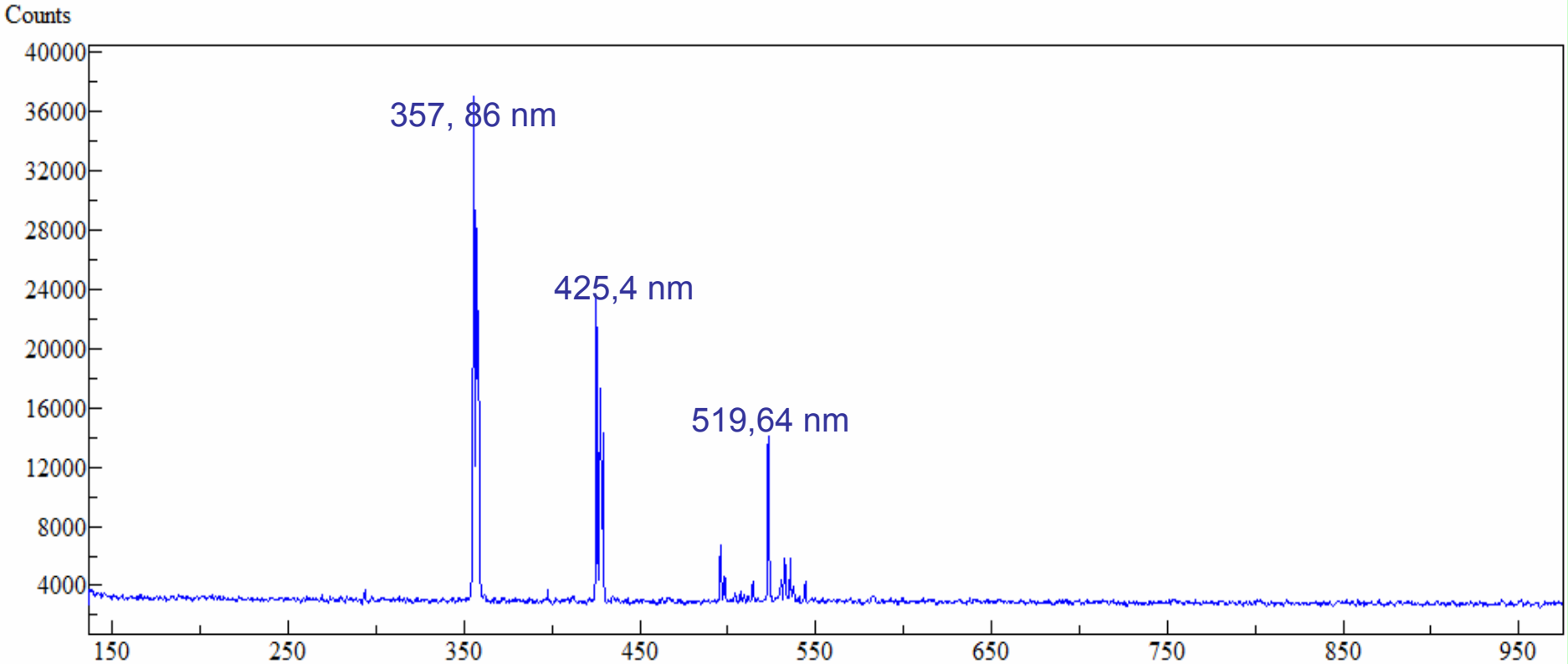

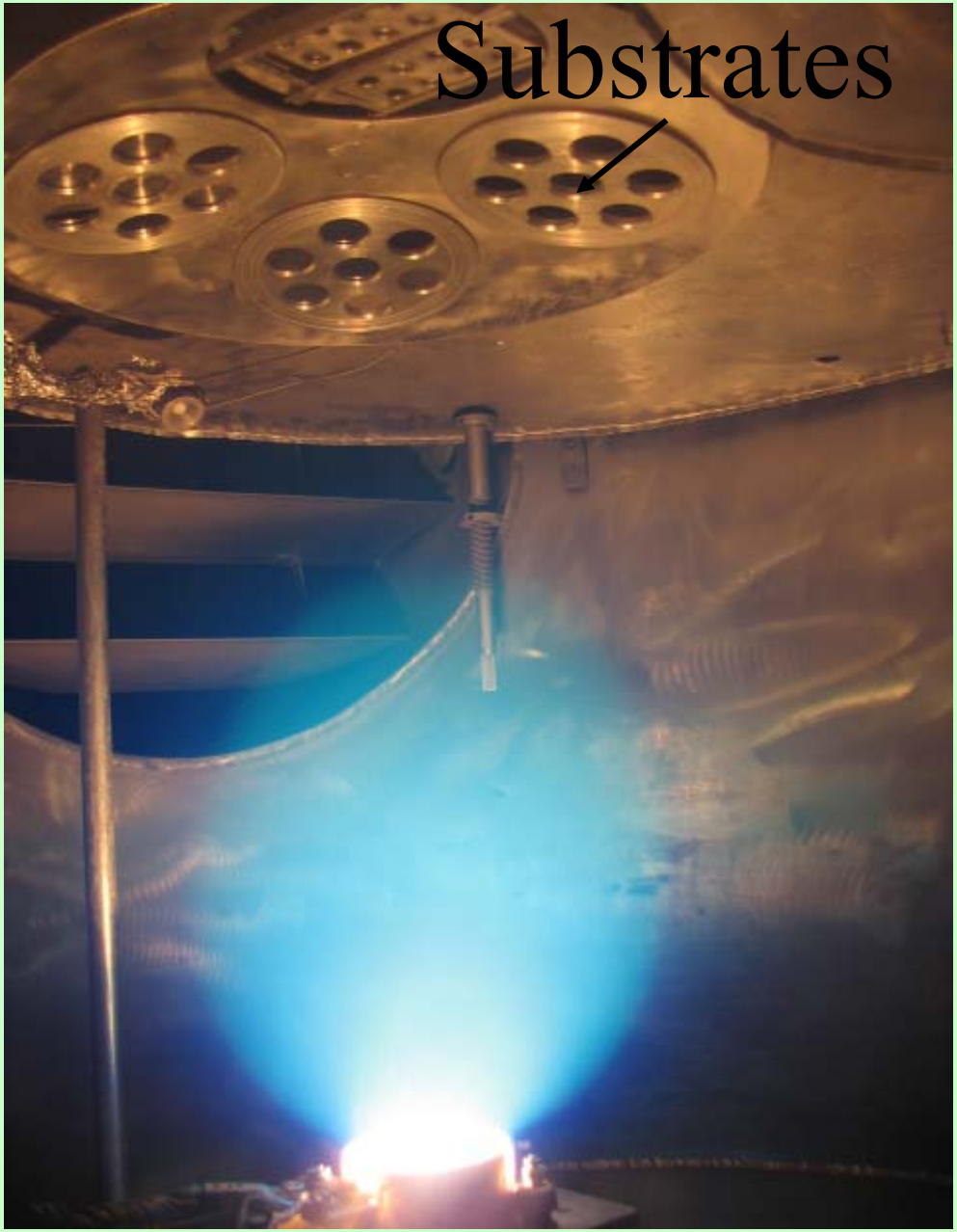
Substrates

Multiple deposition

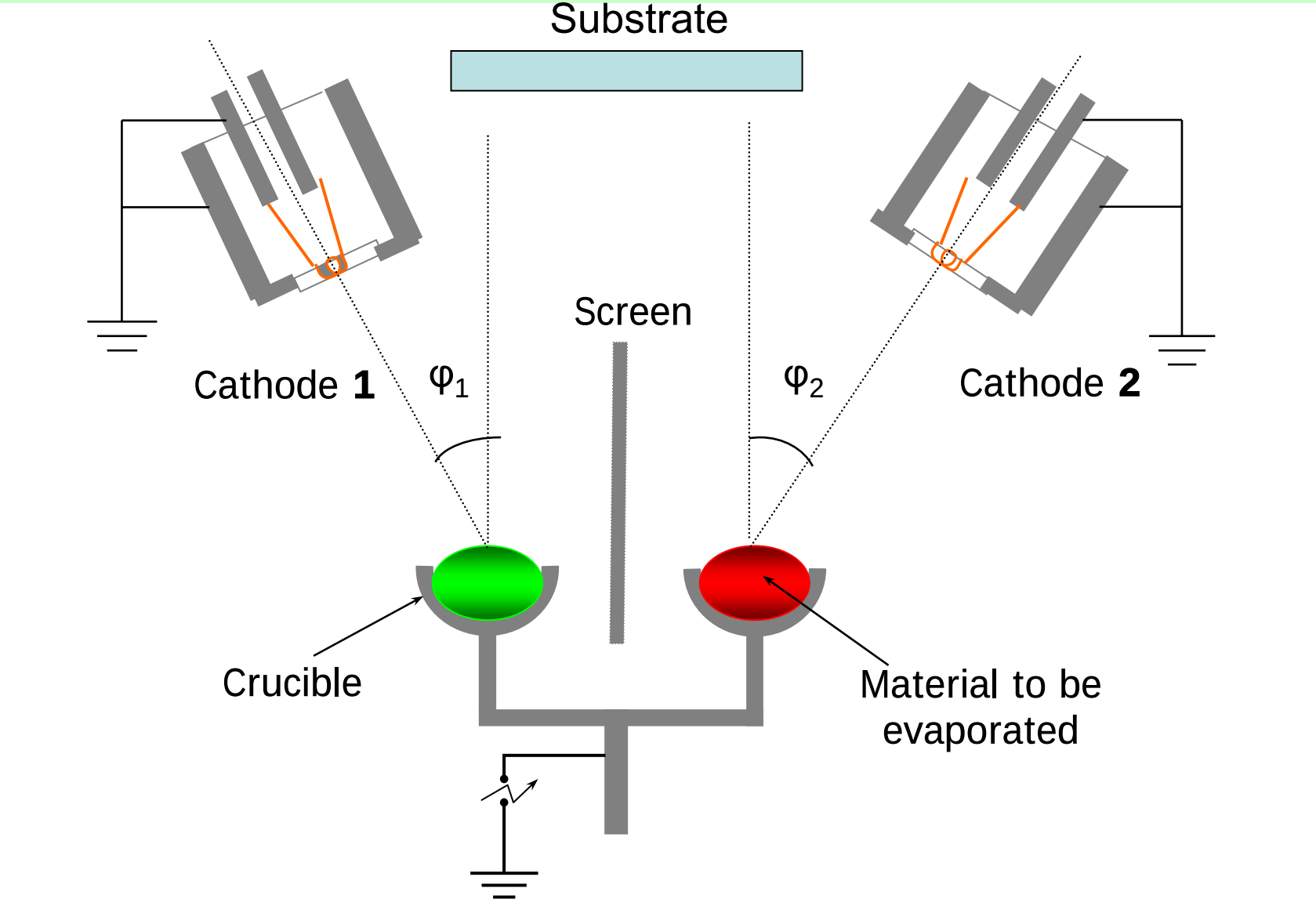

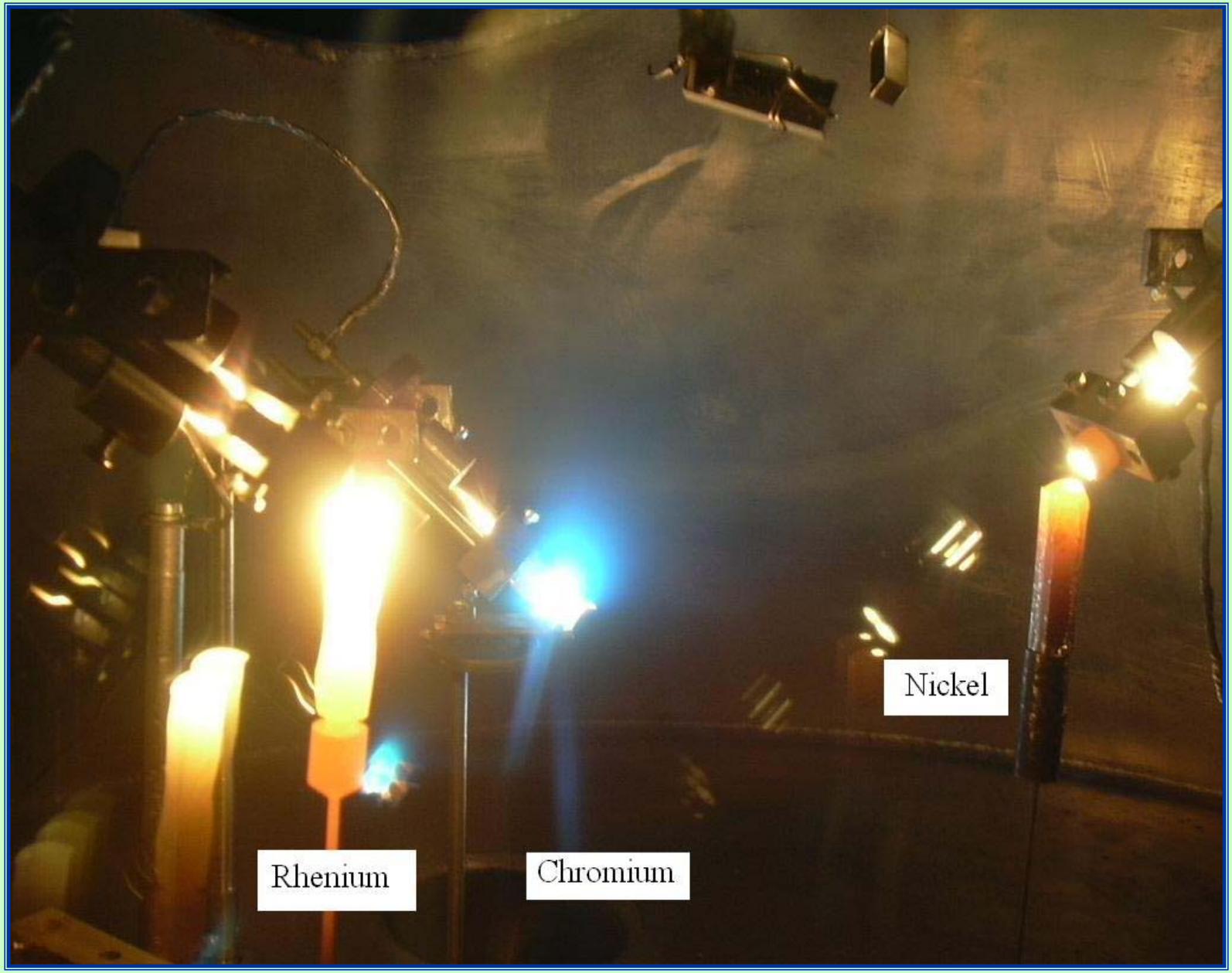

Experimental set-up used for simultaneously depositions of Re, Ni and Cr

TVA parameters

- Interelectrode distance
- Angle φ
- Cathode heating current (I_f)

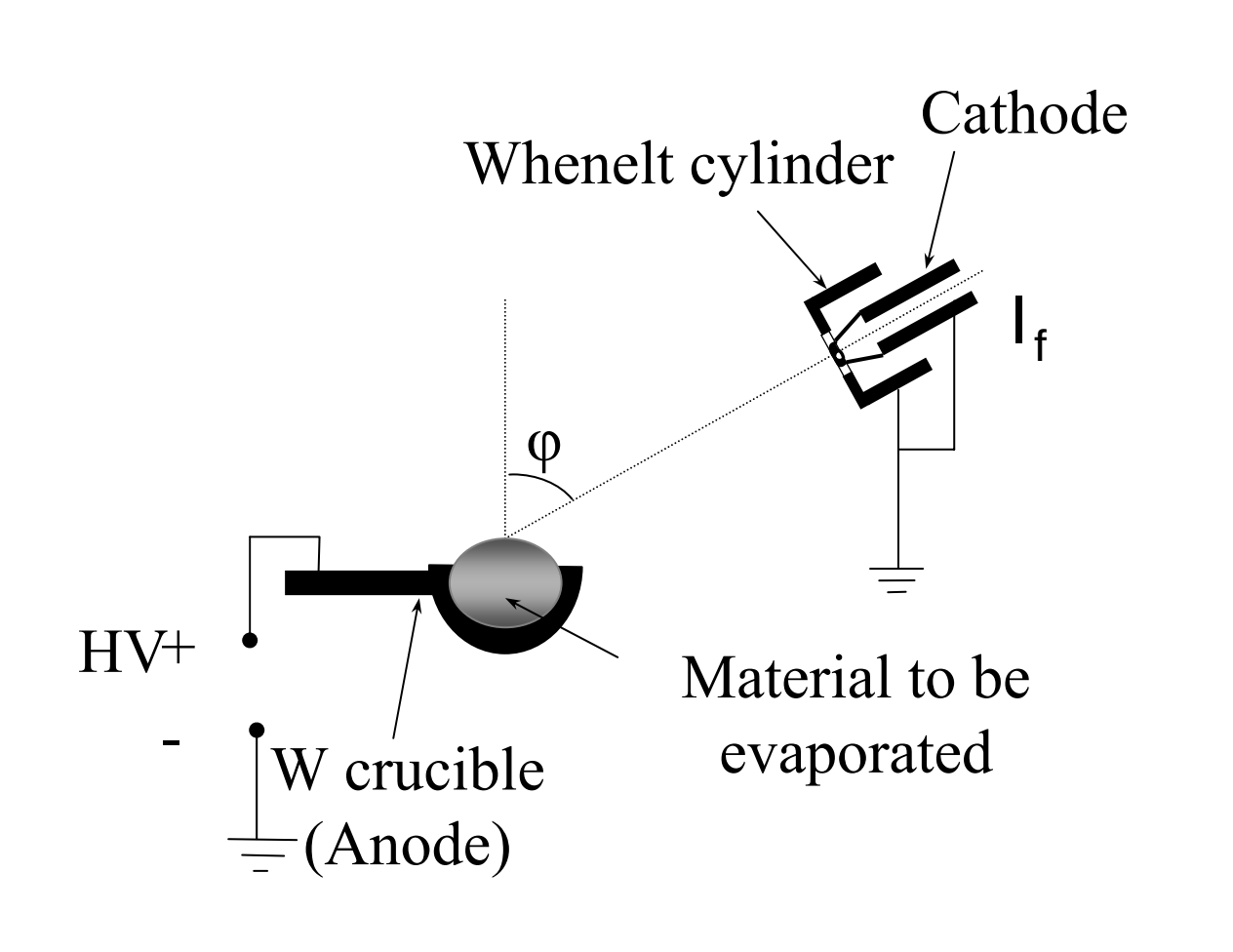

I-V characteristics

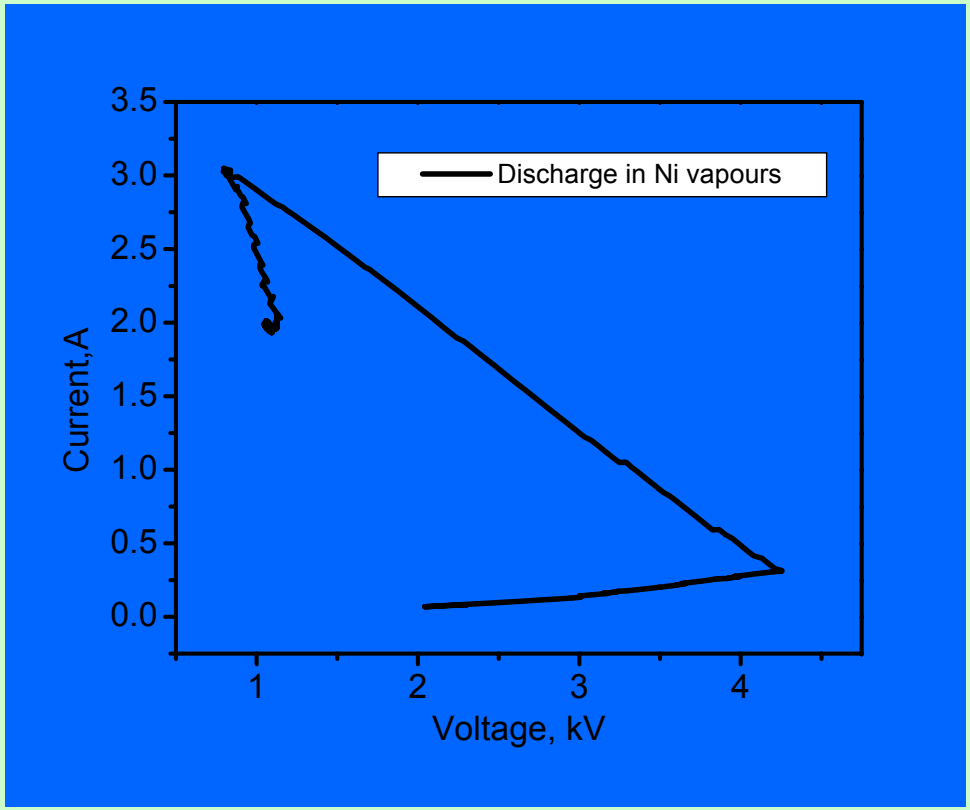

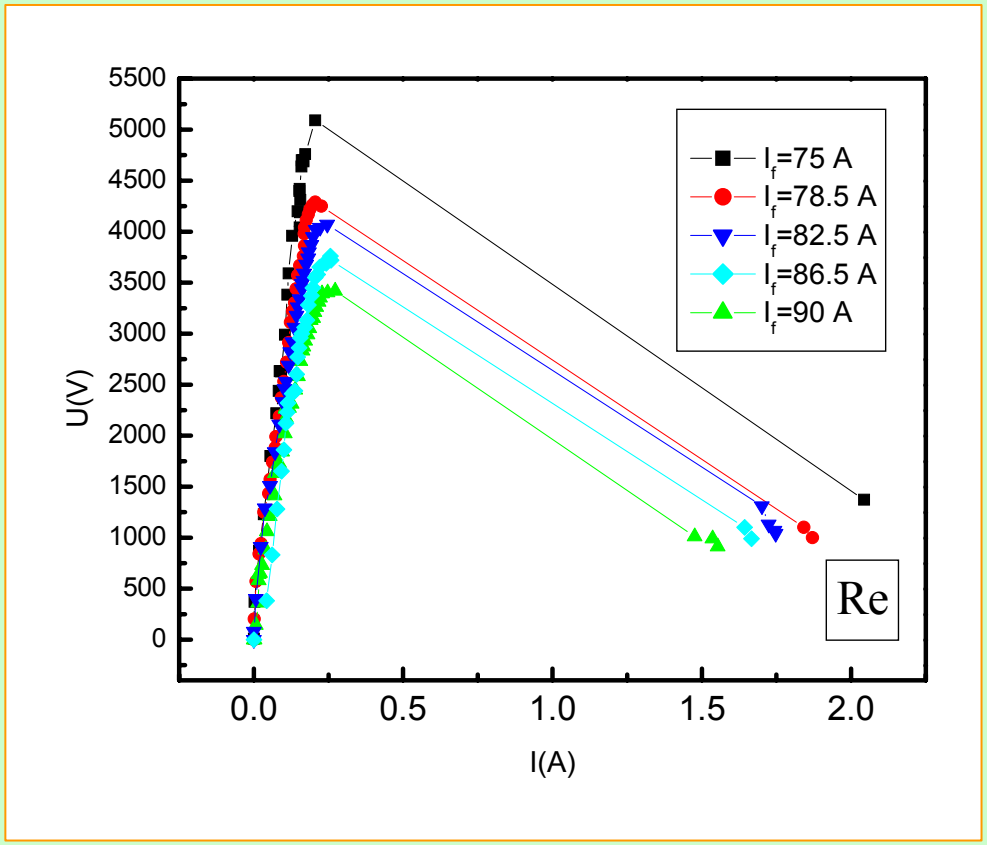

I-V characteristics plasma (Re) as function of the filament current

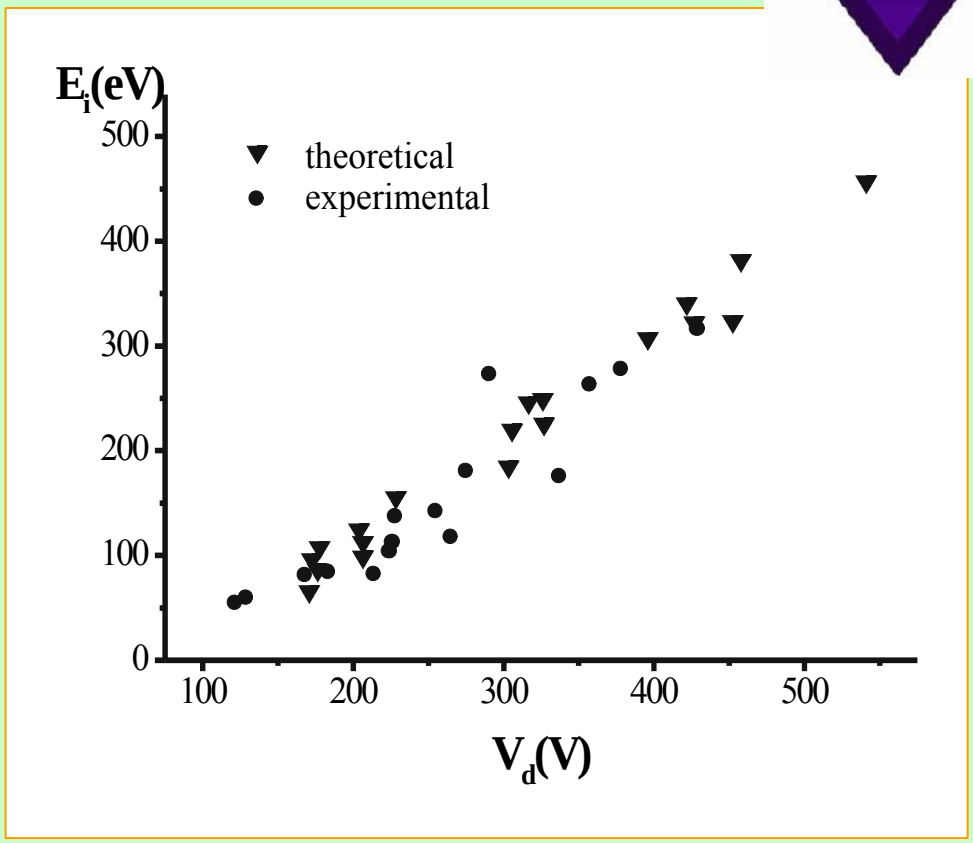

Ion energy vs discharge voltage (V_d)

Cathode heating current (I_f)

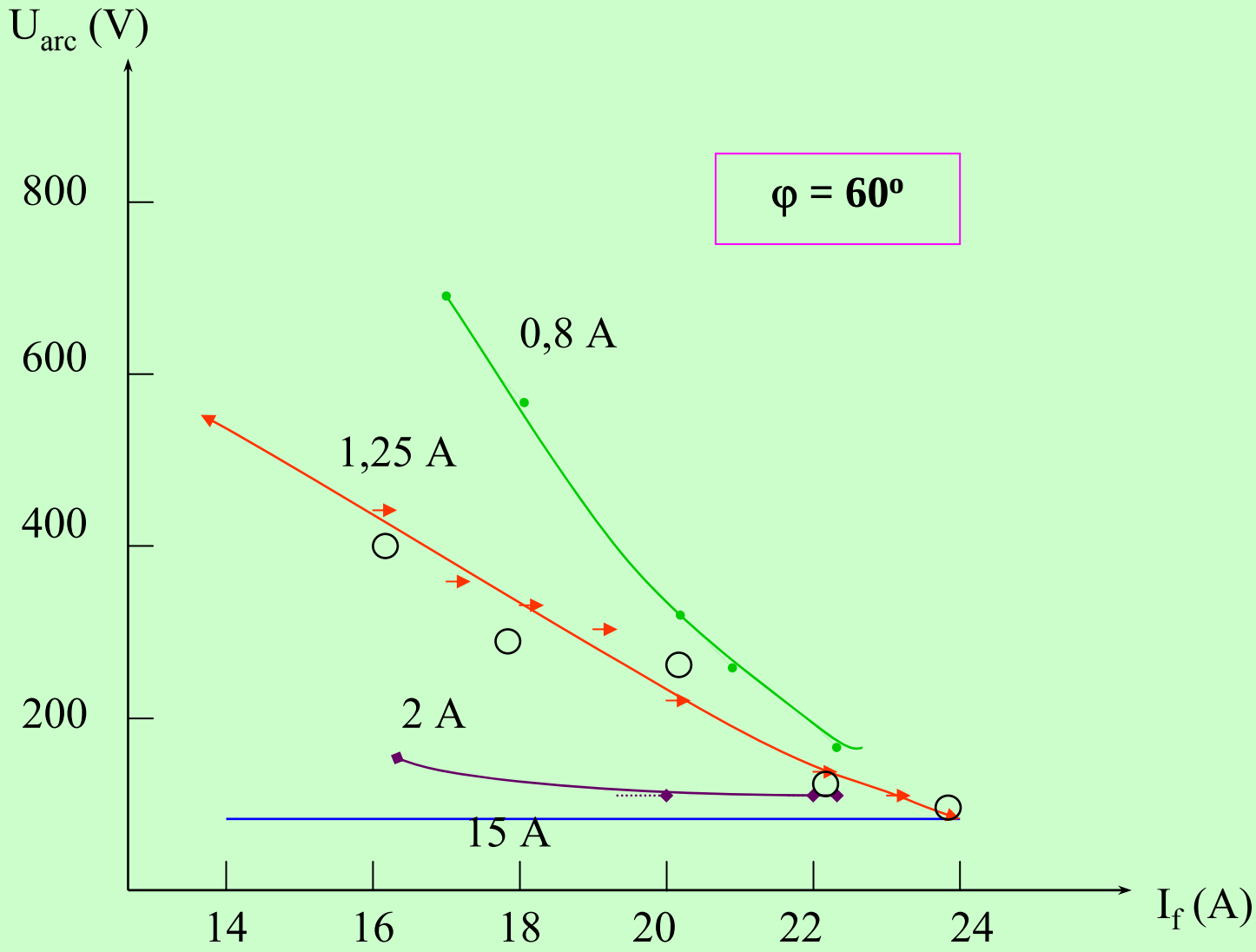

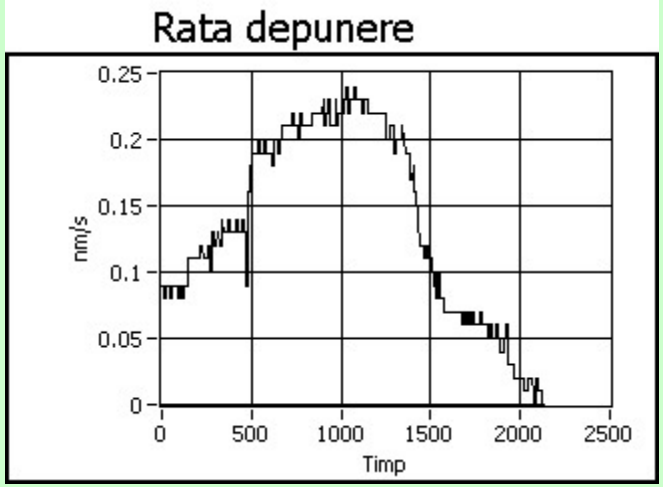
Rata depunere
nm/s
0.25
0.2
0.15
0.1
0.05
0
0
500
1000
1500
2000
2500
Timp

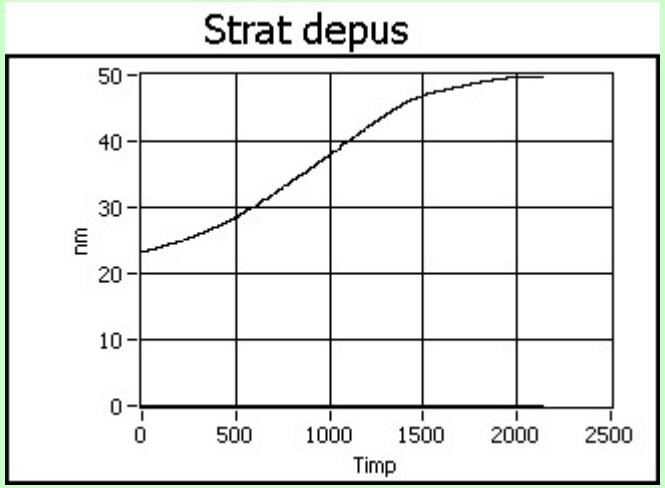
Strat depus
nm
50
40
30
20
10
0
0
500
1000
1500
2000
2500
Timp

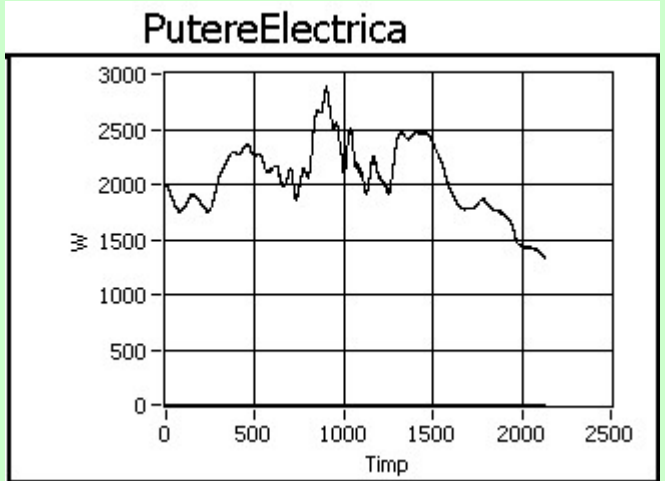
PutereElectrica
W
3000
2500
2000
1500
1000
500
0
0
500
1000
1500
2000
2500
Timp

The main advantages of the TVA method are:

- deposition of pure metal film in high or ultra - high vacuum conditions (<10^{-4}torr);

- no gas consumption and gas incorporation in the growing film;

- the growing thin film is bombarded just during deposition with the ions of the depositing material insuring the compactness of the film;

-the energy of bombarding ions can be controlled and can be even changed during deposition;

- the deposition rate can be easily controlled and can be greater than in the sputtering case (0.1 – 2 nm/s).

TVA apparatus:
Volume ~ 1m^3; Base pressure: <10^{-6} torr
DC Power supplies: 6kV, 5A; 5kV,1A; 3kV, 2A; 0.6kV, 20 A

High-temperature oxidation resistant coatings

Refractory metals such as W, Mo, Ta and Nb are promising candidates for the development of new kinds of heat resisting materials (**One of their most fatal shortcomings is low resistance against oxidation at high temperatures**)

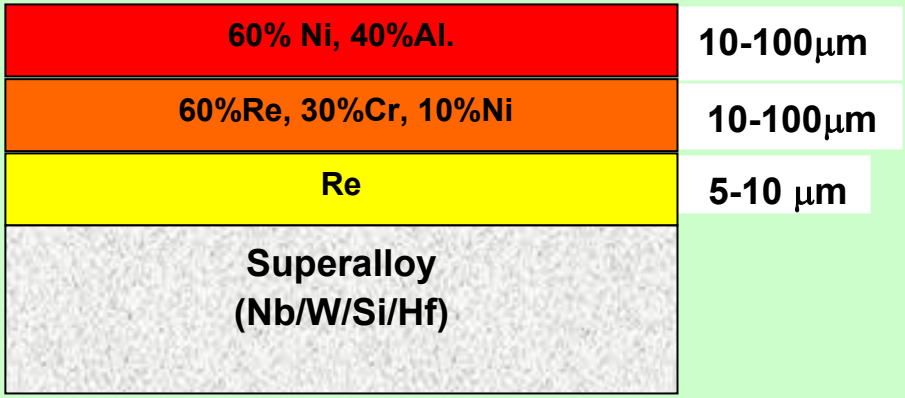

This problem is expected to be solved by forming multi-layered coatings:

- a barrier against coming and outgoing elements (Re),
- a reservoir supplying lost elements (Re-Ni-Cr) and
- a heat resistant layer (Ni-Al).

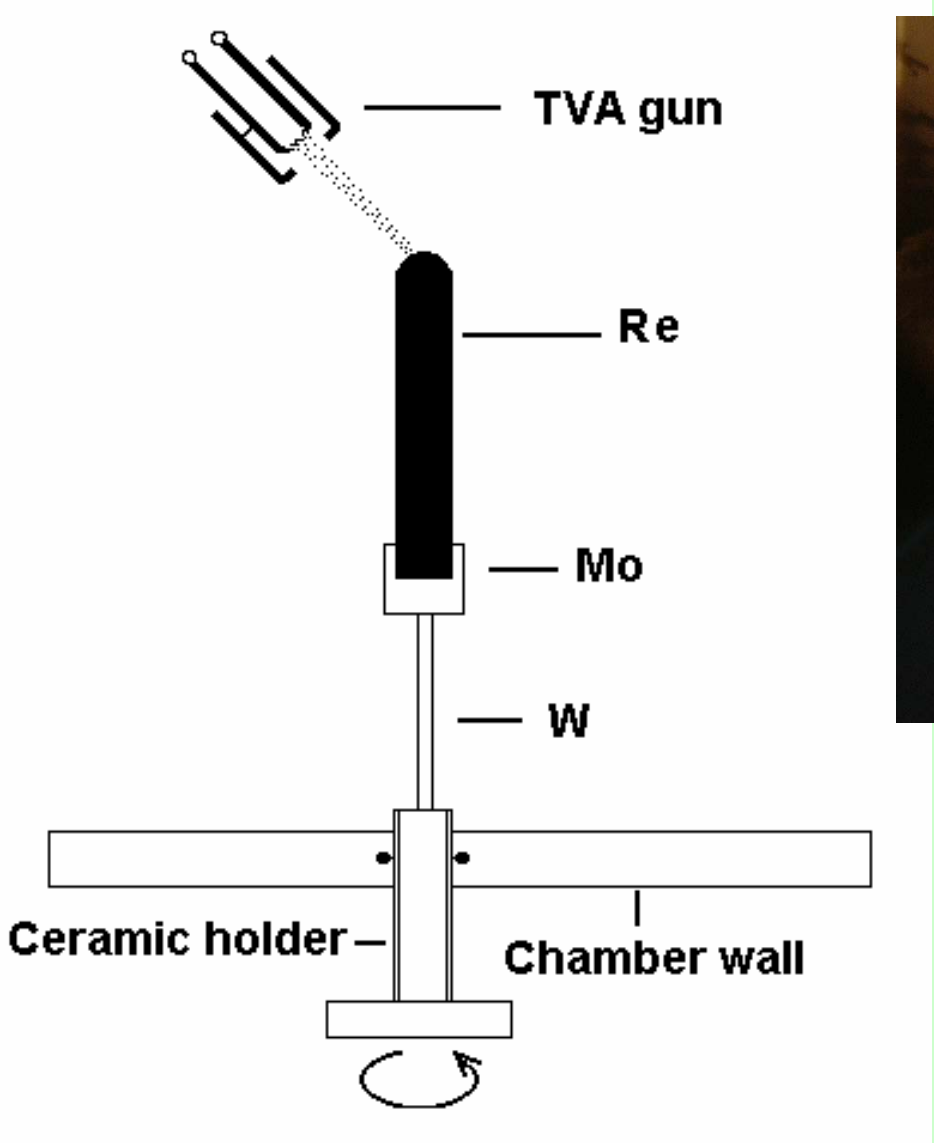

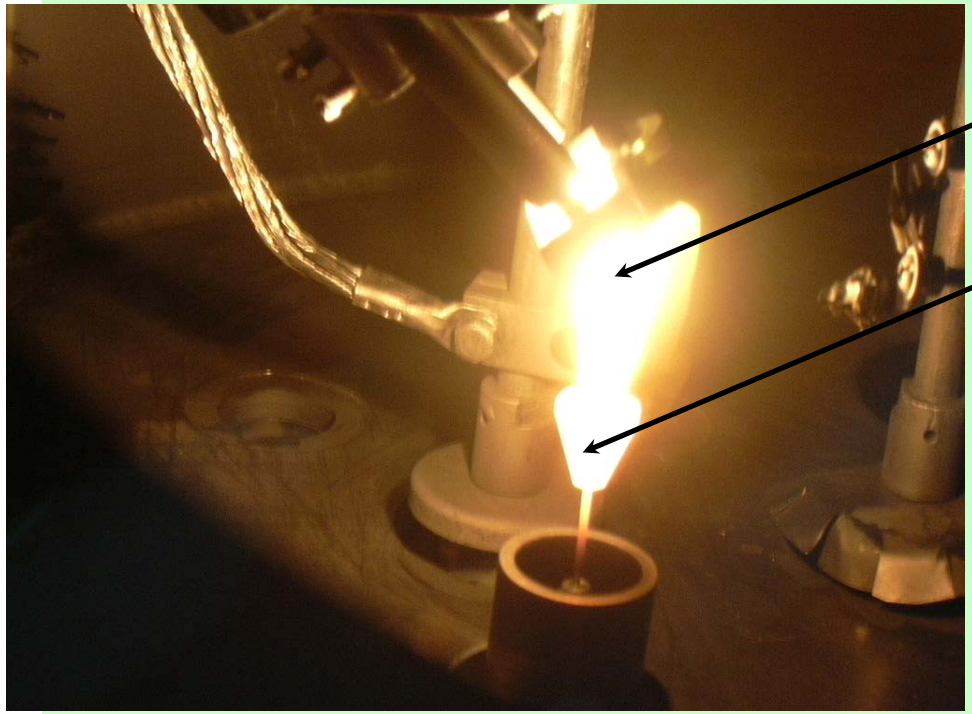

Photograph of the Re ingot during deposition

Cross-sectional SEM Image of Re-Cr film

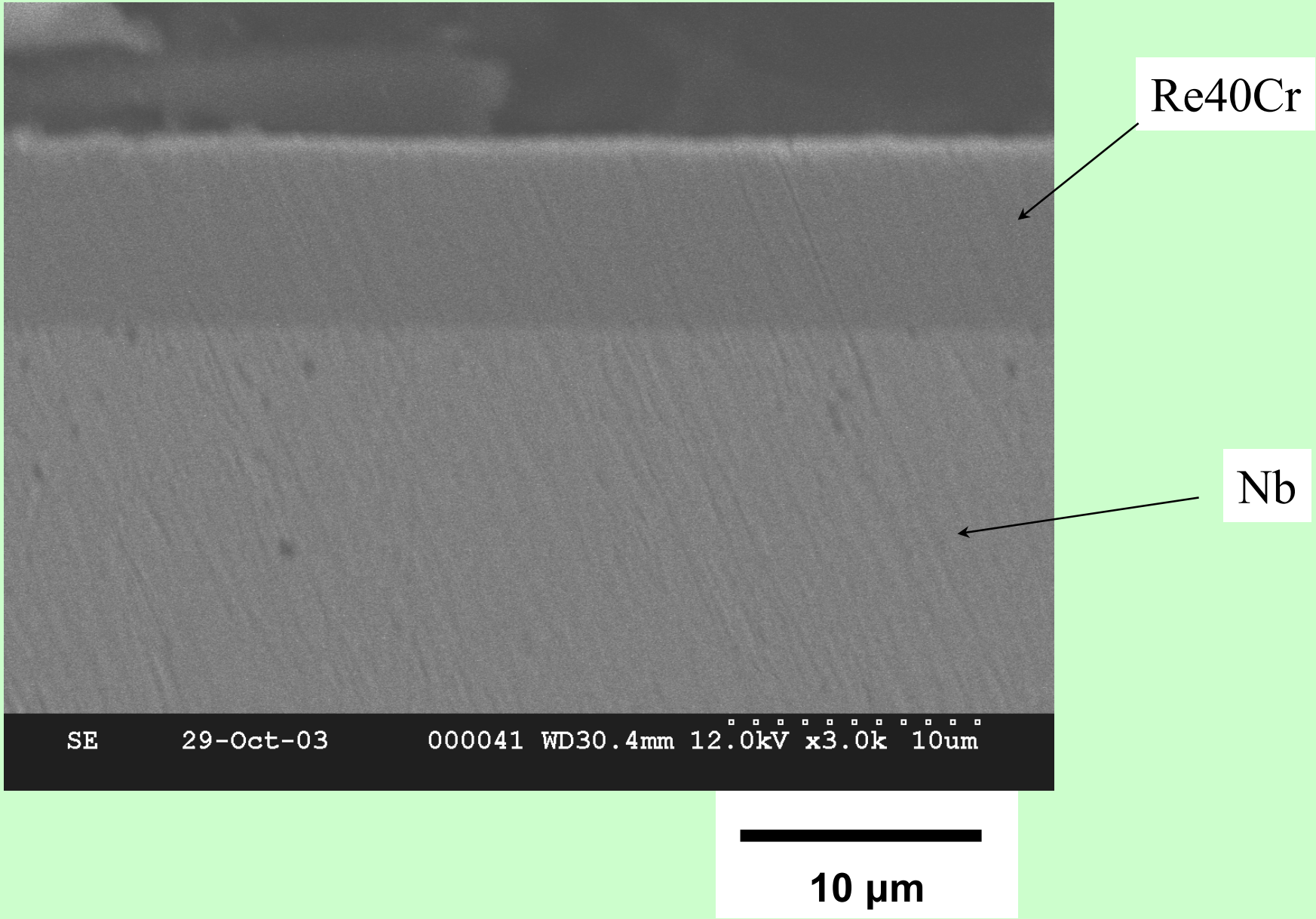

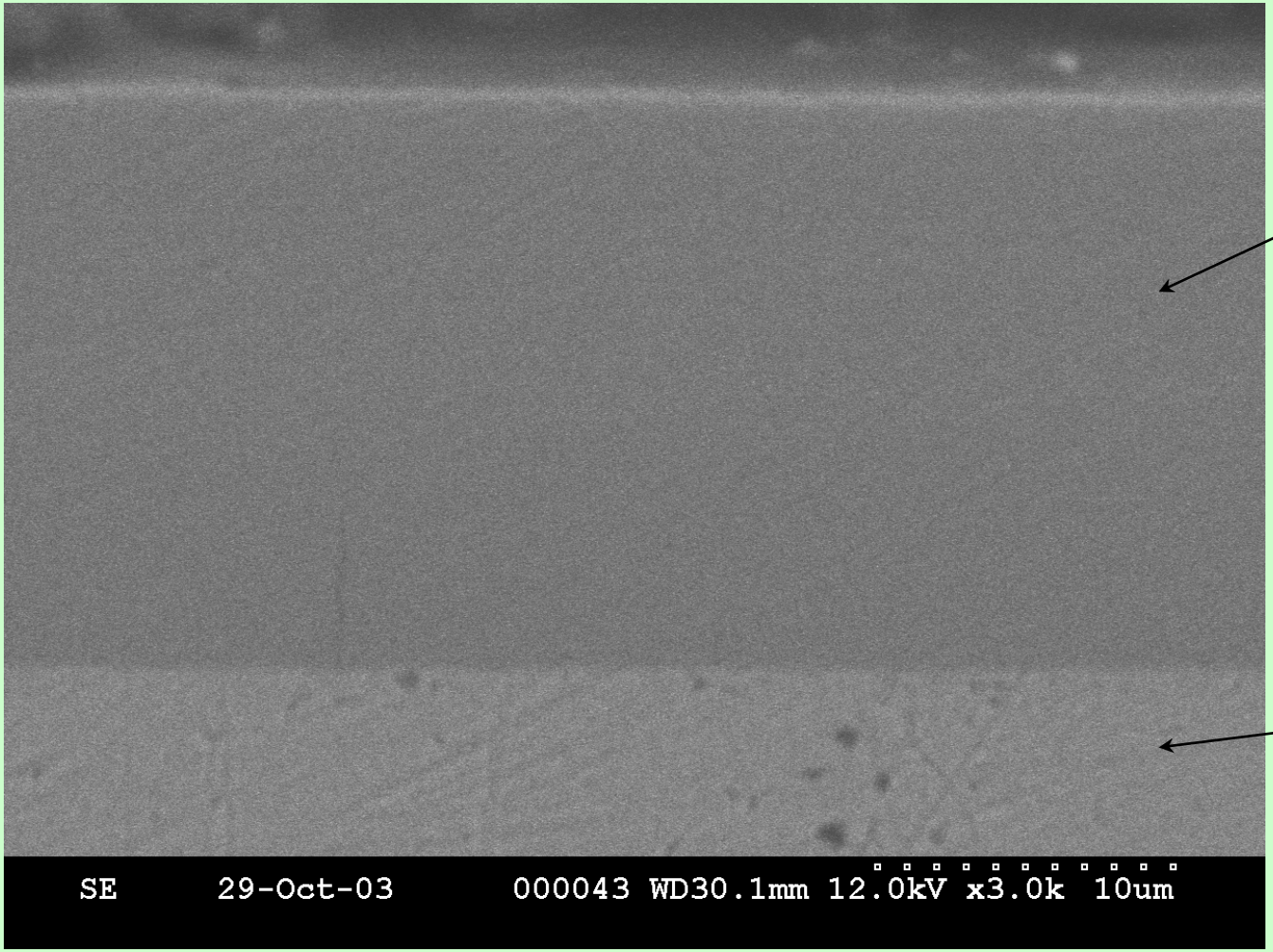

Re30Cr10Ni

Nb

10 μm

Cross-sectional SEM Image of Re-Cr-Ni film

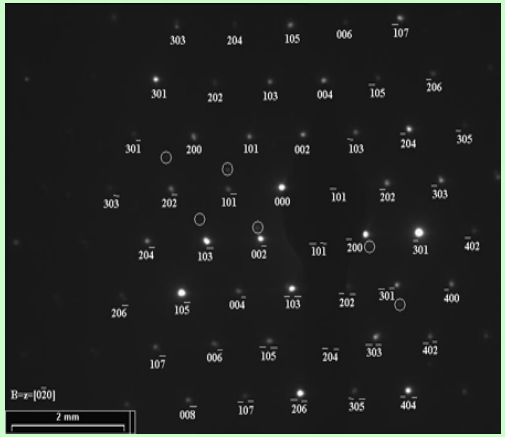

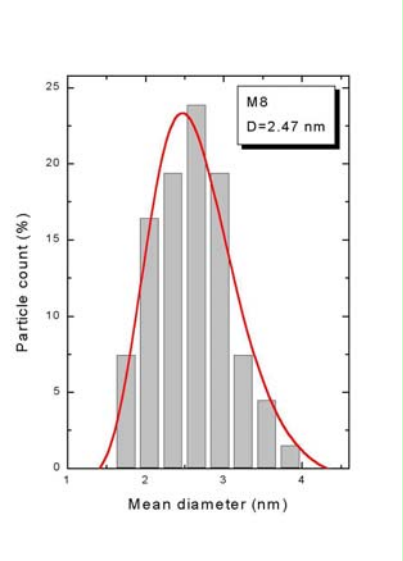

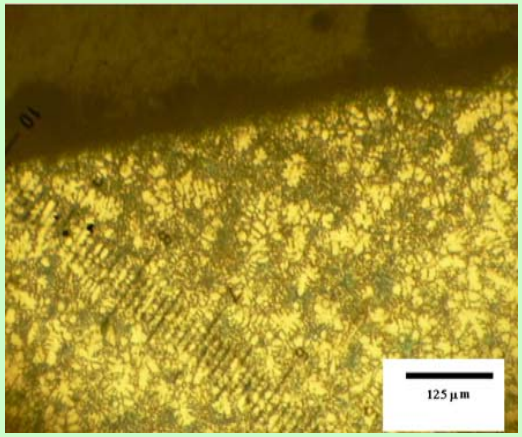

Nb superalloy

(Optical micrograph

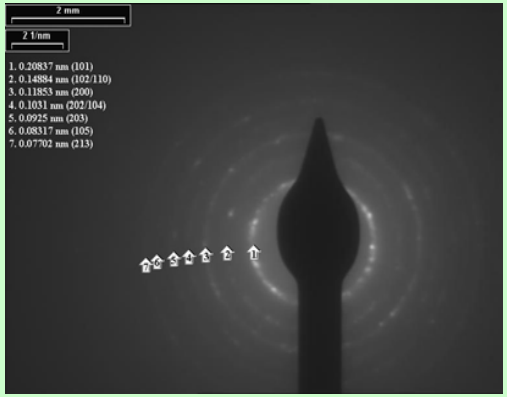

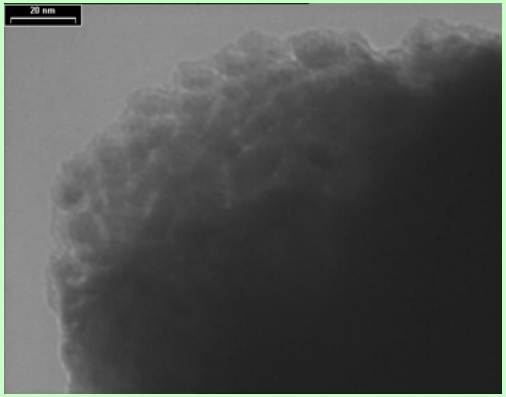

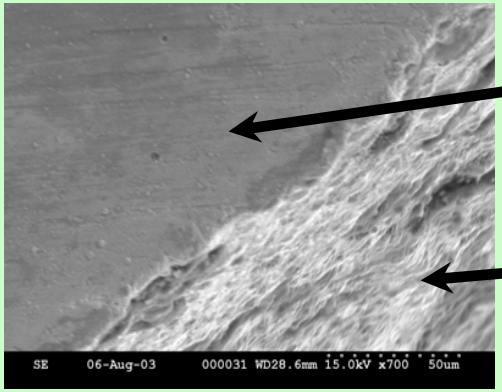

Re

Nb superalloy

SAED **HRTEM** **SEM**

Selected area diffraction (SAED), high resolution transmission microscopy (HRTEM) and scanning electron microscopy (SEM) images of the nanostructured Rhenium film deposited on Nb superalloy by TVA

Differential Thermal Analysis (DTA) and Thermal Gravimetric Analysis (TGA)

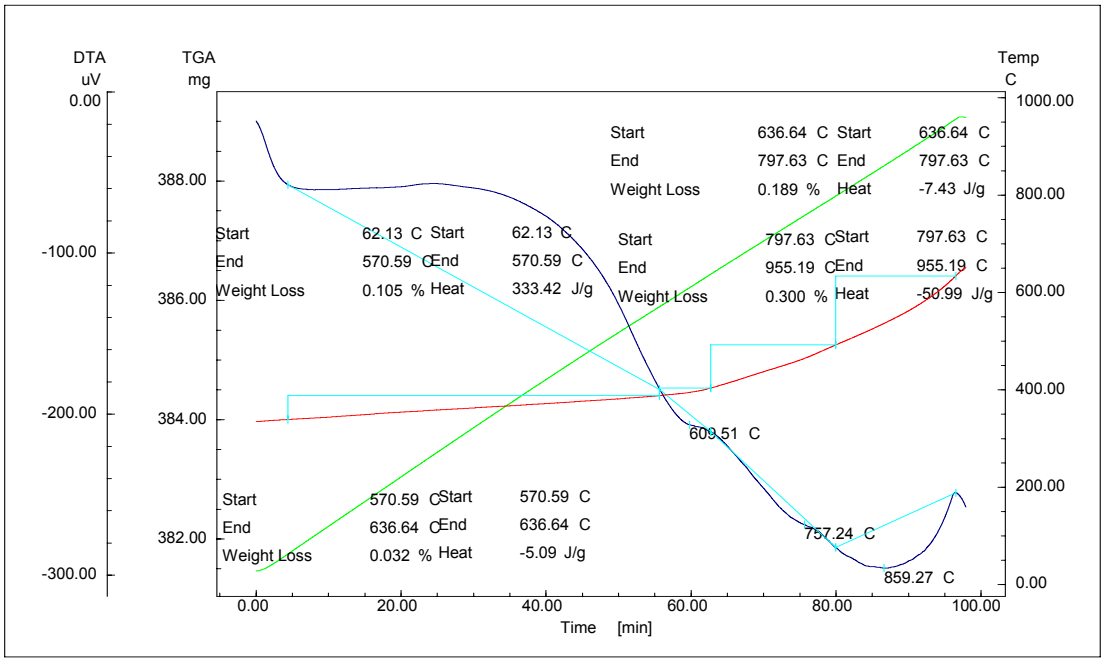

Nb alloy uncoated

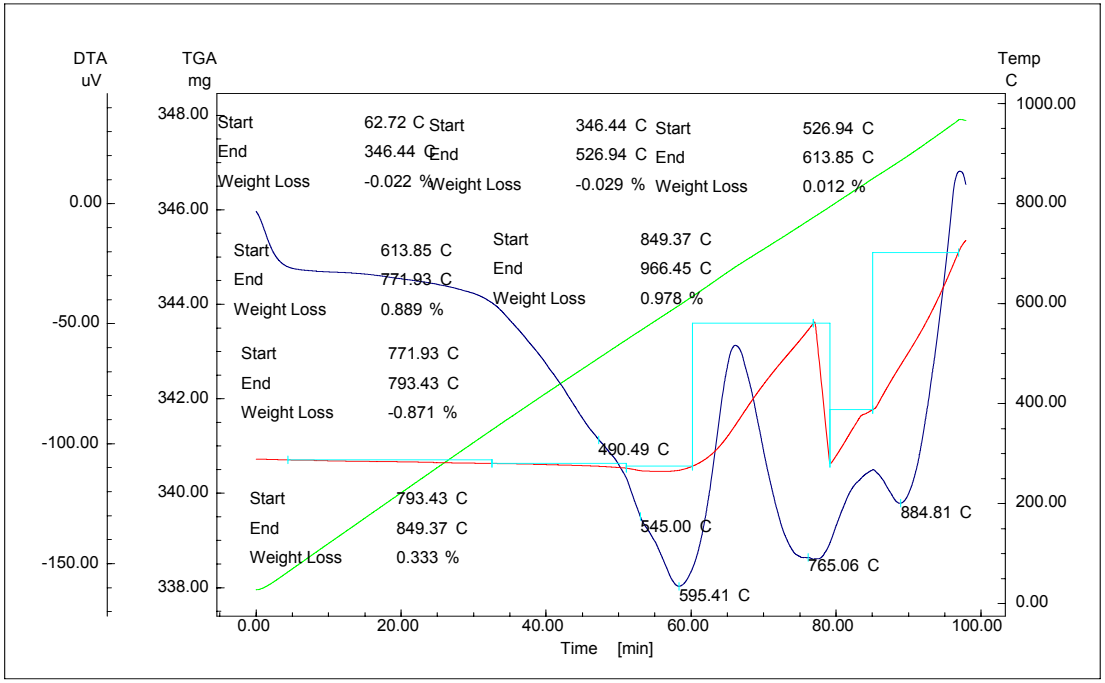

Rhenium coated Nb alloy

Summary of Re-Ni/Cr deposition

By utilizing the present results of experimental and theoretical analyses, it has become possible to make uniform Re coatings onto the Nb alloy at a deposition rate of more than 10 μm/h.

The possibility to form Re-30Cr-10Ni (at.%) alloy coatings was also tested.

HRTEM image of a C film

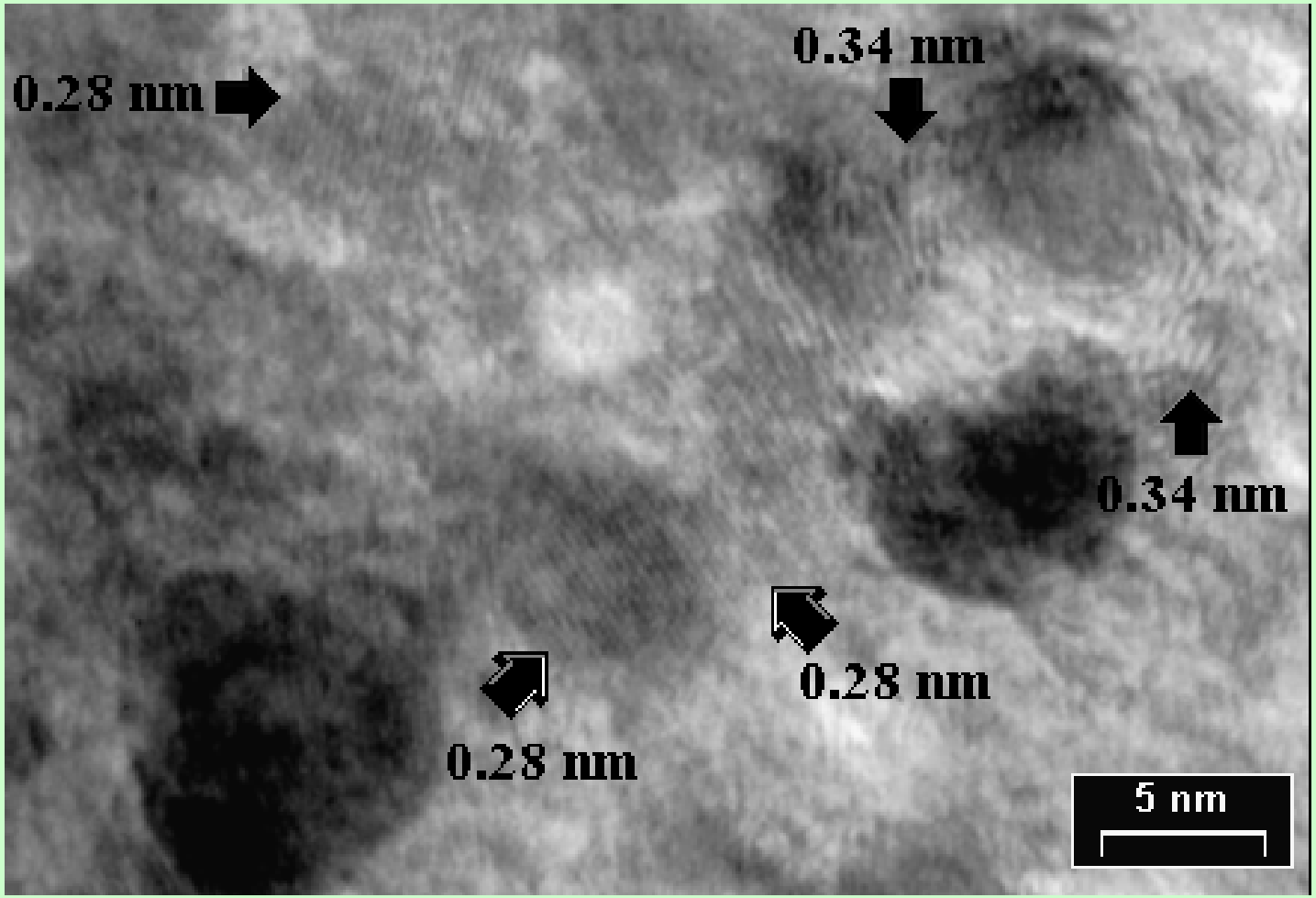

Nanostructured diamond like carbon (DLC) films preparation

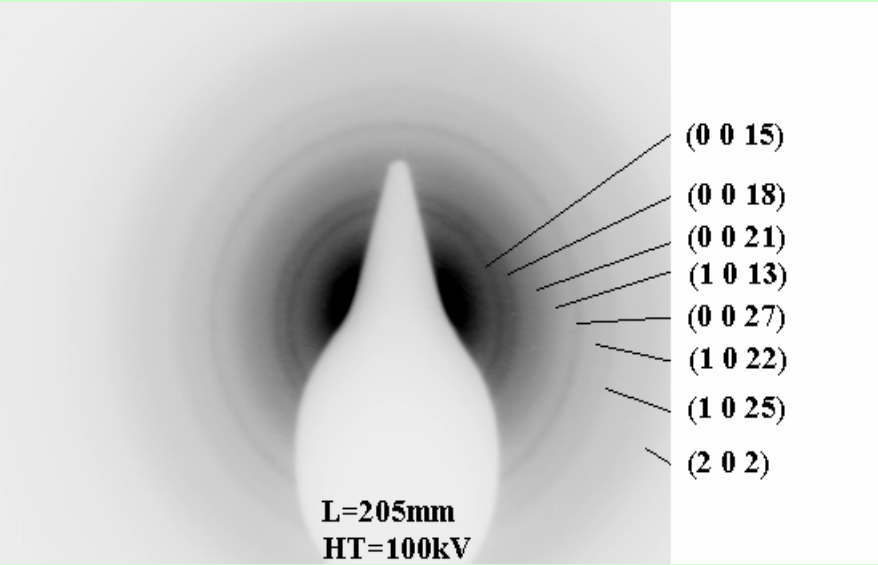

SAED

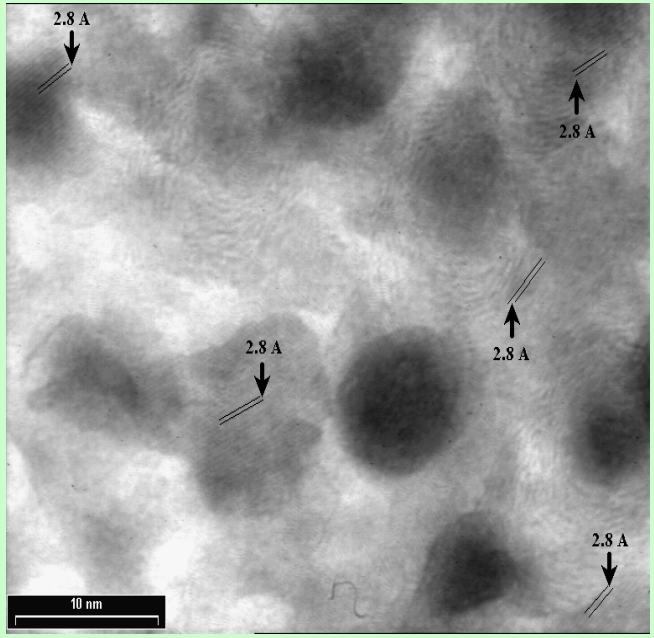

5nm HRTEM

Rhombohedra structures of the film with following parameters: a = 0.25221 nm, c = 4.3245nm (ASTM pattern: 79-1473) corresponding to diamond/carbon.

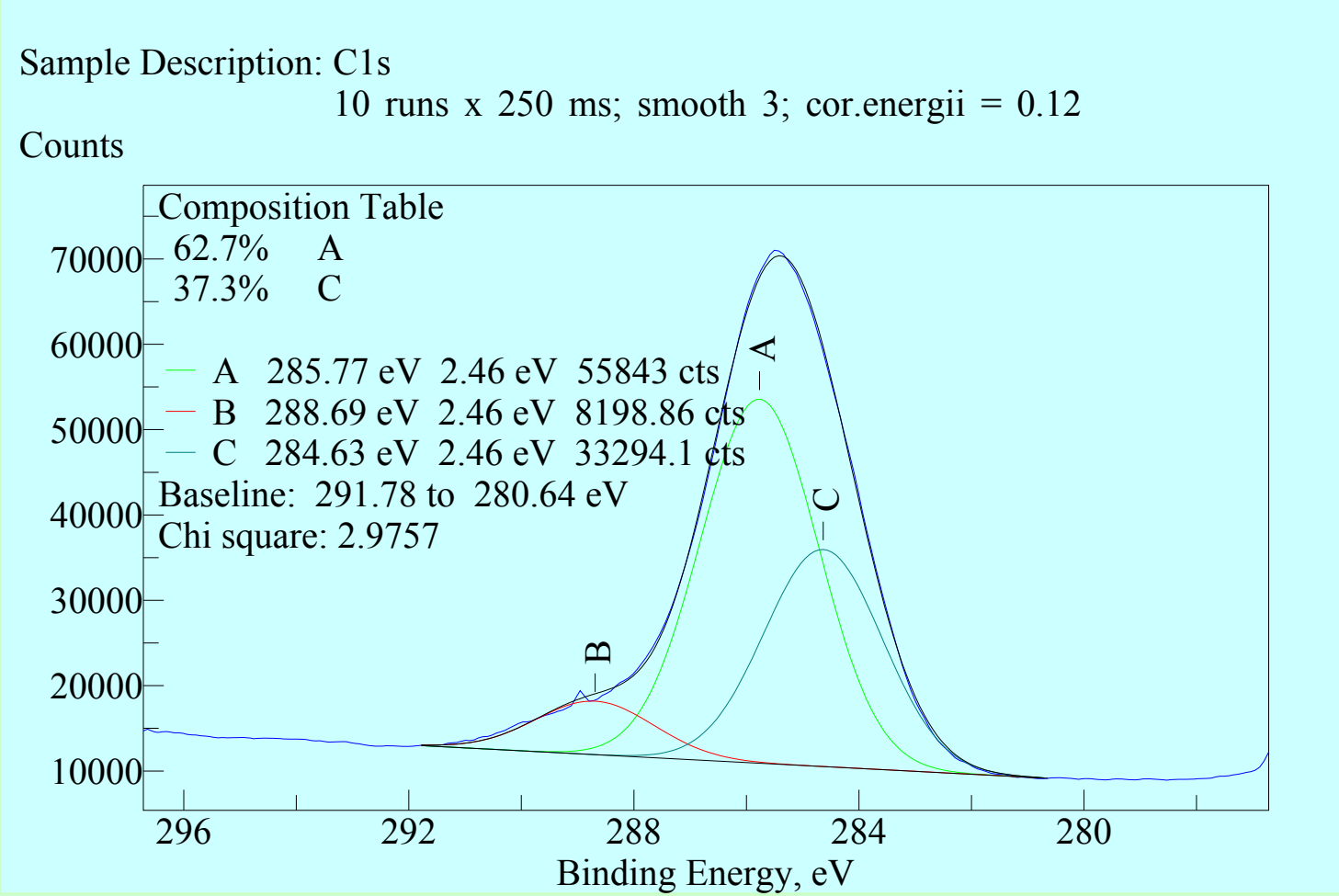

A: sp3; C: sp2; B: carbon-oxygen (CO_2)

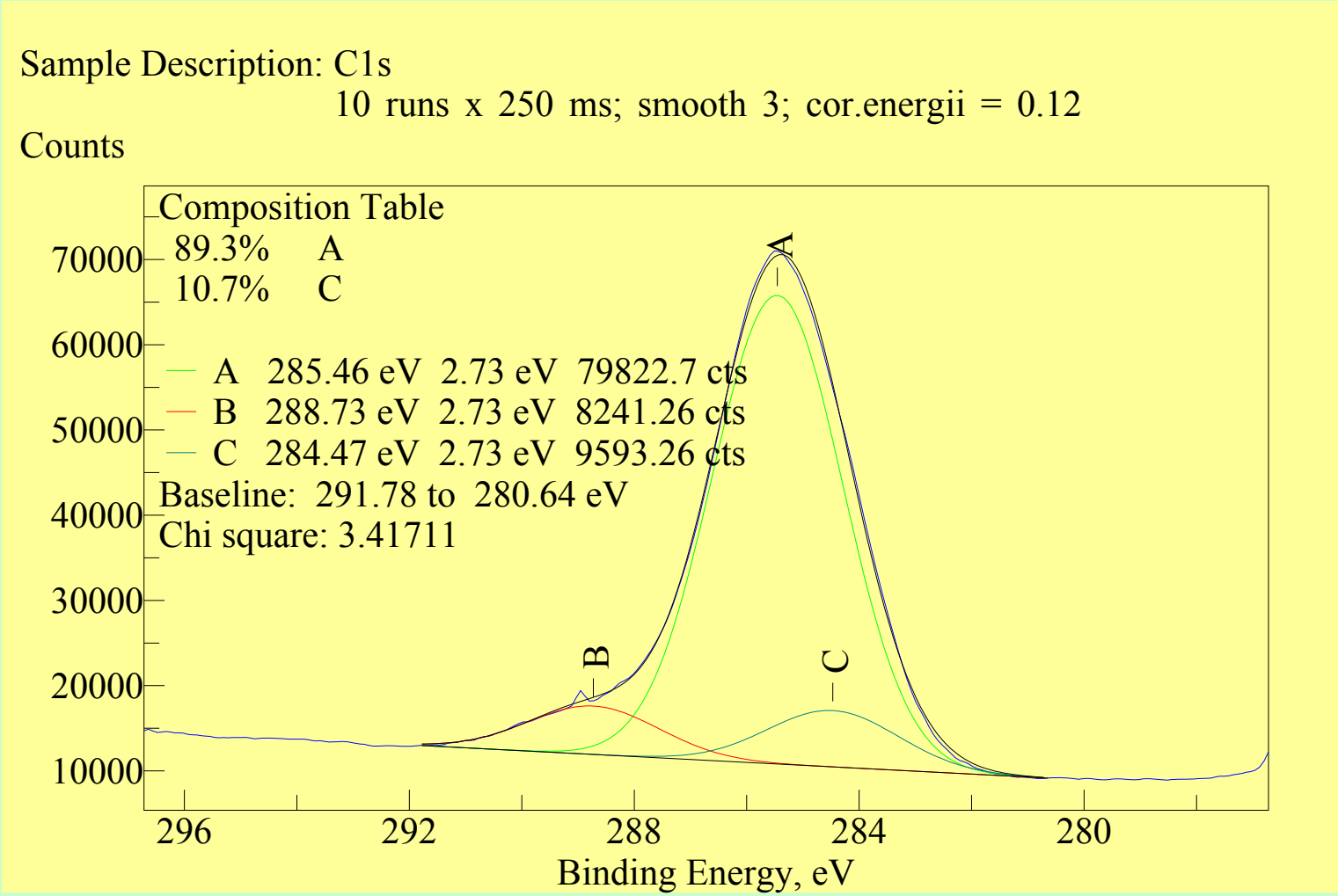

A: sp3; C: sp2; B: carbon-oxygen (CO_2)

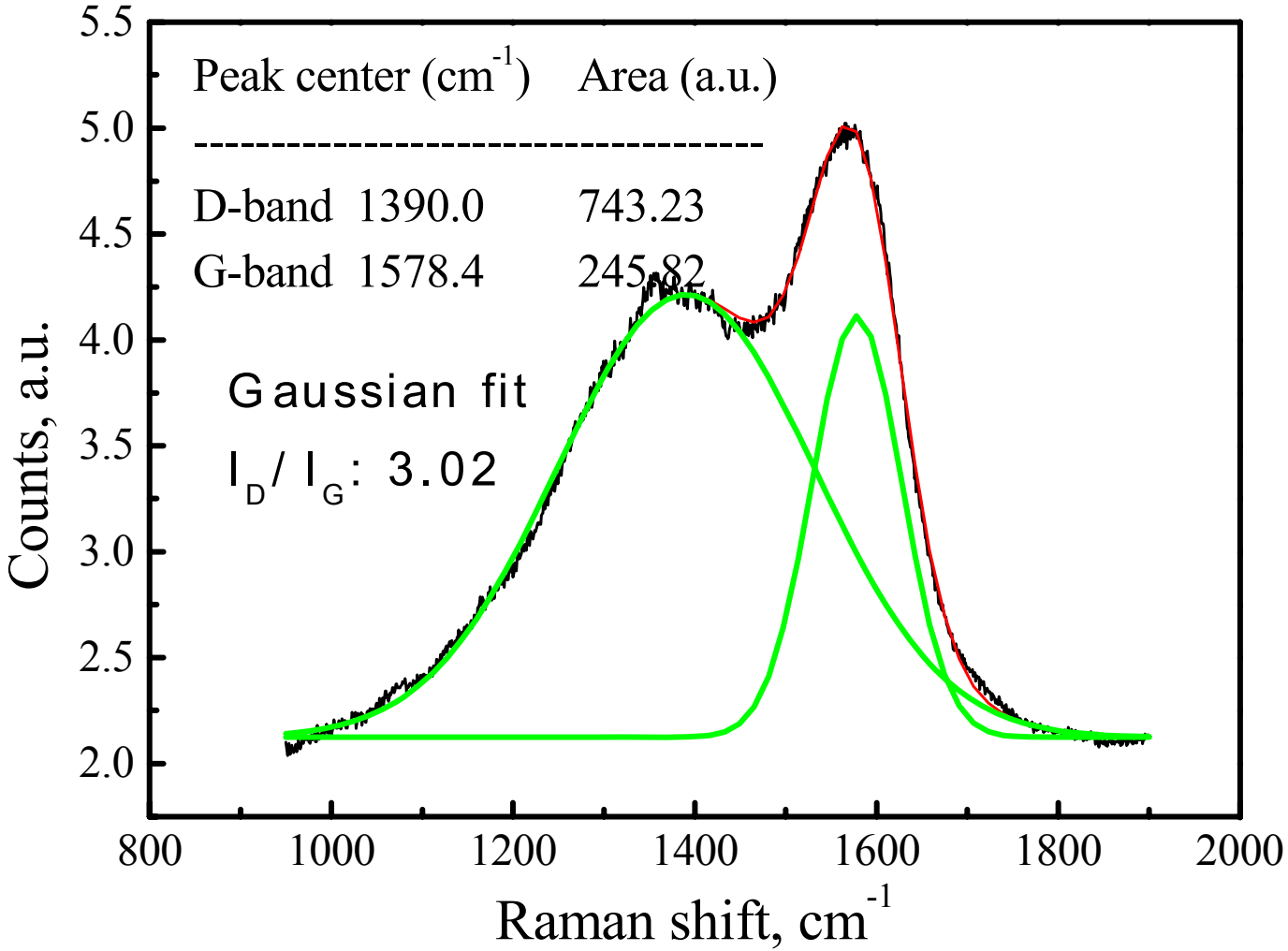

Typical Raman spectrum and Gaussian fit of the 2 peaks assigned asD-band and G-band.

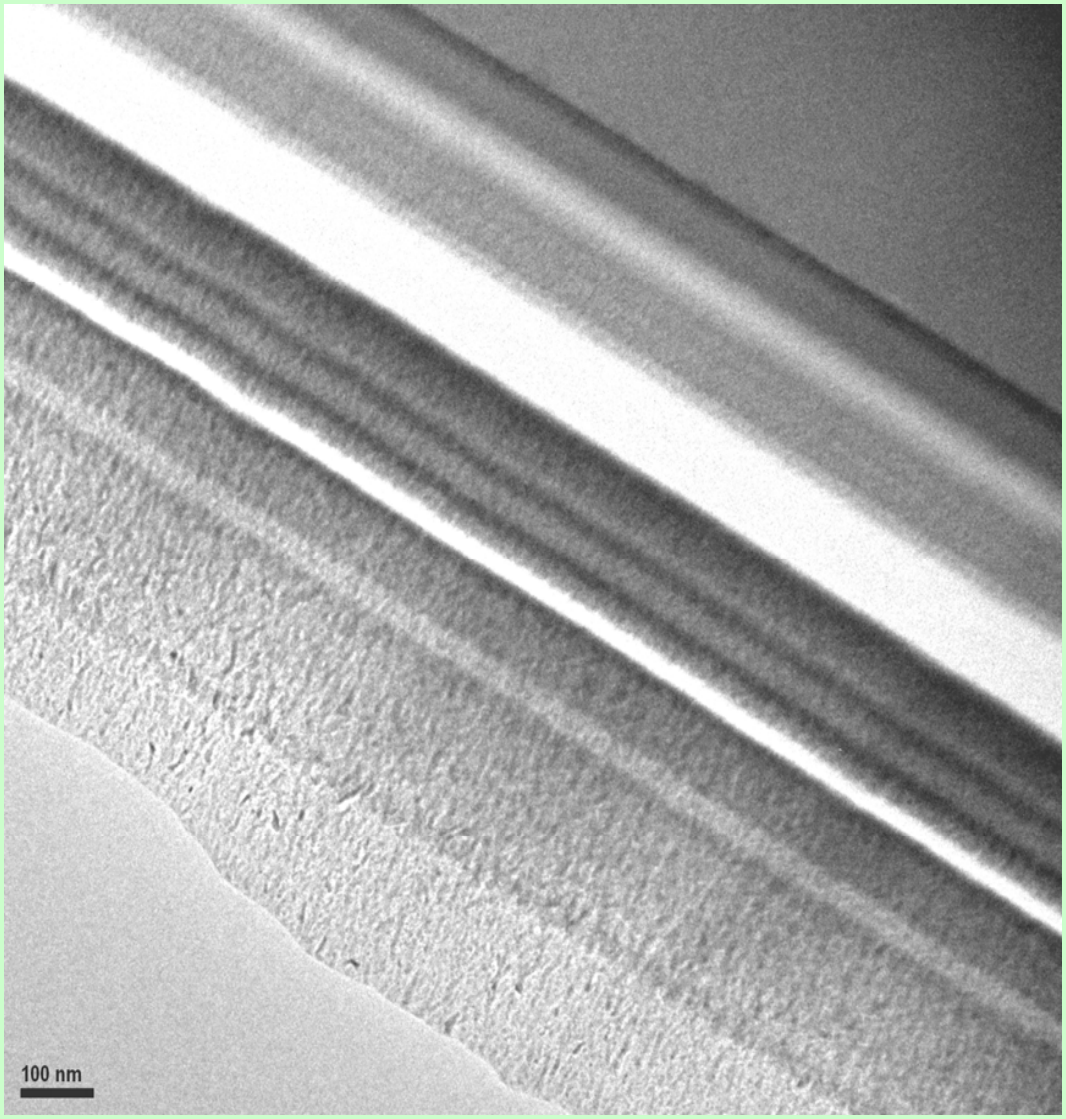

Low magnification image of the whole system (silicon substrate at upper right corner).

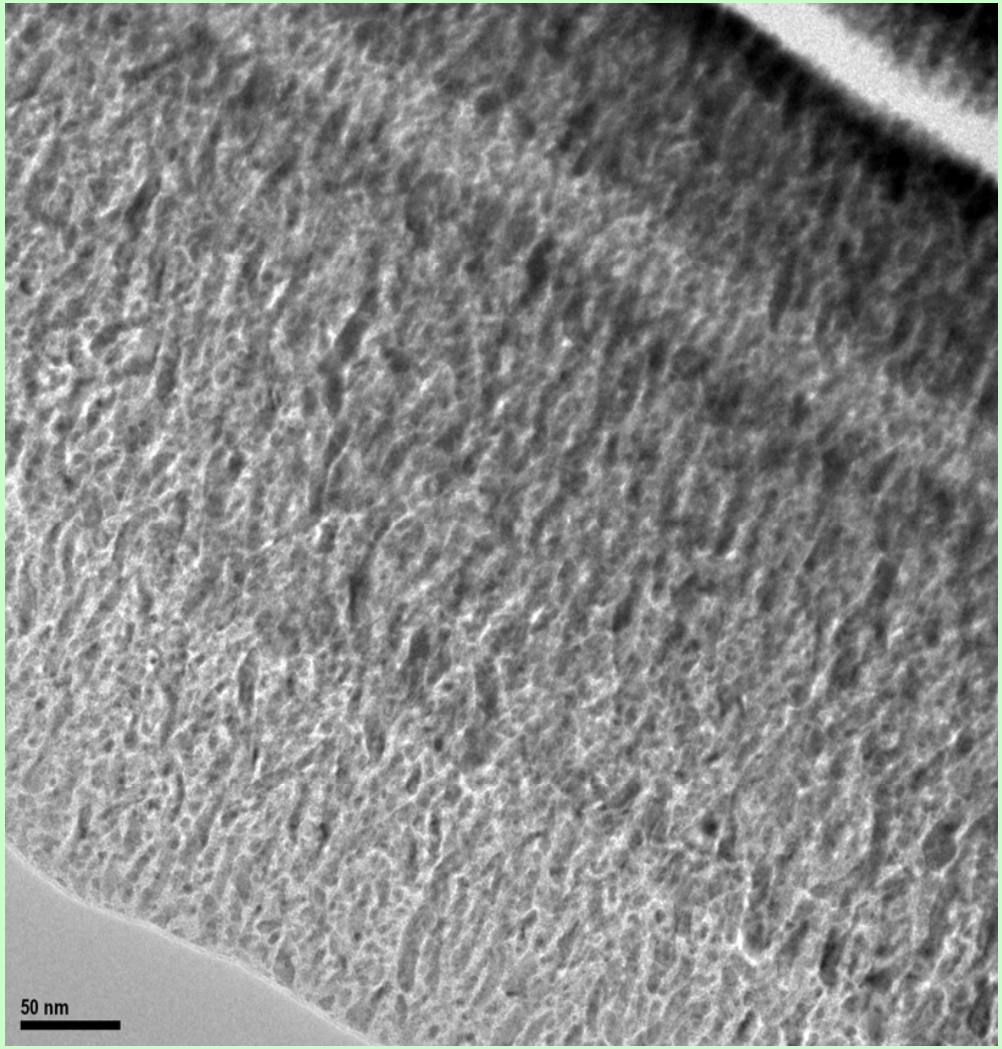

Images of the structure of the upper layer: tubular features with about 10 nm width and 50-100 nm length appear together with small grains with a lateral size of about 5 nm. The mentioned features are surrounded by a brighter matrix.

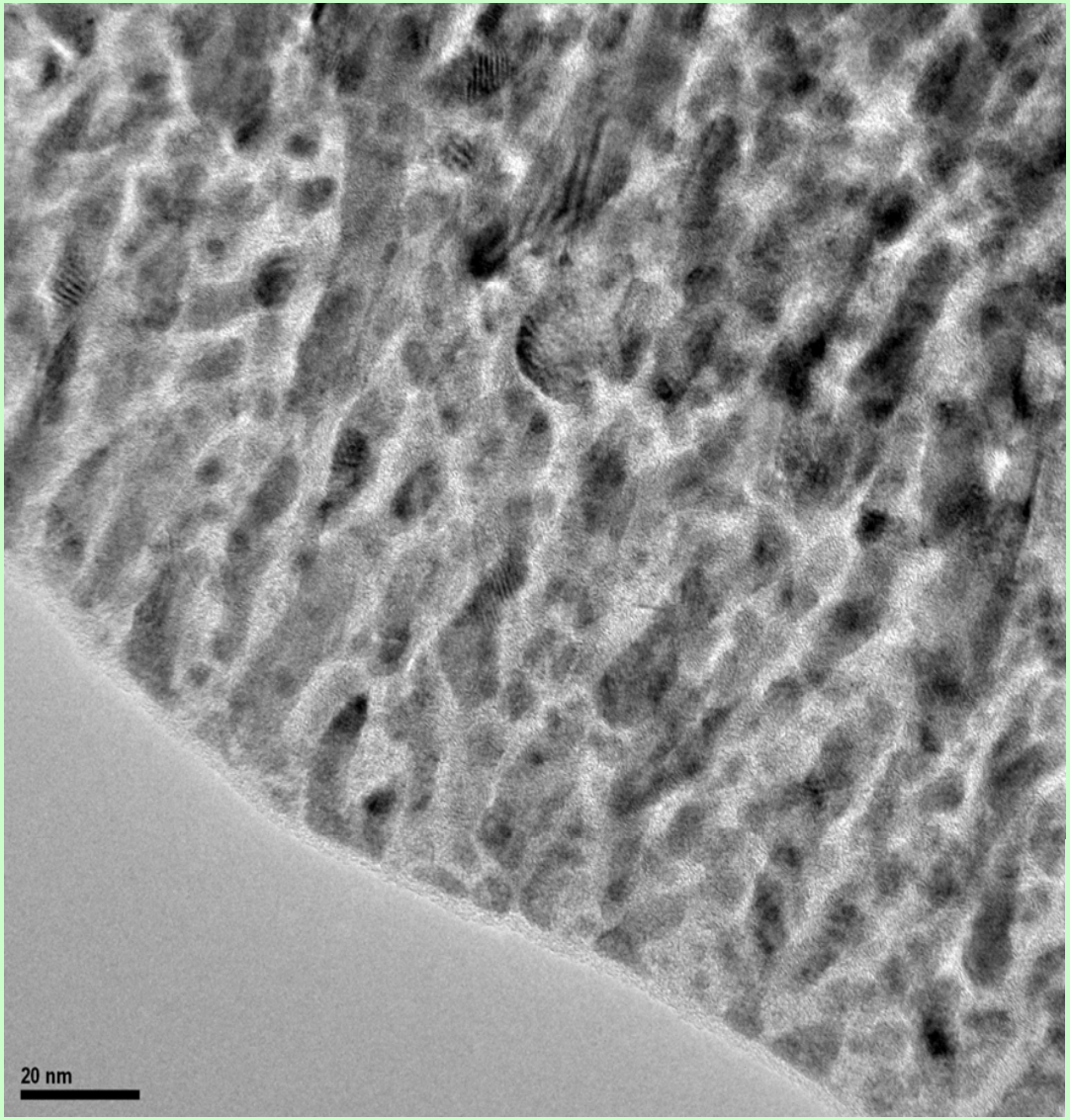

High resolution image of grains in the upper layer: in most of the grains a crystalline structure is visible, while the surrounding matrix is amorphous.

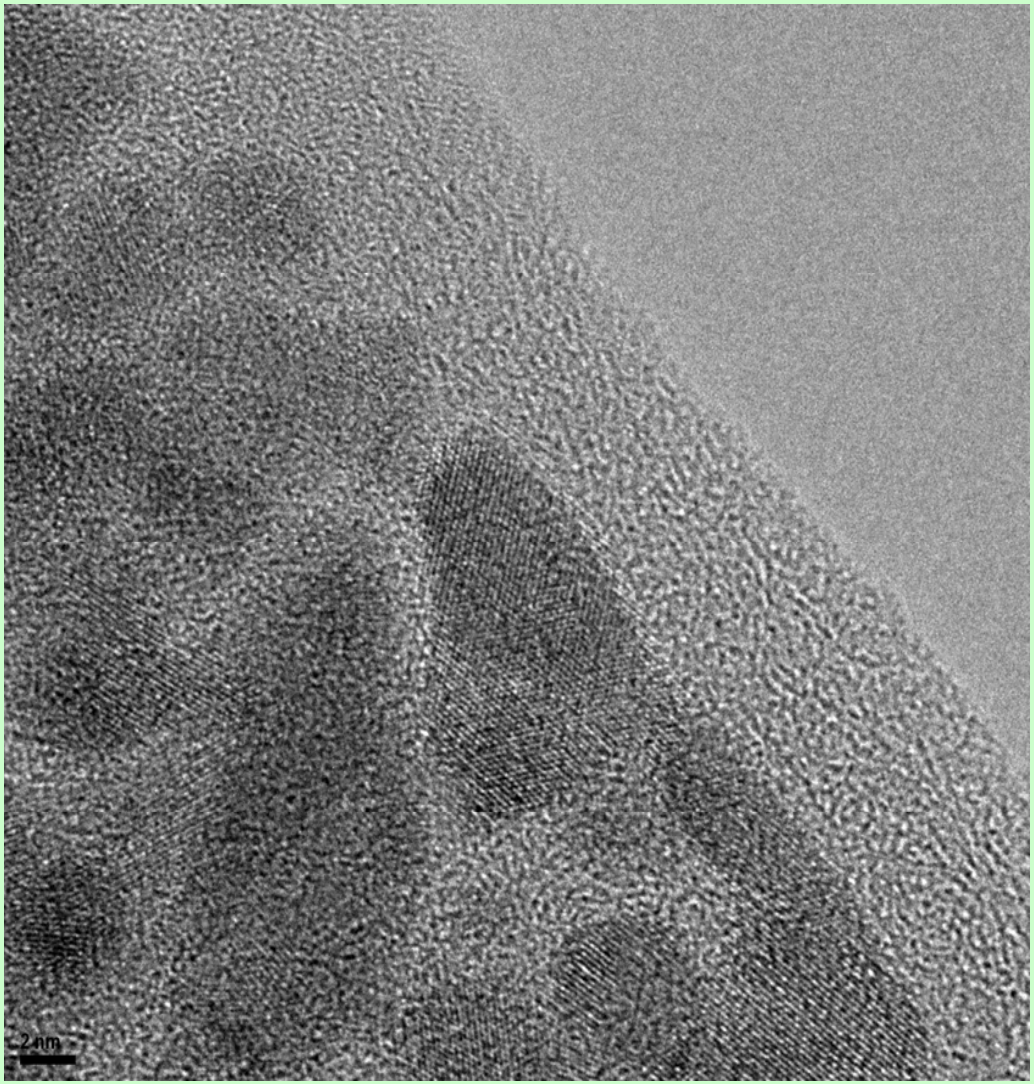

2 nm

High resolution image of grains in the upper layer: in most of the grains a crystalline structure is visible, while the surrounding matrix is amorphous.

W -TEM investigation

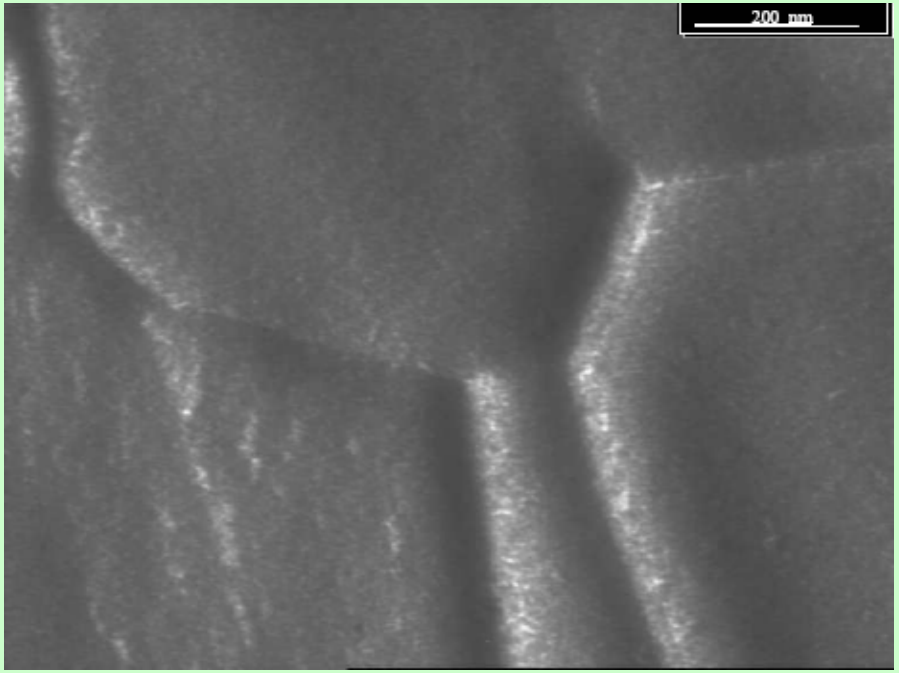

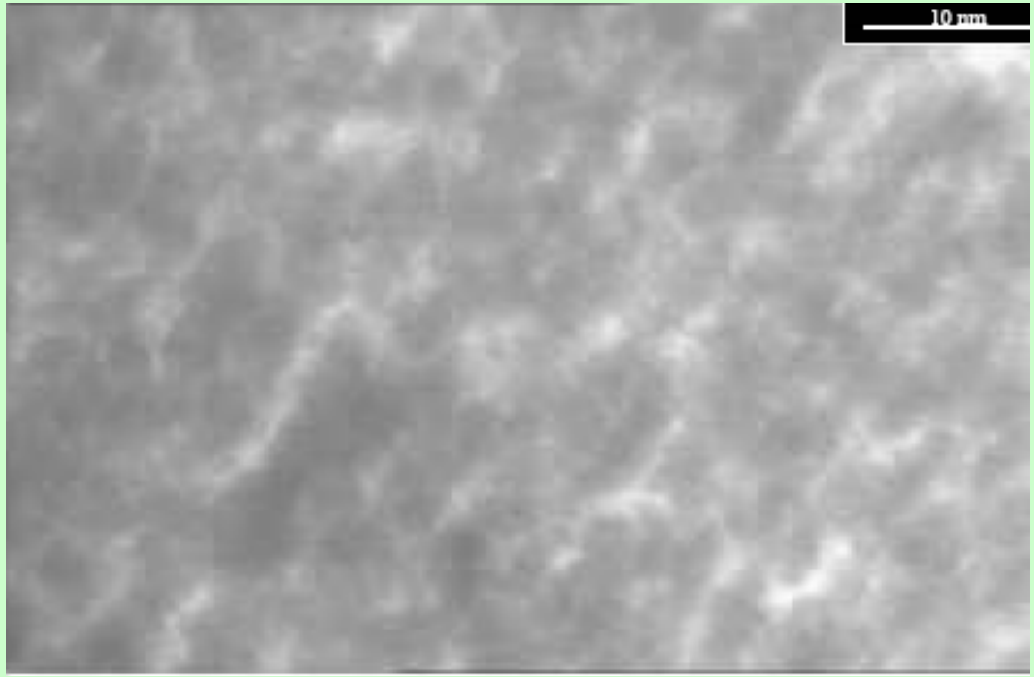

The structure of the deposited W films were studied using TEM electronic microscopy with a magnification of 1.4 M and a resolution of 0.14 nm . The samples of tungsten films deposited on small size NaCl or KCl single crystals have been submitted to TEM examination (after solving the single crystal supports in water). TEM analysis of thin layers (10-20 nm thickness) revealed the nanostructured tungsten film with grain size in the range of 10 nm (left and right). Also in right image one can see clustered tungsten nanoparticles with mean diameters bellow 10 nm.

W-HRTEM AND SAED features

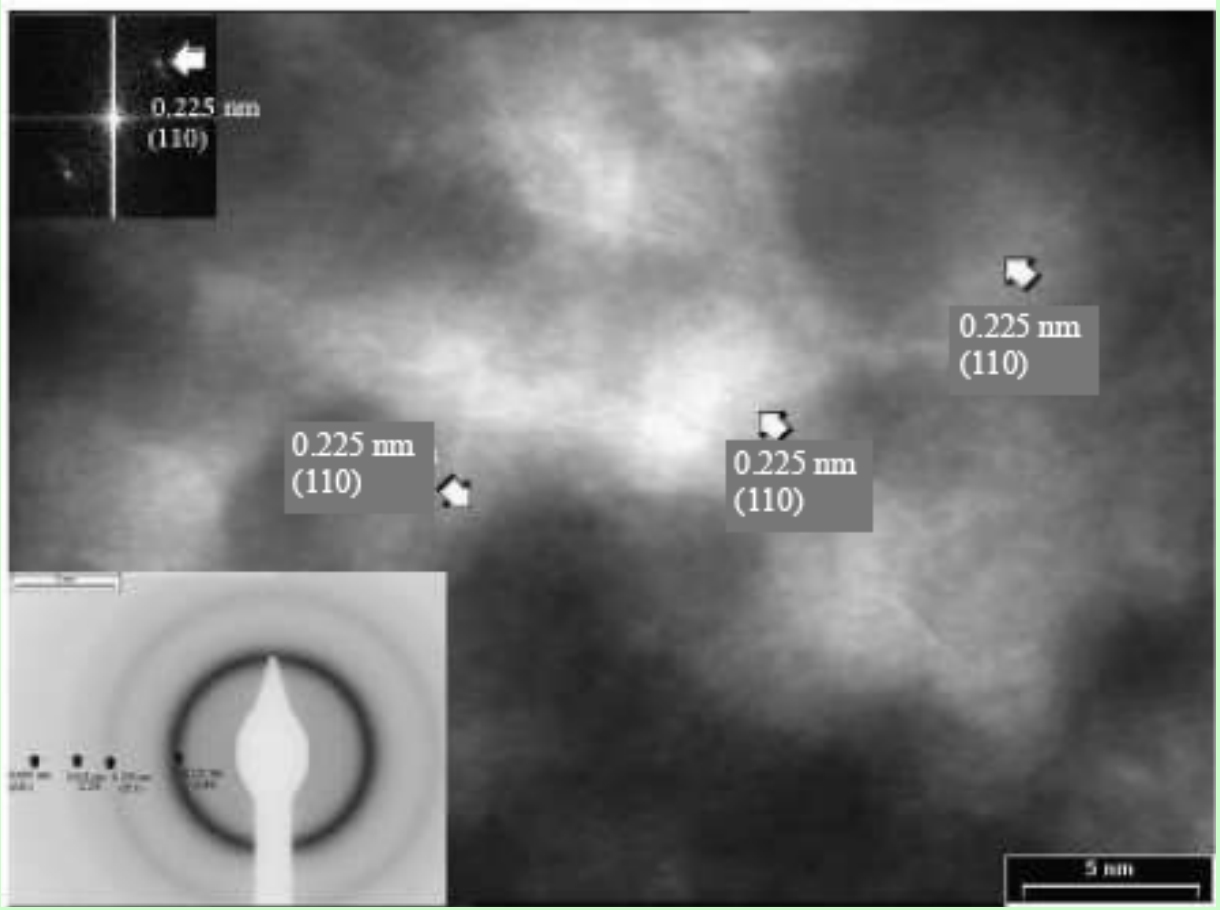

Figure shows HRTEM image of W nanoparticles that exhibits (110) planes. Left inset shows FFT (Fast Fourier Transmission) representation of selected zone. SAED (Selected Area Electron Diffraction) image confirms the cubic structure of W. (SG: Im3m, a = 3.158 nm).

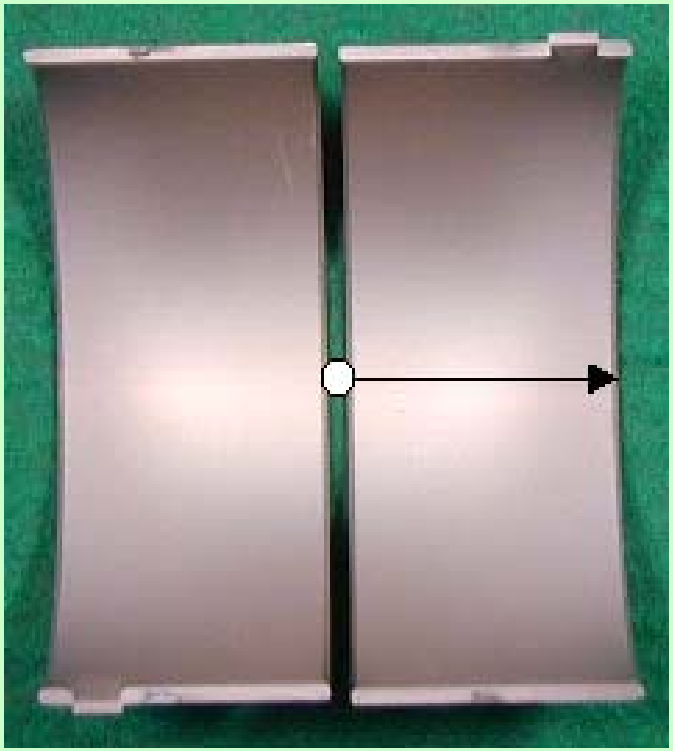

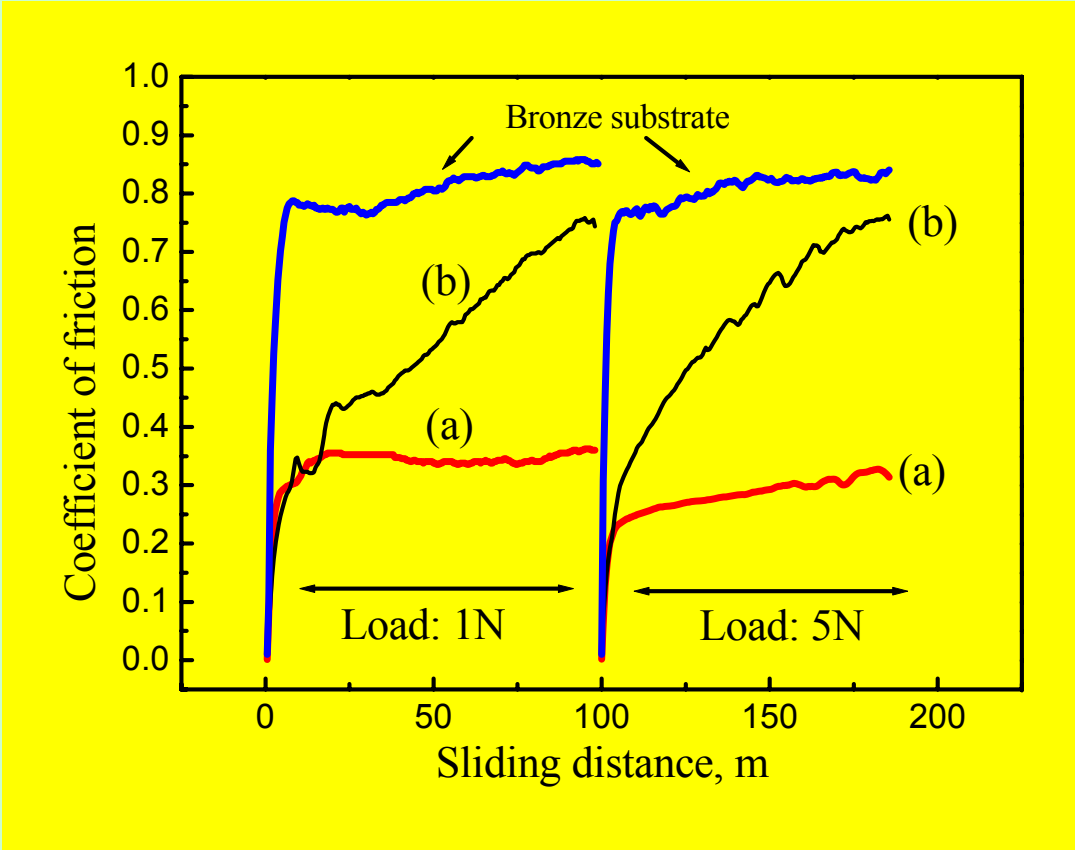

Plain bearings for automotive applications coated with antifriction Ag/DLC overlay

Drastically decrease of the coefficient of friction by increasing the graphite (DLC) concentration in the overlay

sample (a): 44.82 mass%C;

sample (b): 19.27mass%C;

Ag concentration: balance

C-W deposition and characterization

Wear scar on C-W film

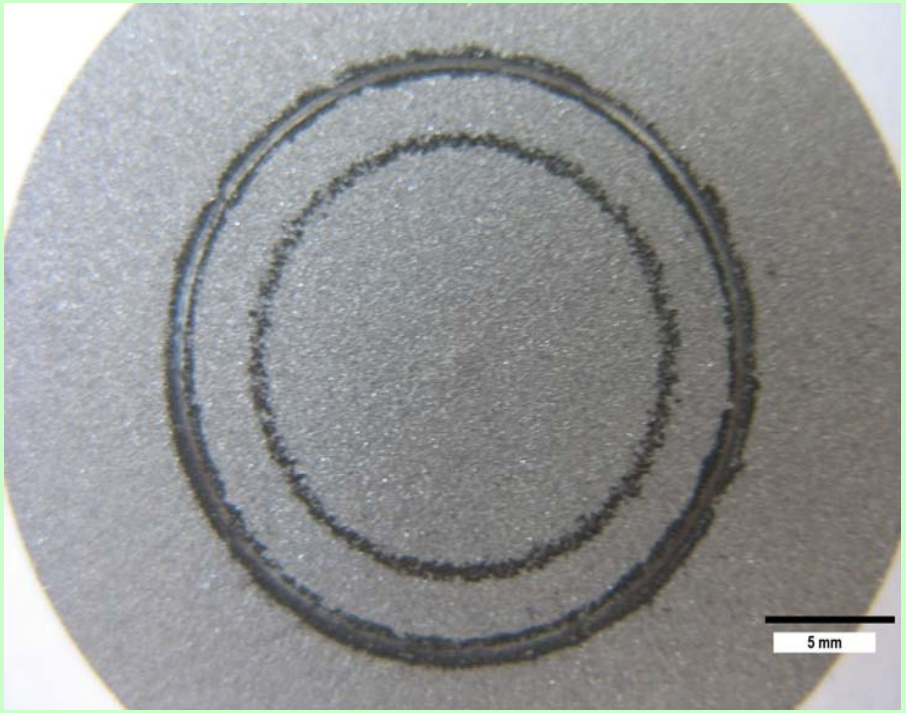

AFM of the wear track

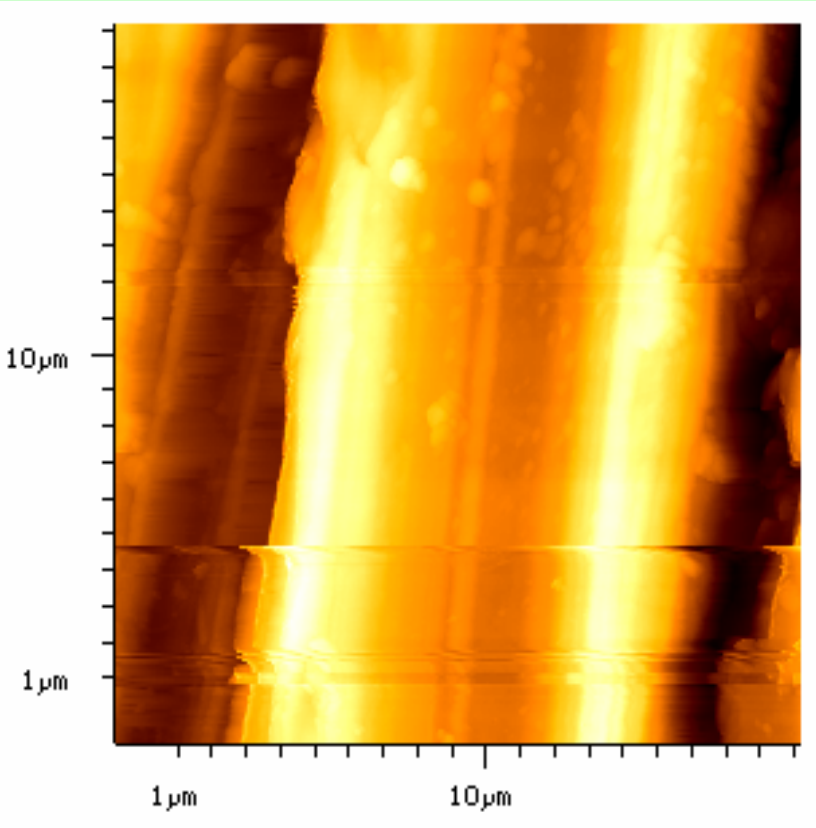

Coefficient of friction C-W

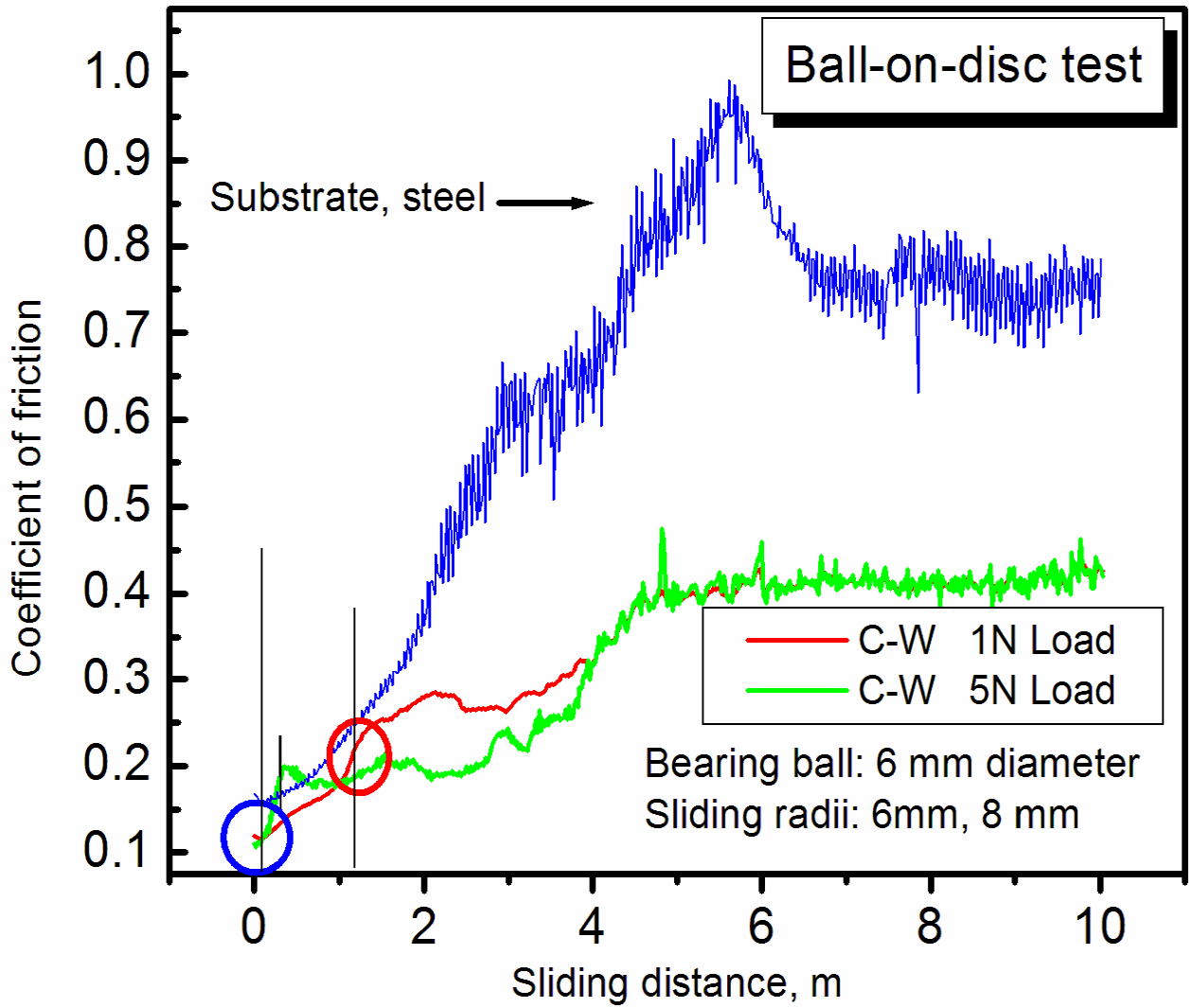

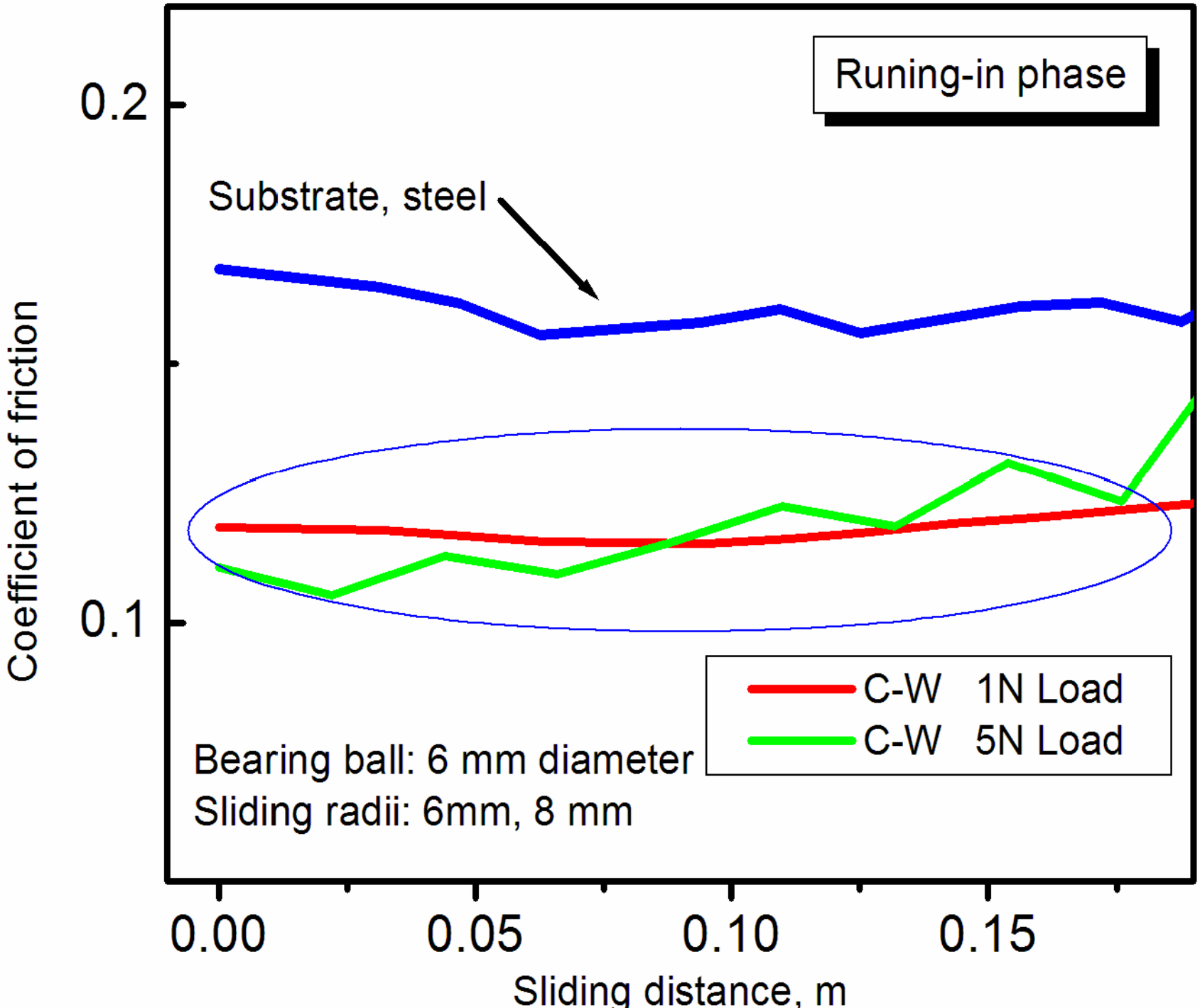
Runing-in phase
Substrate, steel
C-W 1N Load
C-W 5N Load
Bearing ball: 6 mm diameter
Sliding radii: 6mm, 8 mm
Coefficient of friction
0.2
0.1
0.00
0.05
0.10
0.15
Sliding distance, m

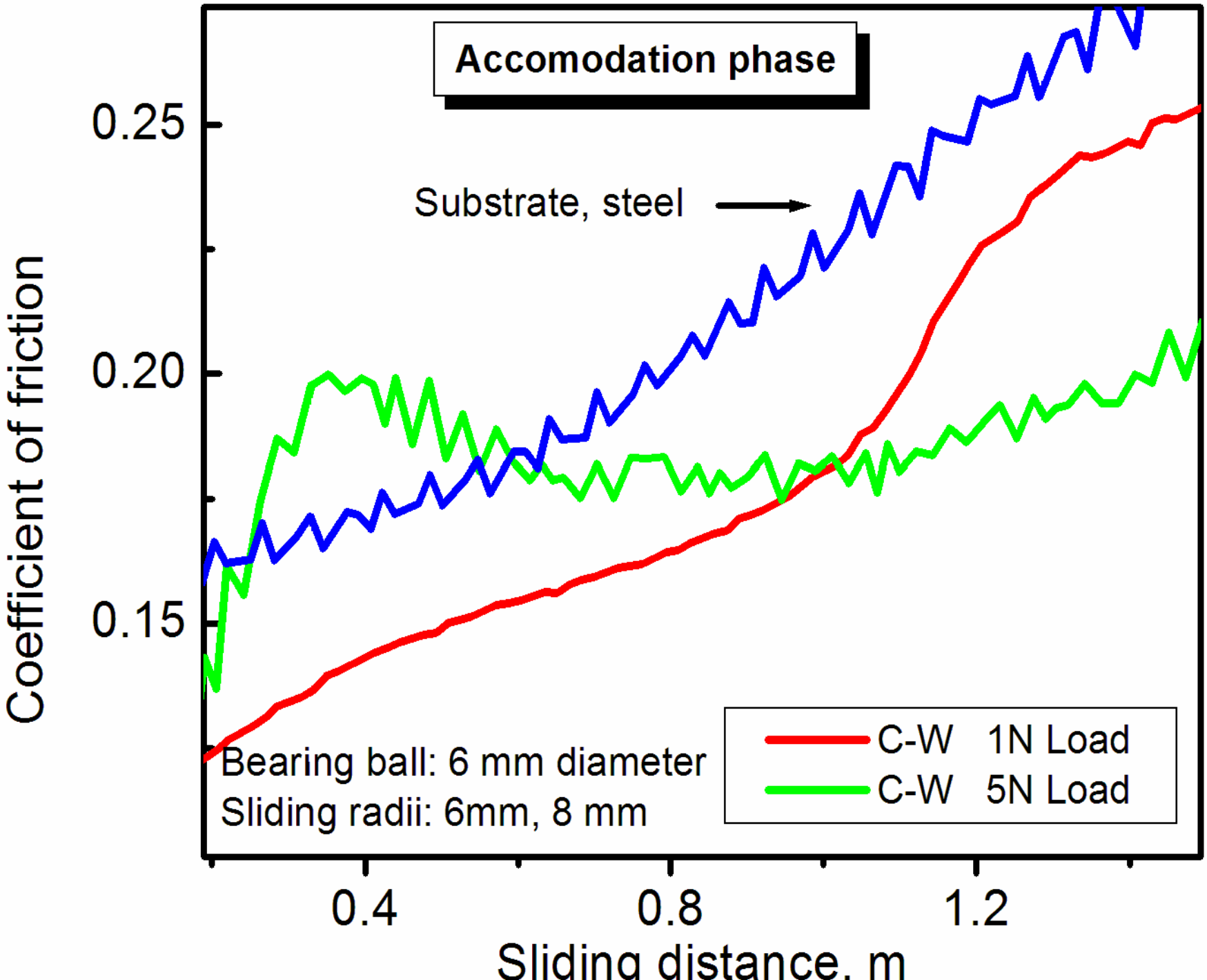
Accomodation phase
Substrate, steel
Coefficient of friction
0.25
0.20
0.15
Bearing ball: 6 mm diameter
Sliding radii: 6mm, 8 mm
C-W 1N Load
C-W 5N Load
0.4
0.8
1.2
Sliding distance, m

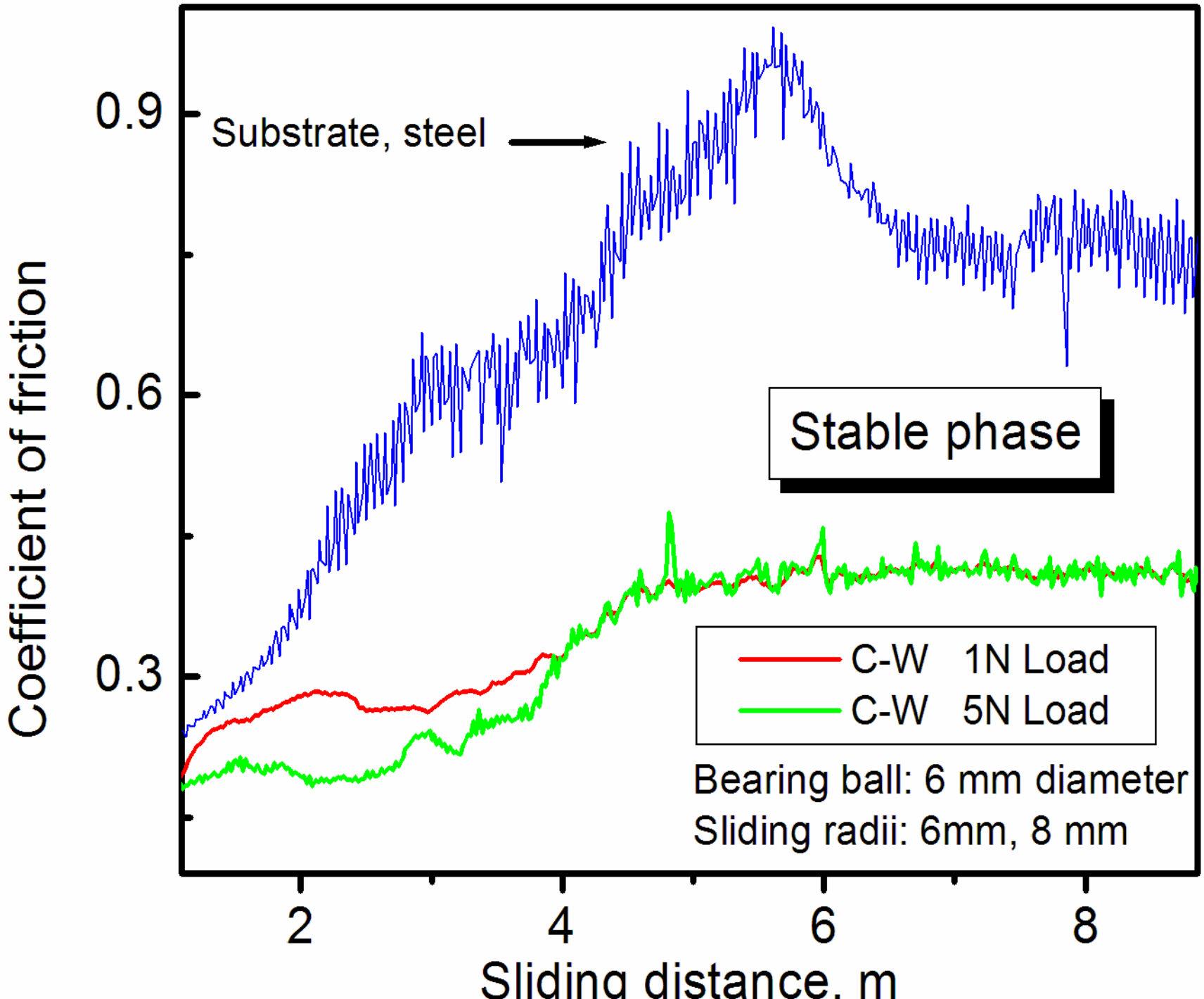
Substrate, steel
Stable phase
C-W 1N Load
C-W 5N Load
Bearing ball: 6 mm diameter
Sliding radii: 6mm, 8 mm
Coefficient of friction
0.9
0.6
0.3
2
4
6
8
Sliding distance, m

Sample	Distance to W rod (mm)	Thickness (μm)	Hardness (GPa)	W (at%)	C (at%)
C-W 1	200	1.4	8	5.2	94.8
C-W 2	220	1.6	11	9.5	89.5
C-W 3	240	1.9	10	15	85
C-W 4	260	2.0	14	20	80
C-W 5	275	2.1	16	25	75

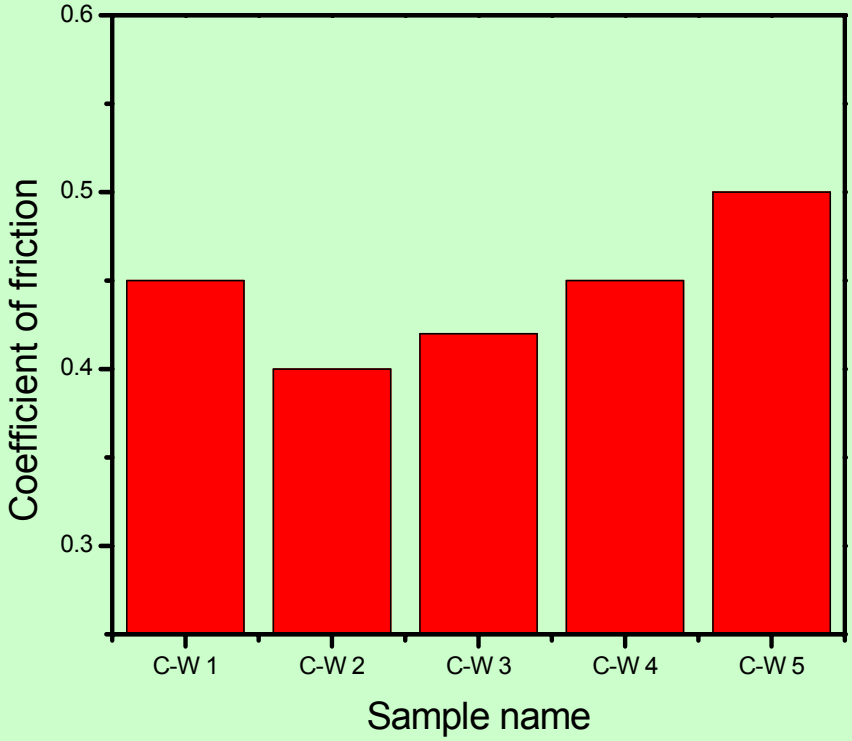

Coefficient of friction C-Ni

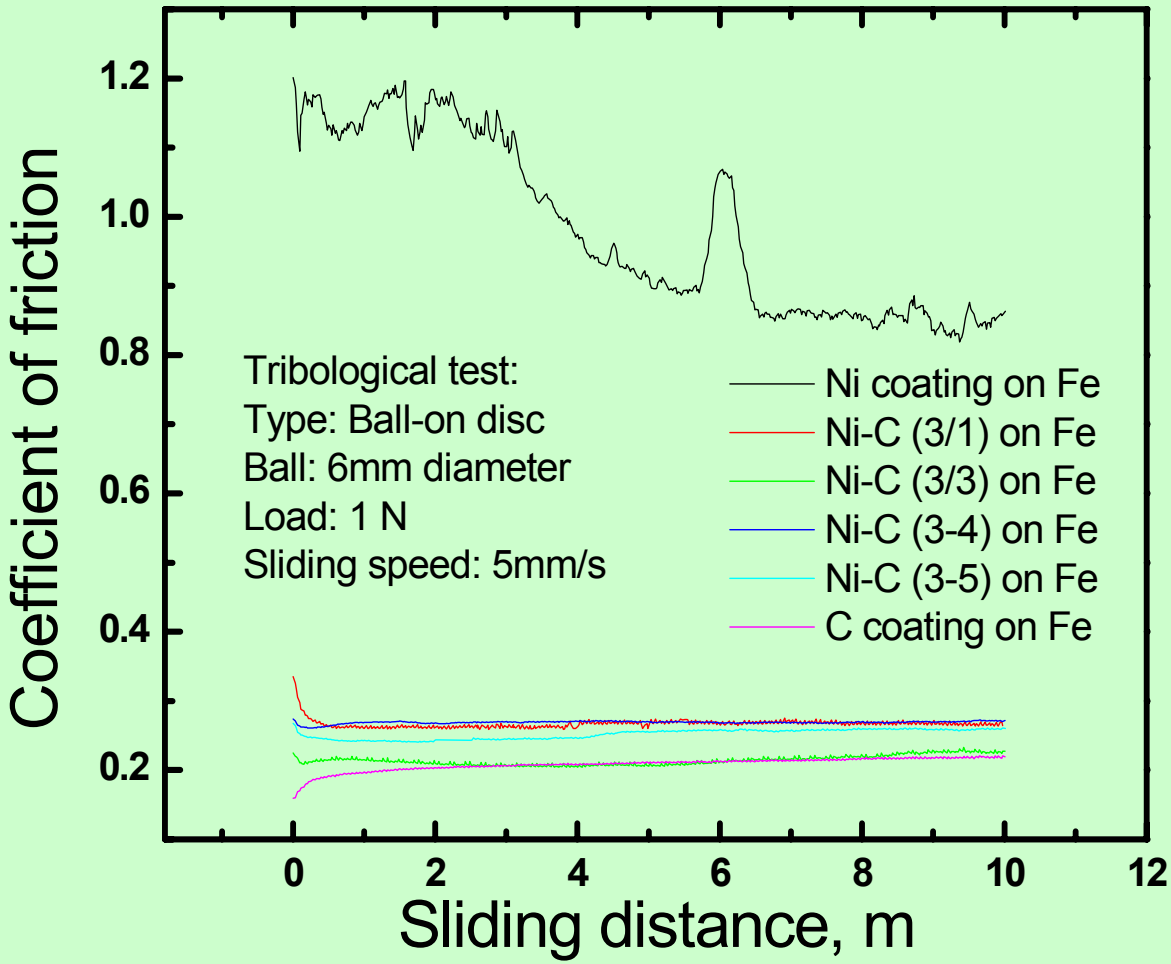

Coefficient of friction C-Ni

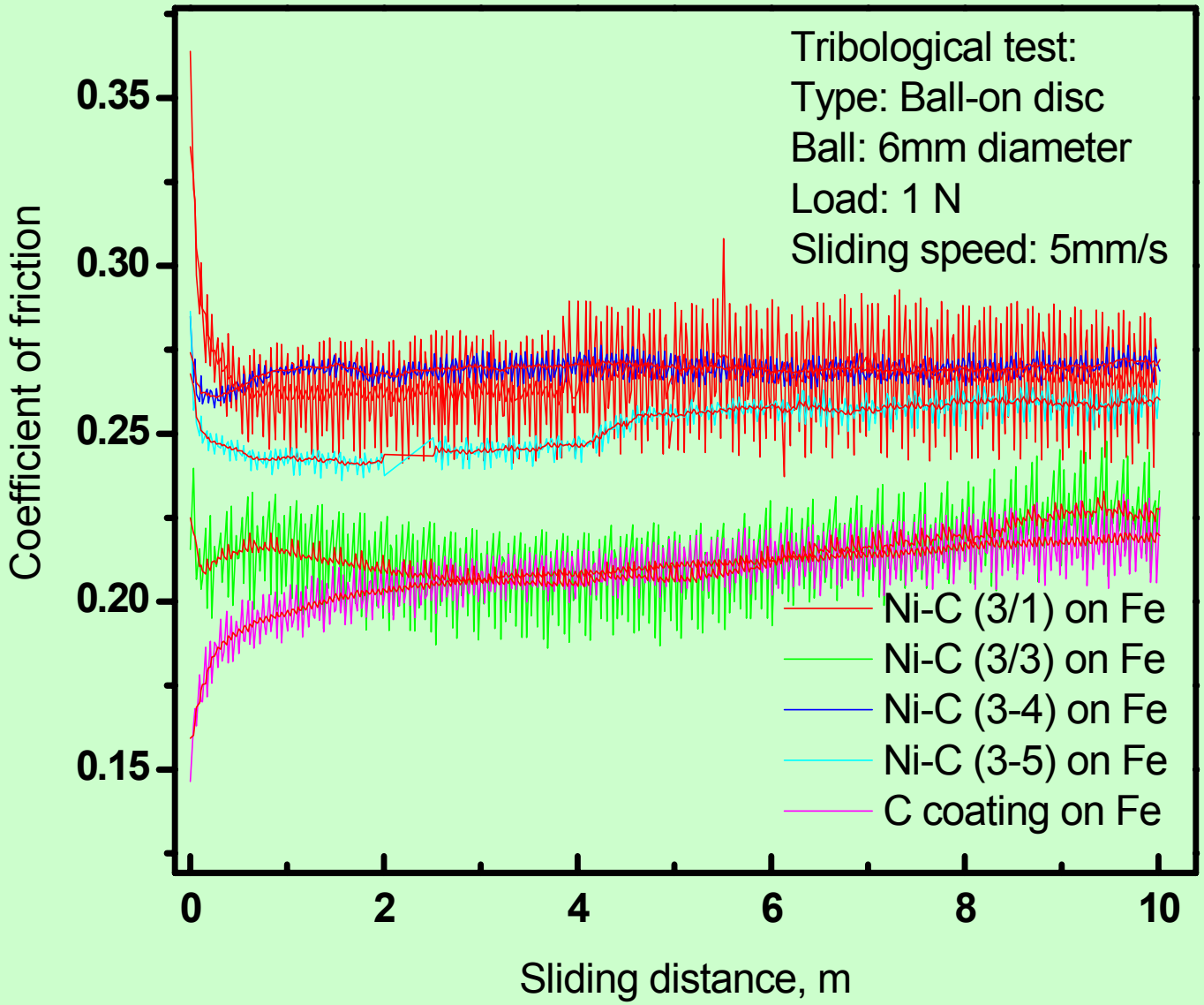

CONCLUSIONS

•The carbon-metal films were identified as a nanocrystals complex (5 nm average diameter) surrounded by amorphous structures with a strong graphitization tendency.

•The Raman spectra showed typically D and G-bands of the amorphous carbon. By XPS were identified C-C (sp^3 bonds) and C=C (sp^2 bonds) depending on process parameters and carbon-tungsten relative concentrations.

•The coefficients of friction of the prepared films were in the range of 0.15-0.25, for C-Ag, 0.15-0.25 for C-Ni and 0.4 –0.45 for C-W, three to five times lower than the uncoated substrates.

GMR FILMS

The GMR effect, discovered in 1986-1988, means the very large change in resistance in a magnetic ultrathin multilayer film. The GMR effect is due to the spin-dependent scattering in thin magnetic multilayer.

Physical properties of the magnetic superlattices:

Very small thickness of the layer (nm range)

- change of the magnetic moment
- surface or interface anisotropy
- low-dimensional effects

Multilayer effects

- interlayer coupling
- exchange interaction

Technological applications:

Magnetic sensors:	- high sensitivity for low fields
Magentic read heads:	- high linear voltage versus field

GMR EXPERIMENTAL RESULTS

The resistance measurements were performed by four point probing method on the Co-Cu, or Co-Ag granular specimens mounted between two magnetic poles of an electromagnet being able to furnish a magnetic filed varying from zero to 1.5 T.

The measurement geometry was of current-in-plane (CIP) type. The magnetic field was in the plane of specimen and perpendicular to the current direction.

The experimentally obtained curves are presented in the following figures:

The GMR effect for an Ag-Co film. I

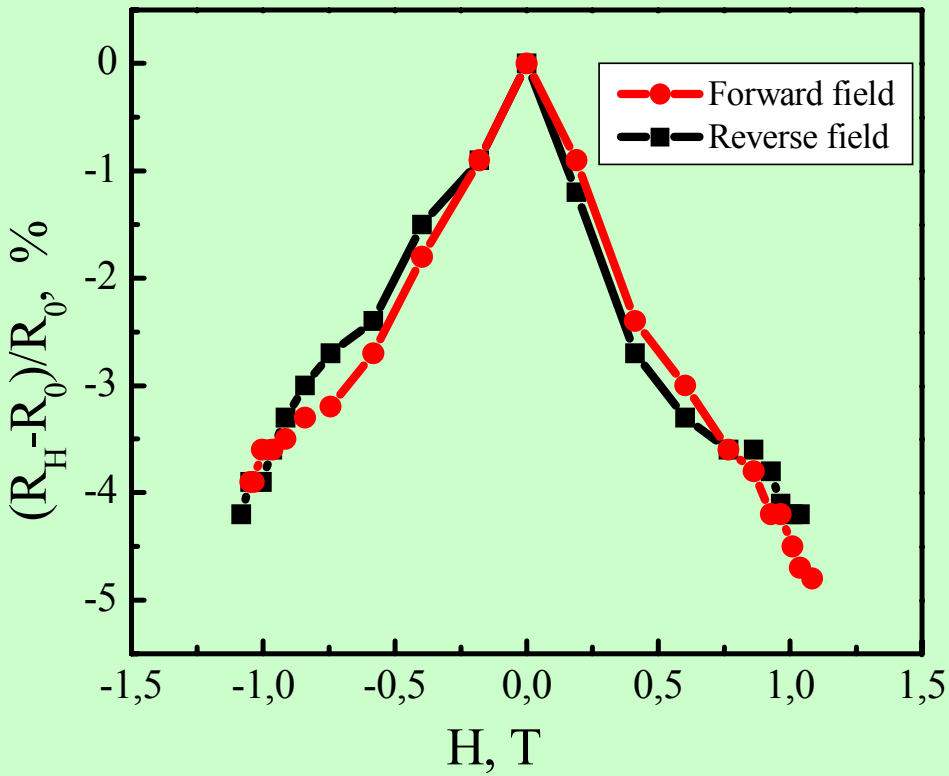

Film thickness: 129 nm.

Deposition time: 6 minutes.

The relatively small curve decreasing along the wings which can indicate a graduate cluster orientation change in the magnetic field due to their different dimensions or to their different interactions with the Cu neighboring atoms.

This film was obtained using: 24 A for both filaments,

Ag case: 200 mA discharge current; 300V; 30 cm distance to anode

Co case: 600 mA discharge current;1900 V; 34 cm distance to anode

The GMR effect for an Ag-Co film. II

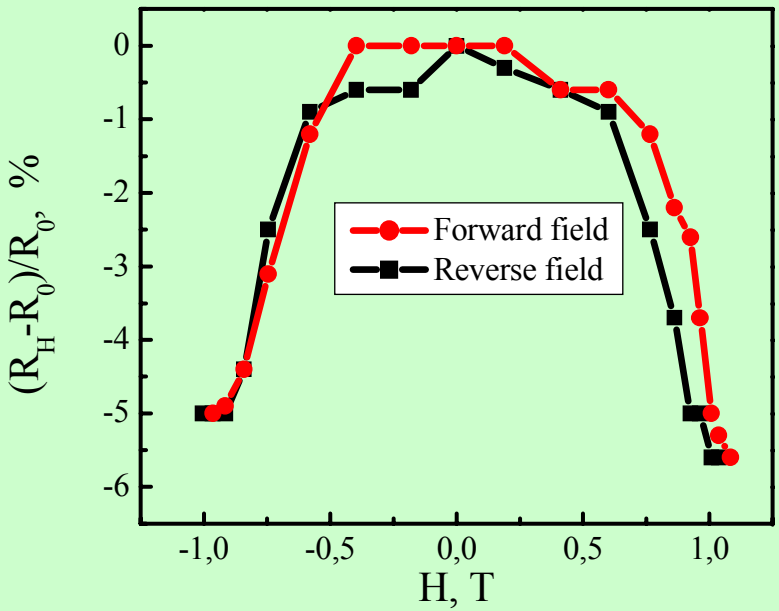

Here we can also find out a small difference between the two curves corresponding to the two different magnetic field variations.

The wing variations are more rapid in this case indicating a more uniform distribution of the formed cobalt clusters during the deposition. (all clusters magnetic moments are aproximately of the same magnitude and it makes possible to change their orientation at the same magnetic field intensity.

The GMR effect exhibited by a Ag-Co specimen prepared in the same experimental conditions as the specimen presented in the former figure but having other position, namely 30 cm from the Co crucible and 34 cm from the Ag one.

The position of the specimen can determine very different GMR effect. In this case the maximum GMR effect was 5.5% that is greater than in the case of the sample characterized in the former figure.

The GMR effect for an Co-Cu film. I

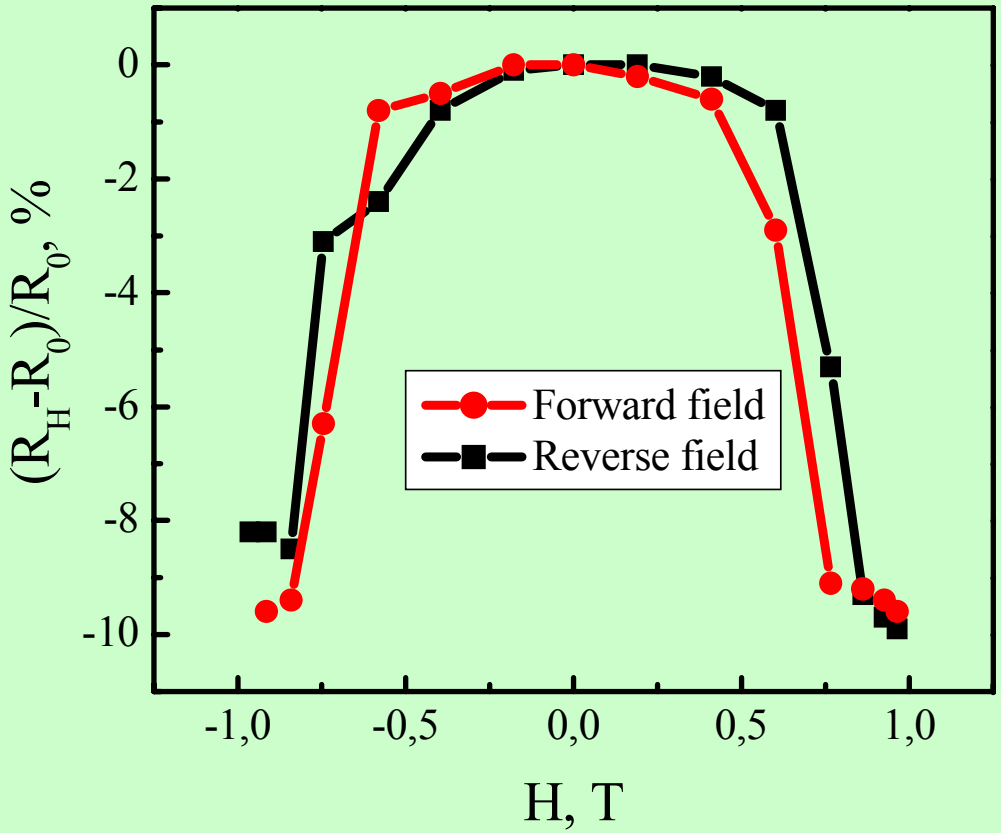

Total thickness: 404 nm

Deposition time: 10 min.

The specimen was not thermally treated after deposition.

The maximum GMR effect was greater in this case, namely of 10%.

This film was obtained using: 24 A for both filaments,

Cu case: 240 mA discharge current; 600V; 26 cm distance to anode

Co case: 250 mA discharge current;1550 V; 26 cm distance to anode

The GMR effect for an Co-Cu film. II

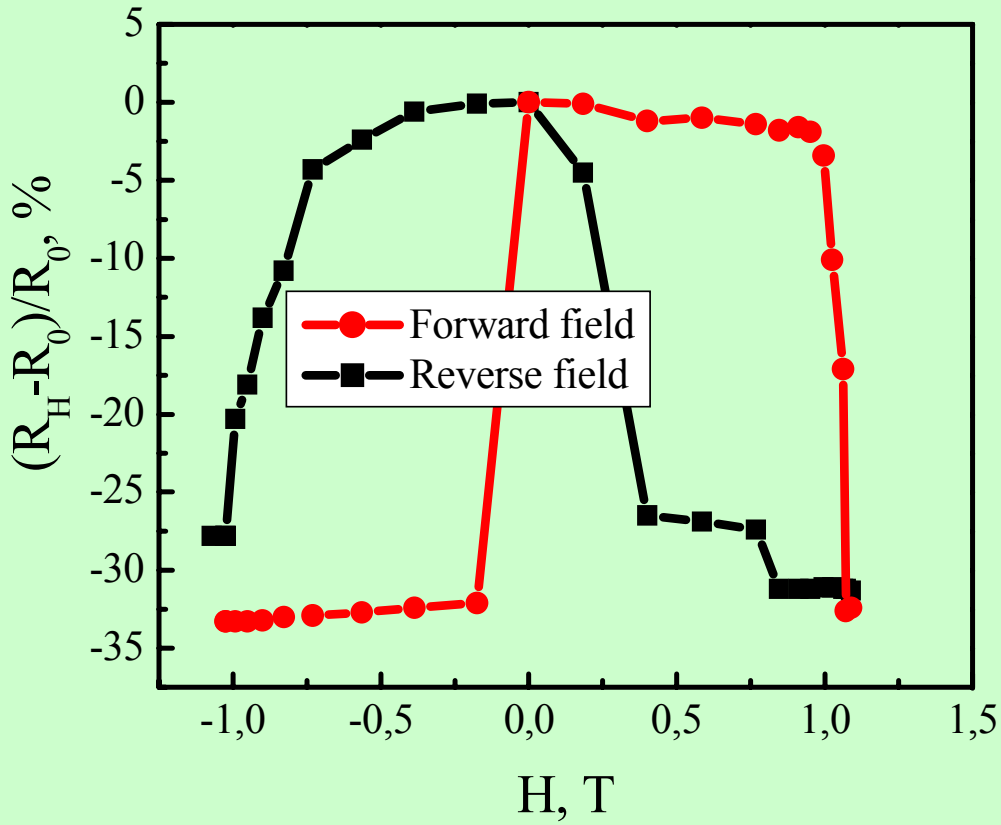

The wing gradients are very sharp and of the great values.

The maximum GMR effect of the Co-Cu specimen post-deposition treated being in this case **33%.**

Co-Cu specimen, thermally treated, (450 ^{0}C for 60 minutes) prepared in the same conditions as the former specimen. The specimen was positioned 24 cm from Co crucible and 32 cm from Cu crucible, therefore closer to the Co source than the former specimen.

One can directly observe a great difference between forward and reversed field variation this indicating a great **coercitive magnetic force**.

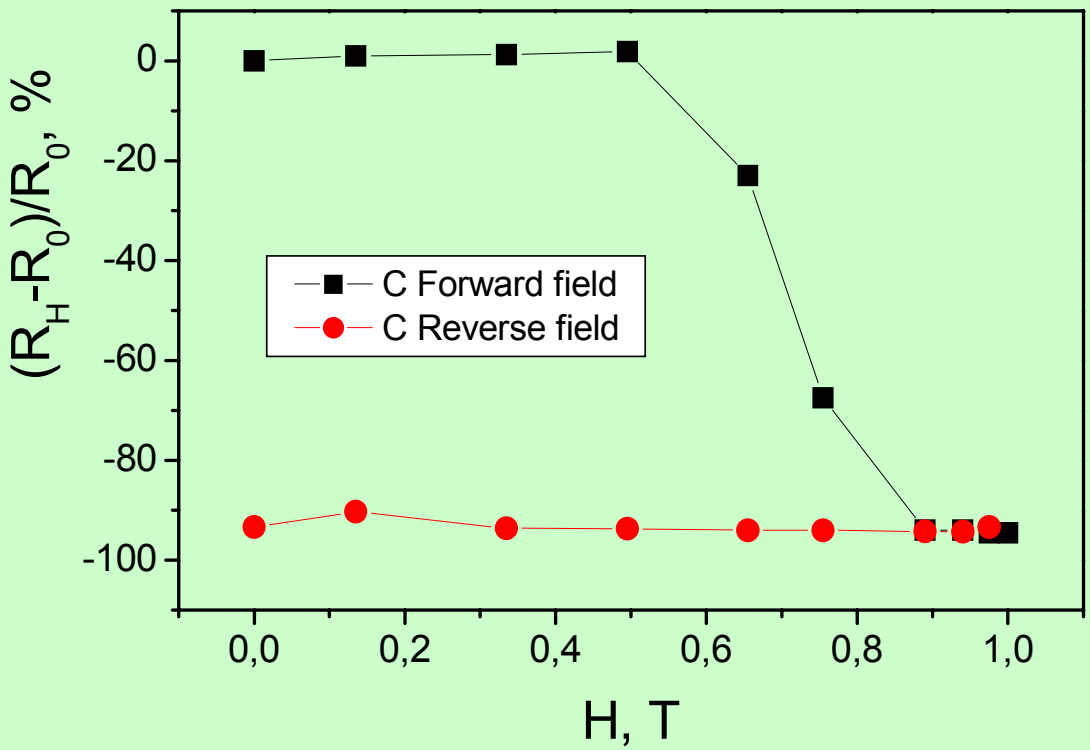

- **The GMR effect attains very high values of 94% having very great variation.**
- **Its resistance once decreased remains as such even for zero magnetic fields (does not increase).** That means that the magnetic clusters are so strongly coupled with one another that they remain parallel oriented for ever, no matter the magnetic field value is. This property could be used in reading magnetic heads manufacturing where one layer must remain constant in orientation for low magnetic fields.

Coatings for fusion technology applications

Beryllium Coatings on Metals:

Development of Process and Characterisation of Layers

Optical emission spectroscopy diagnostic of Be plasma

TVA plasma in pure berylllium vapors

OES acquisition system: quartz lens, optical fiber, SM242 Spectrometer, PC.

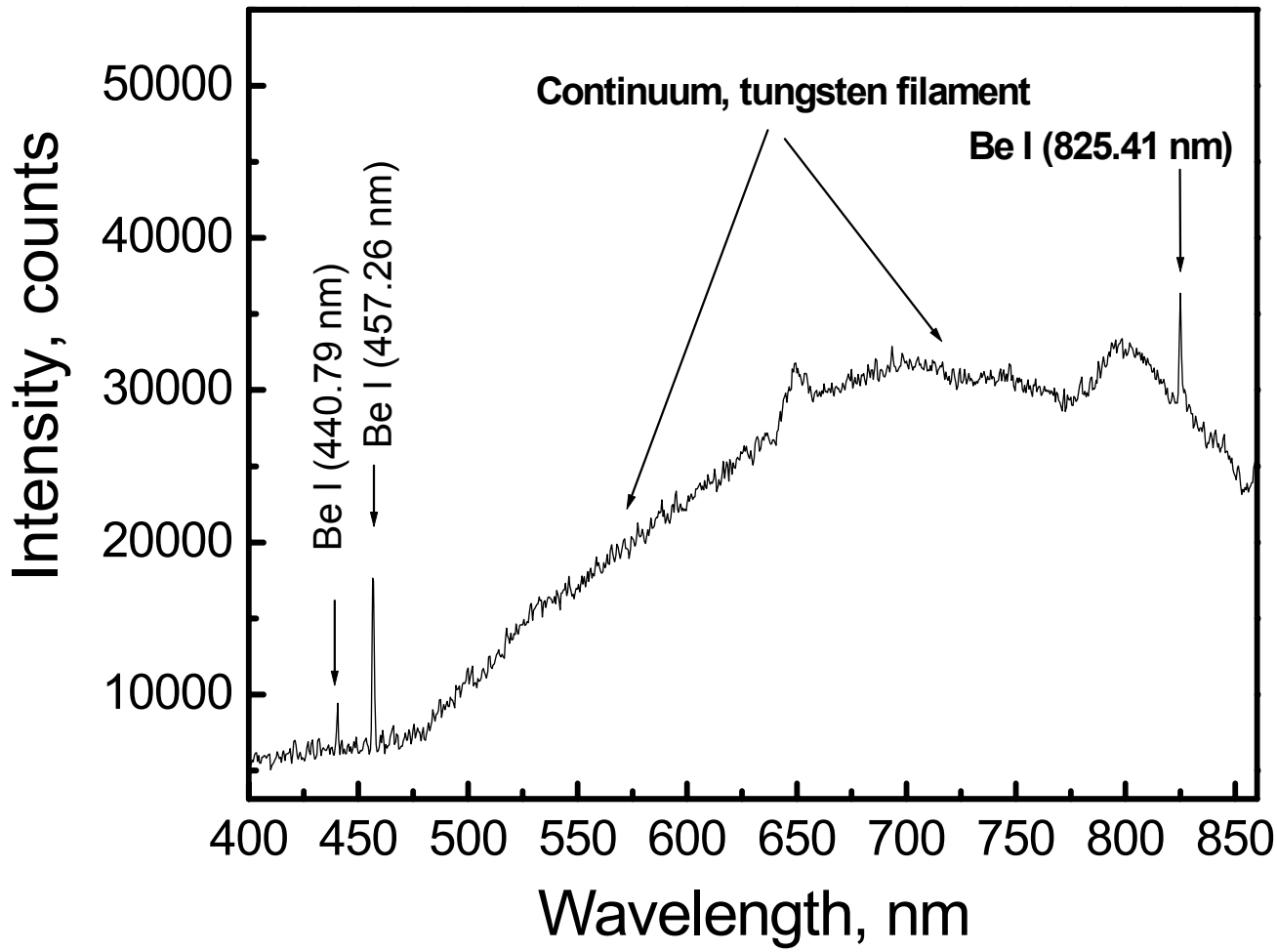

Typical emission spectrum of beryllium plasma

Electron temperature

Assuming PLTE, and $kT_e \ll E_u$:

$$T_e = \frac{-(E_1 - E_2)/k}{\ln\left[\frac{I_2 A_1 g_1 \lambda_2}{I_1 A_2 g_2 \lambda_1}\left(\frac{E_2}{E_1}\right)^{1/2}\right]}$$

-indexes 1, 2 refer to the two spectral lines;
-E_1 and E_2 are the upper level energies
-g_1 and g_2, statistical weights
-A_1 and A_2, transition s probabilities,
-λ_1 and λ_2 are the spectral lines wavelengths,
-I_1 and I_2 the measured lines intensities.

Electron temperature estimation

Be I wavelength (nm)	Transition probability (s^{-1})	Statistical weight	Energy of the upper level (eV)	Measured intensity (counts)	T_e
λ_1 = 457.266	A_1 = 7.9 E+7	g_1 = 5	E_1 = 7.98809	I_1 = 14086 I_1' = 10379	T_e = 7960K T_e' = 6620K
λ_2 = 825.406	A_2 = 3.8 E+7	g_2 = 1	E_2 = 6.78809	I_2 = 7257 I_2' = 3502	T_e = 0.686 eV T_e'= 0.571 eV

Process optimization:

- The kind of material to be used for crucible
- Glow discharge cleaning
- Anode-cathode distance
- View angle for the sample
- Electrical parameters of the discharge
- Deposition rate.

The viewing angle

The substrates were settled at distance of 150 mm from the anode, on a holder in contact with a hot plate of 150 mm x 200 mm. The view angle was chosen as the samples to be settled at the viewing angles between 20 and 50 degree from the horizontal line.

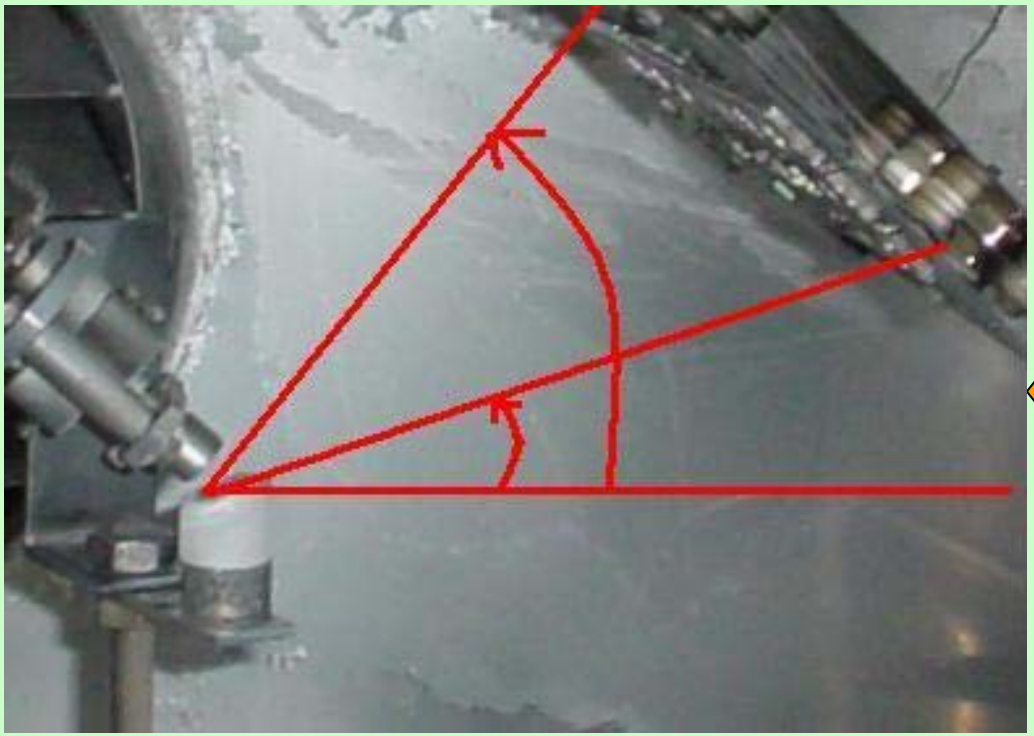

Typical arrangement used for Be depositions

NEW CATHODE-ANODE CONFIGURATION

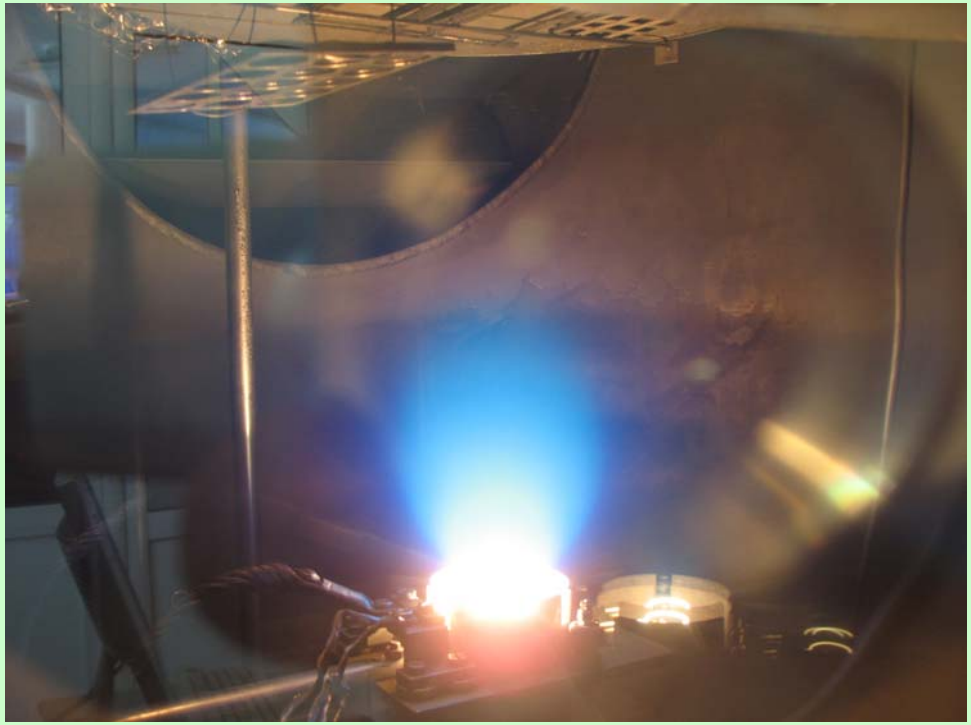

Electrical parameters of the discharge

Optimum electrical parameters of TVA discharge for Be deposition (compared with those of W and Ni) were found to be:

Material	Discharge Voltage	Discharge current
Be	**850 ± 250 V**	**450 ± 20 mA**
W	1500 ± 250 V	1000 ± 100 mA
Ni	1200 ± 200 V	800 ± 100 mA

Deposition rates

Using optimized parameters, deposition rate was found to be
5 ± 0.5 nm/s for Be,
1 ± 0.5 nm/s for W and
2 ± 0.5 nm/s for Ni.

Be film characterisation

- RBS
- Auger
- XRD
- WDS
- AFM
- SEM
- Adherence
- Micro-radiography

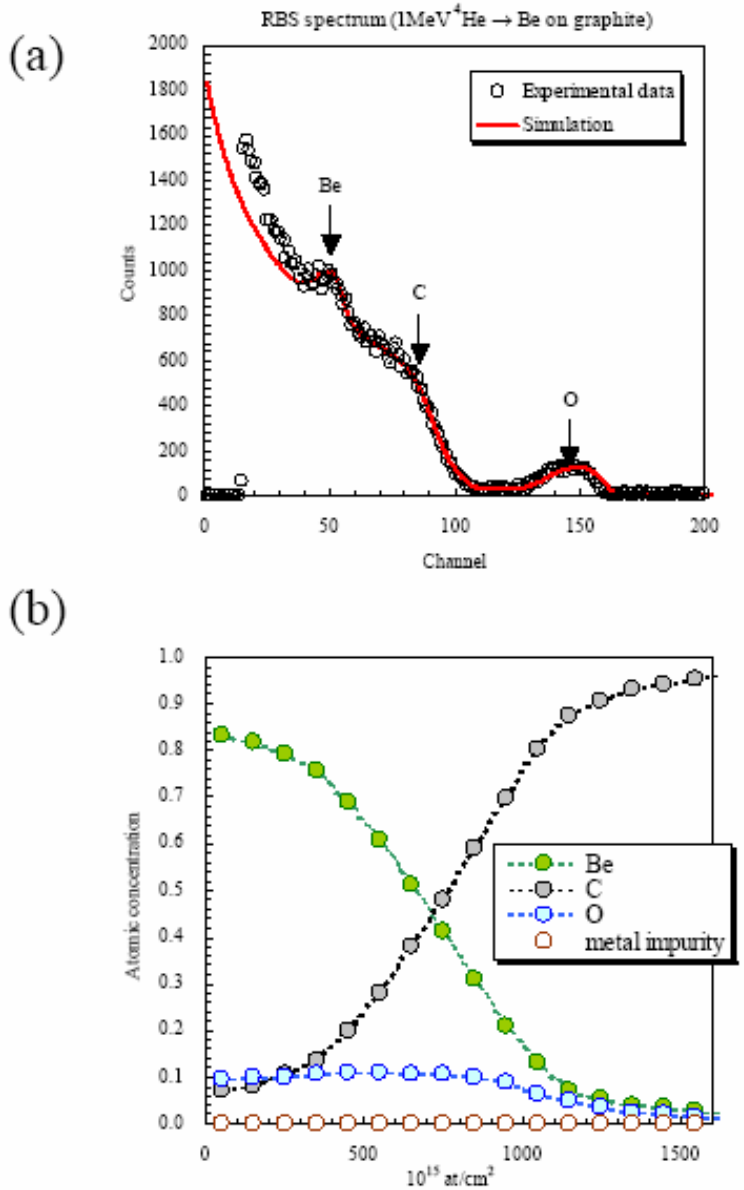

Fig. (a) the RBS spectrum obtained from 2-GR-1. (b) depth profiles of each element calculated from the RBS spectrum by using SIMNRA program.

RBS

1 MeV ^{4}He ion beam to obtain the Rutherford Backscattering Spectrum from the sample surface.
Be on graphite
Peaks: Be, O in the film and C substrate.

Oxygen content ~10 at% through the layer

RBS analysis performed by K.Sugiyama

Auger analysis

O: 6.33%, C: 4.7%, Be:89.97%

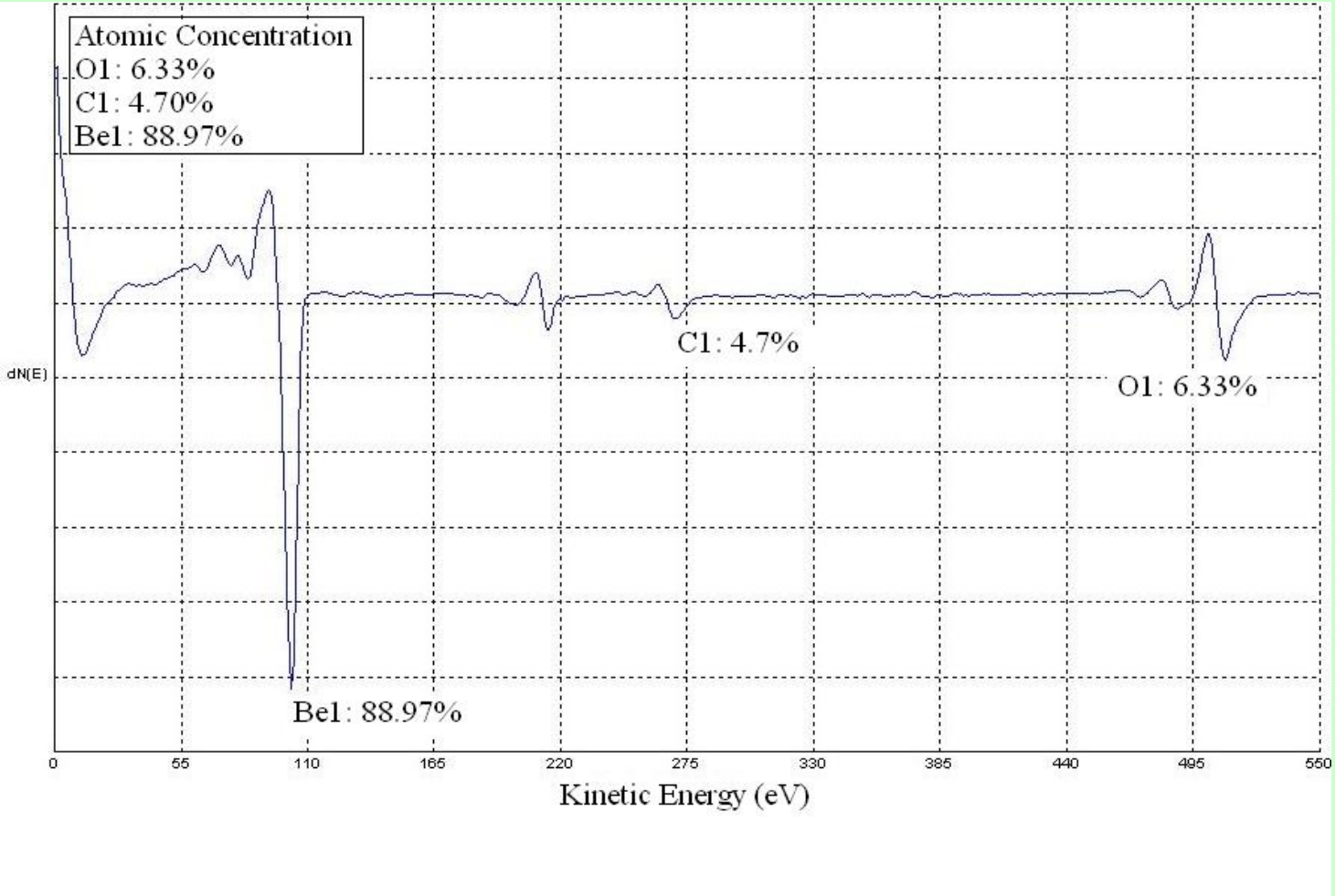

PHI-Perkin Elmer model 3017 Auger spectrometer

(Kinetic energy range; 0-3200 eV, resolution; 0.6%)

XRD

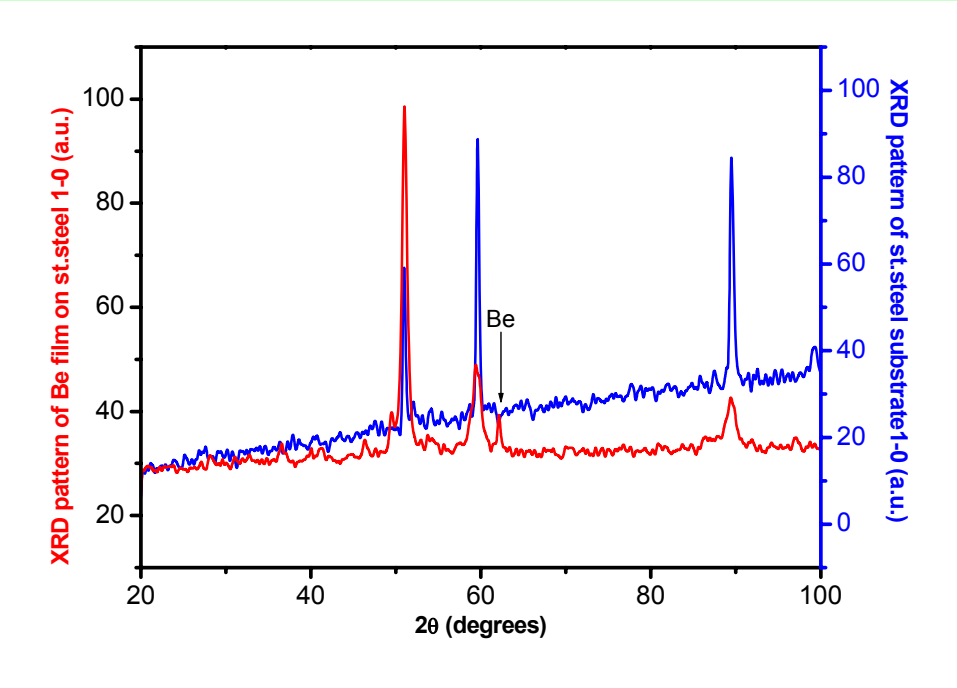

XRD pattern of Be coating on stainless steel

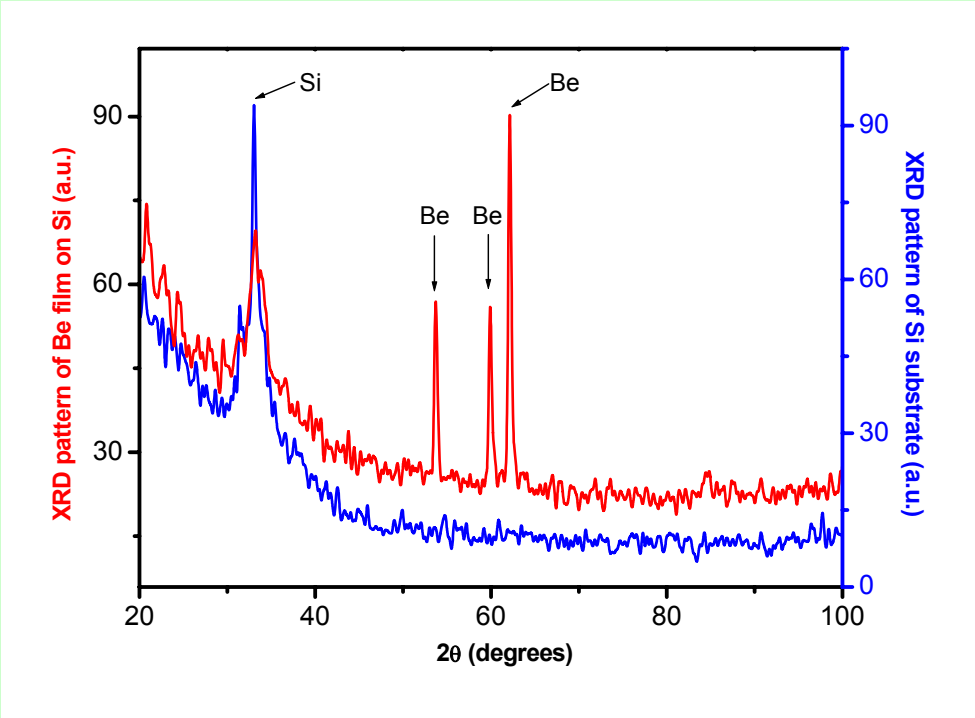

XRD pattern of Be coating on silicon

AFM

The film surfaces morphology was investigated at *"Al. I. Cuza"* University, Iasi by AFM in the taping mode with standard silicon nitride cantilever NSC21 having a force constant of 17.5 N/m, 210kHz resonance frequency and tip with radius of curvature less than 10 nm. The AFM measurements were performed at room temperature and ambient pressure.

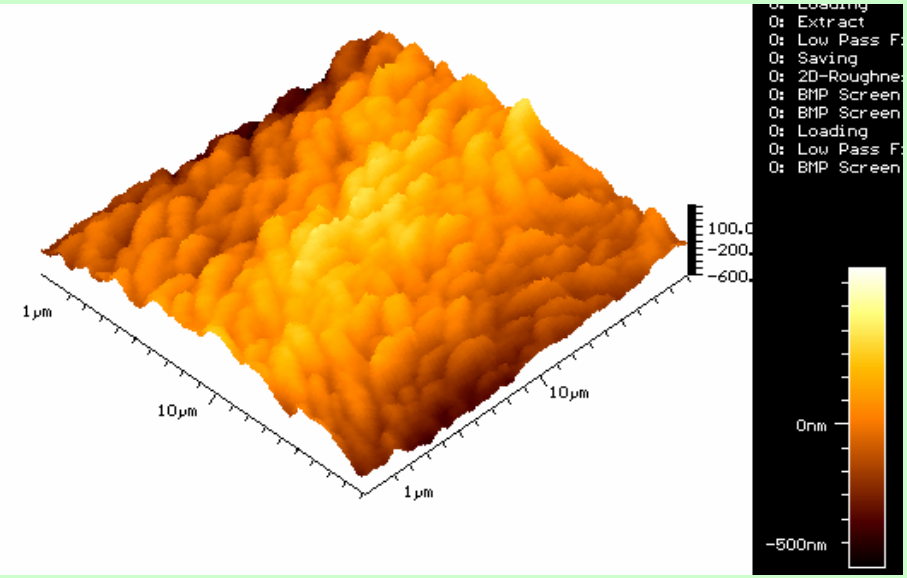

Be on Silicon substrate
(less than 300 nm peak to valley roughness)

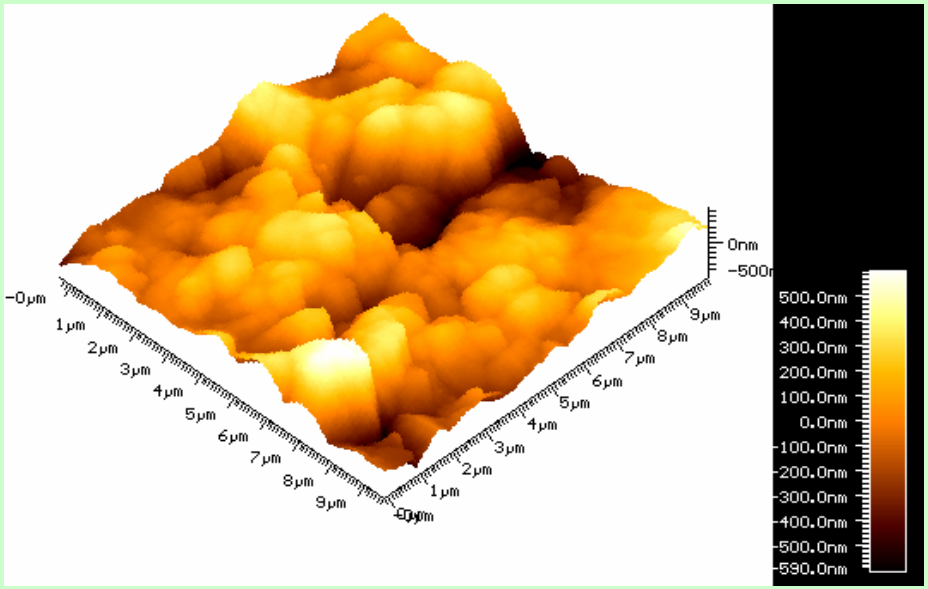

Be on Graphite substrate
(1000 nm peak to valley roughness)

SEM

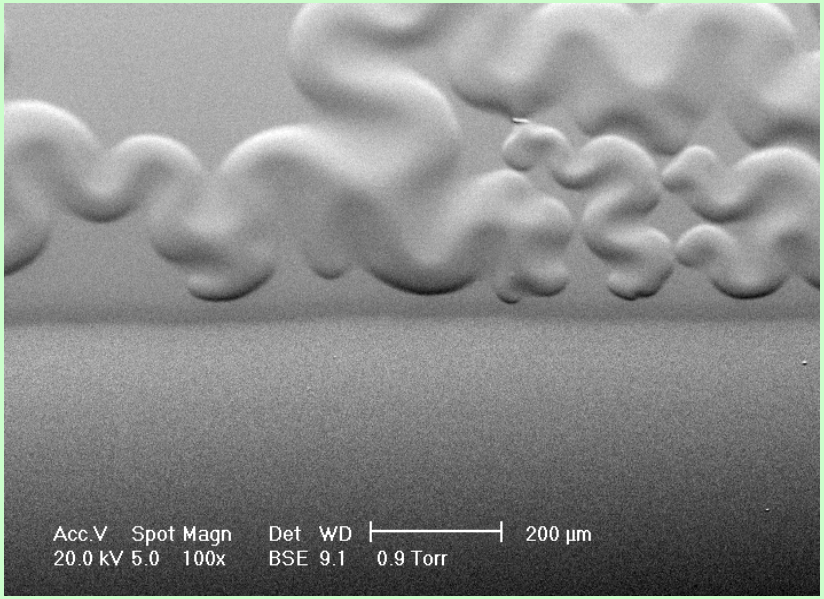

Be on glass

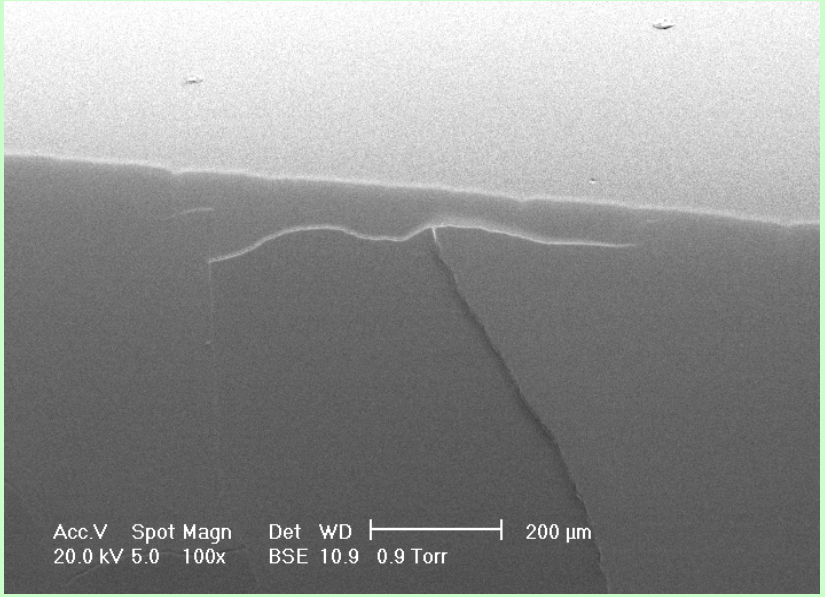

Be on Si

Be coatings
(substrates at RT)

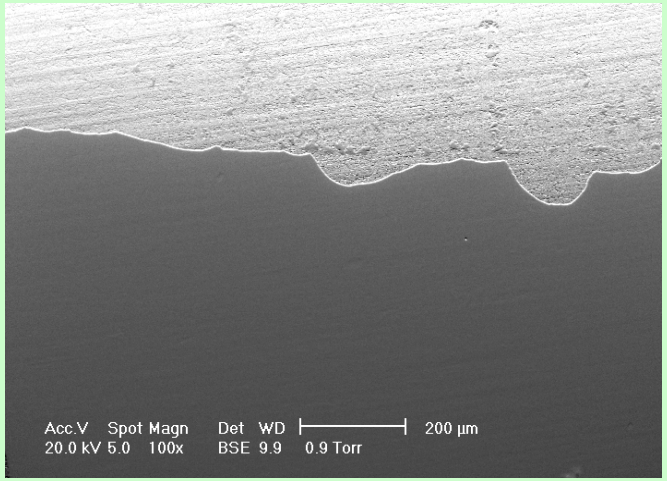

Be on st.steel

SEM

Substrate	SEM image 1000x	SEM image 5000x	SEM image 10000x
Stainless steel	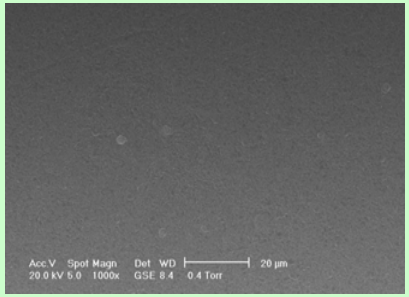	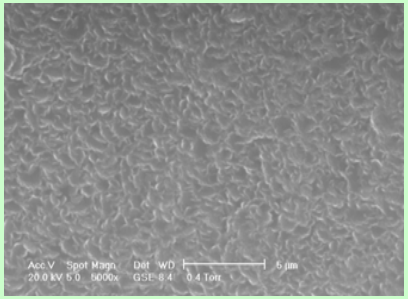	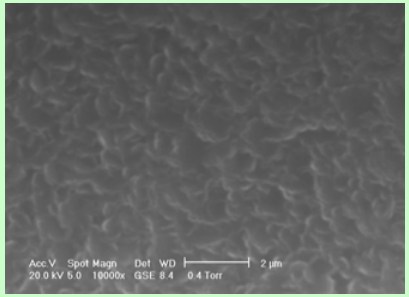
Glass	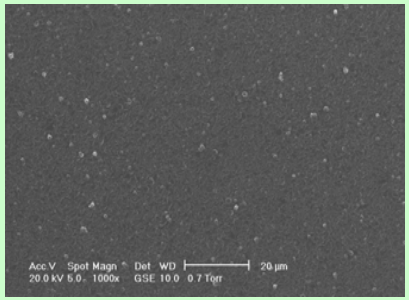	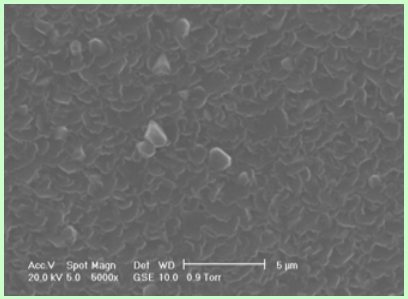	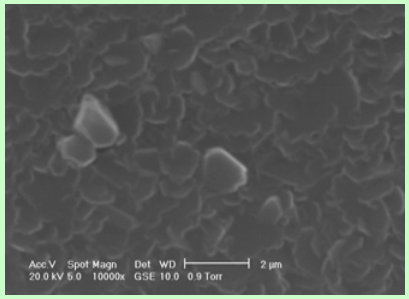
Silicon wafer (back side)	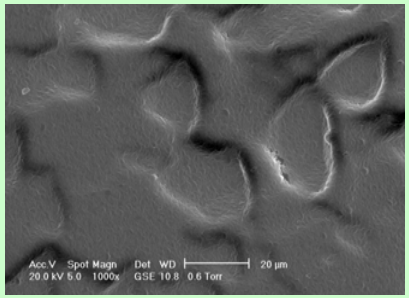	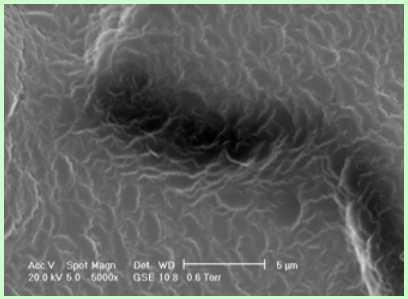	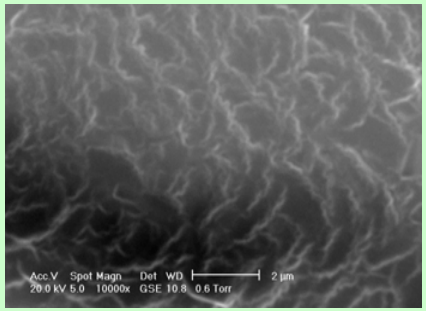

Be Marker Layers for ILW

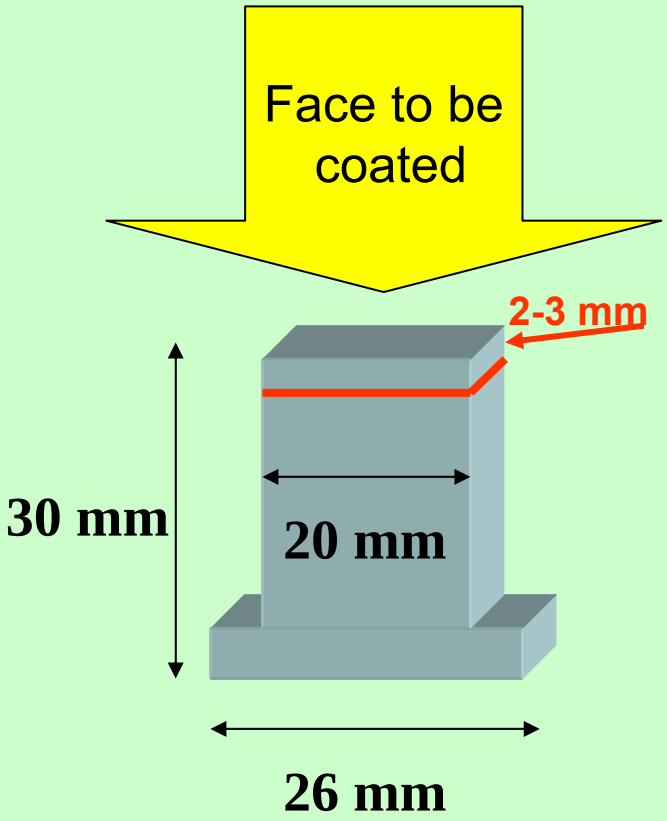

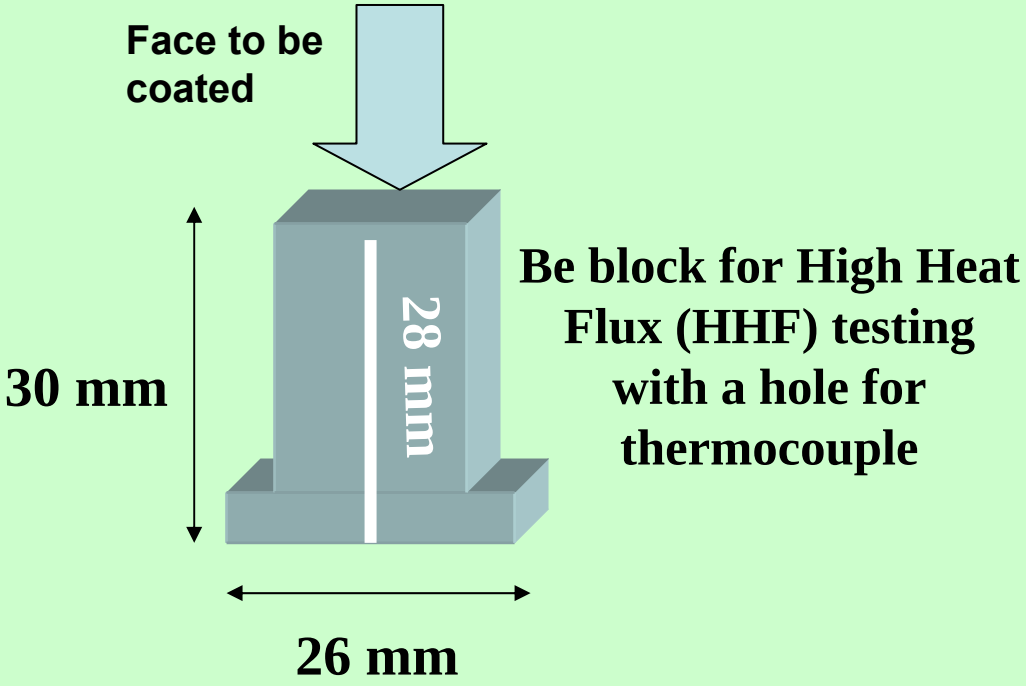

Metal Interlayer: W, Ni ?

W deposition

W deposition on Be block

SEM analysis

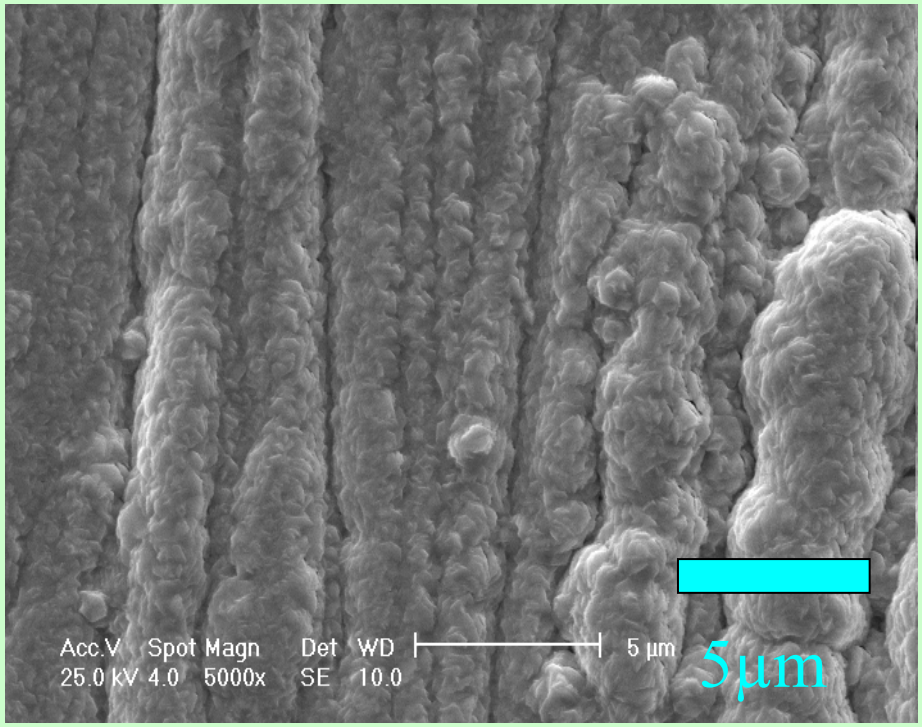

W film (on Fe substrate) analysis using Scanning Electron Microscope XL 30 ESEM PHILIPS (5000 x)

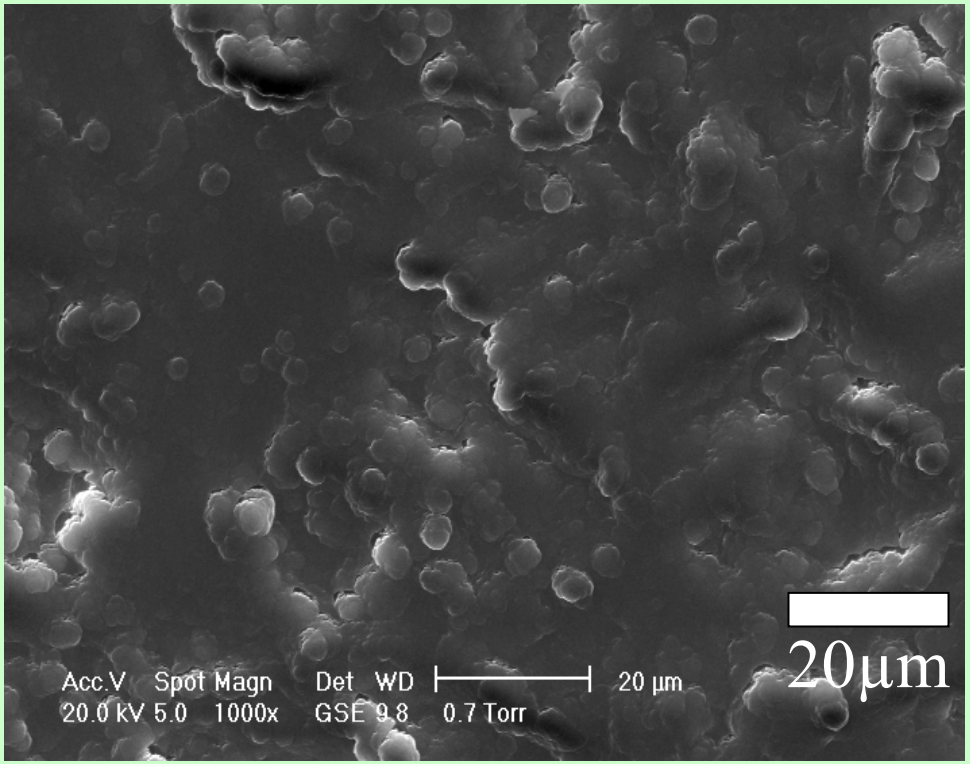

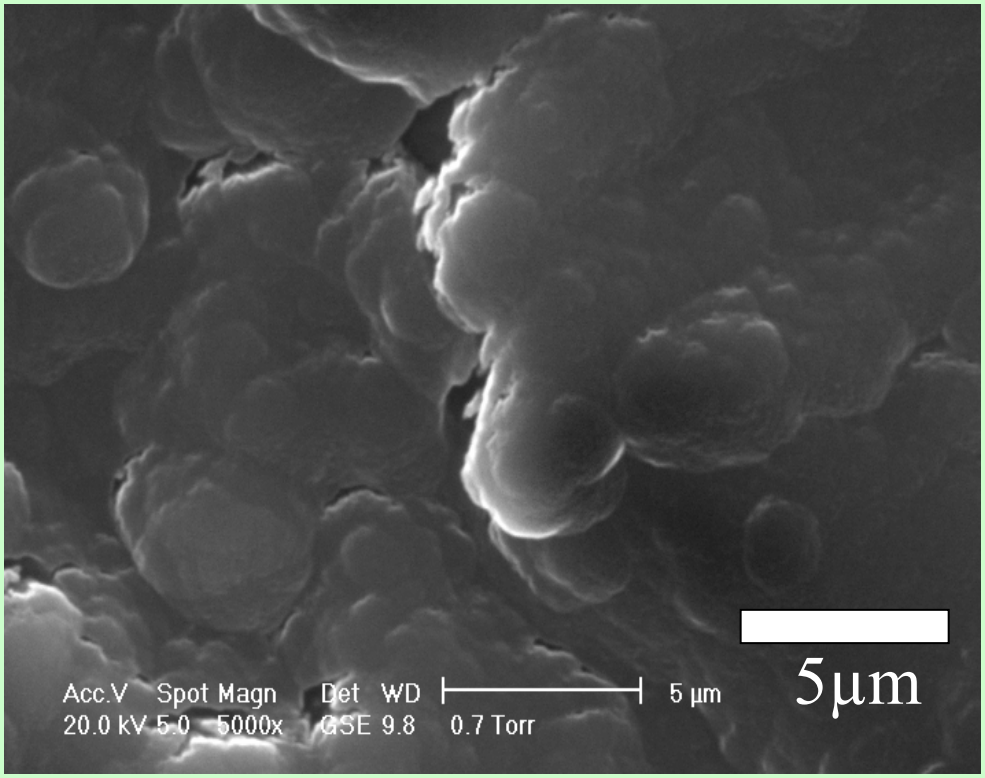

Ni film (on St. Steel substrate) analysis using Scanning Electron Microscope XL 30 ESEM PHILIPS (1000 x and 5000 x)

Coeff. of Thermal Expansion:

Ni = 13.1 x 10^{-6}/K,

W = 4.4 x10^{-6}/K,

Re = 6.2x 10^{-6}/K,

Cr = 6.2 x 10^{-6}/K and

Be = 11.5 – 16.5 x 10^{-6}/K, (20-500°C)

Be film / Ni Interlayer / Be block

Ni (2.5 ± 0.5 μm) and Be (7.5 ± 0.5 μm)

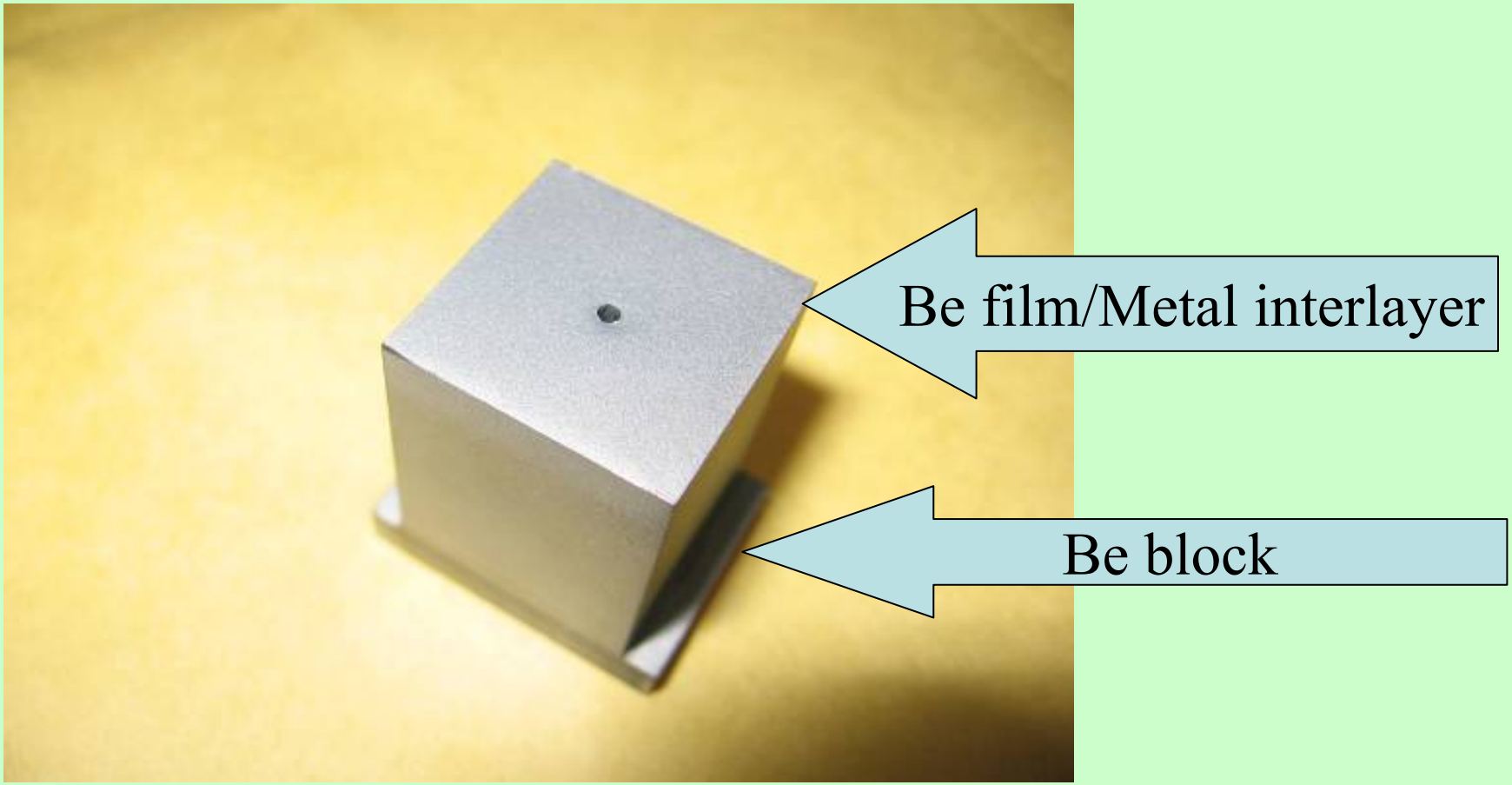

Cross-section of Be blocks

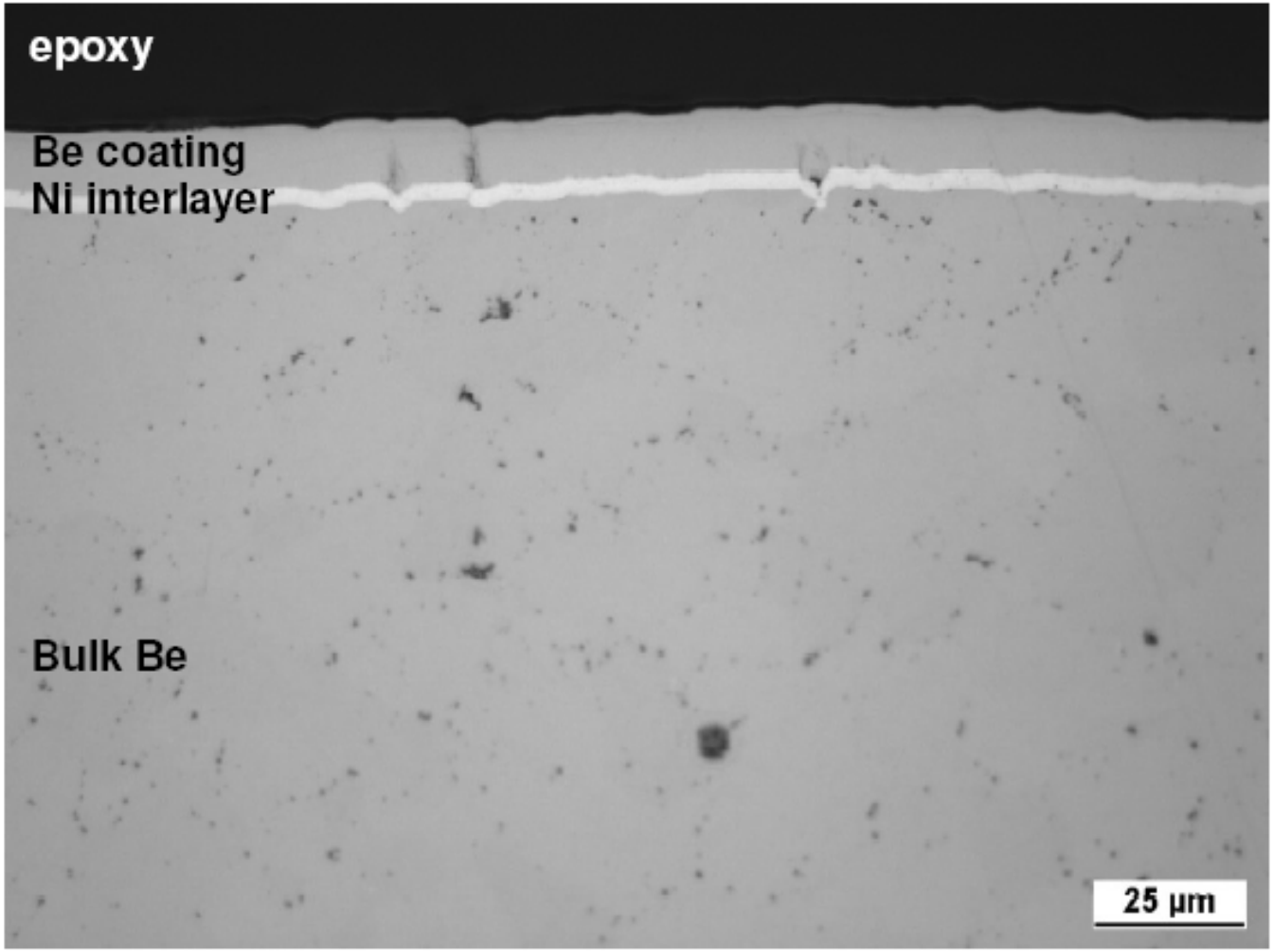

Fig. 16 TC28, 50 cycles of 3.5 MW/m^2 for 10s, optical image.

Impurity analysis of Be blocks

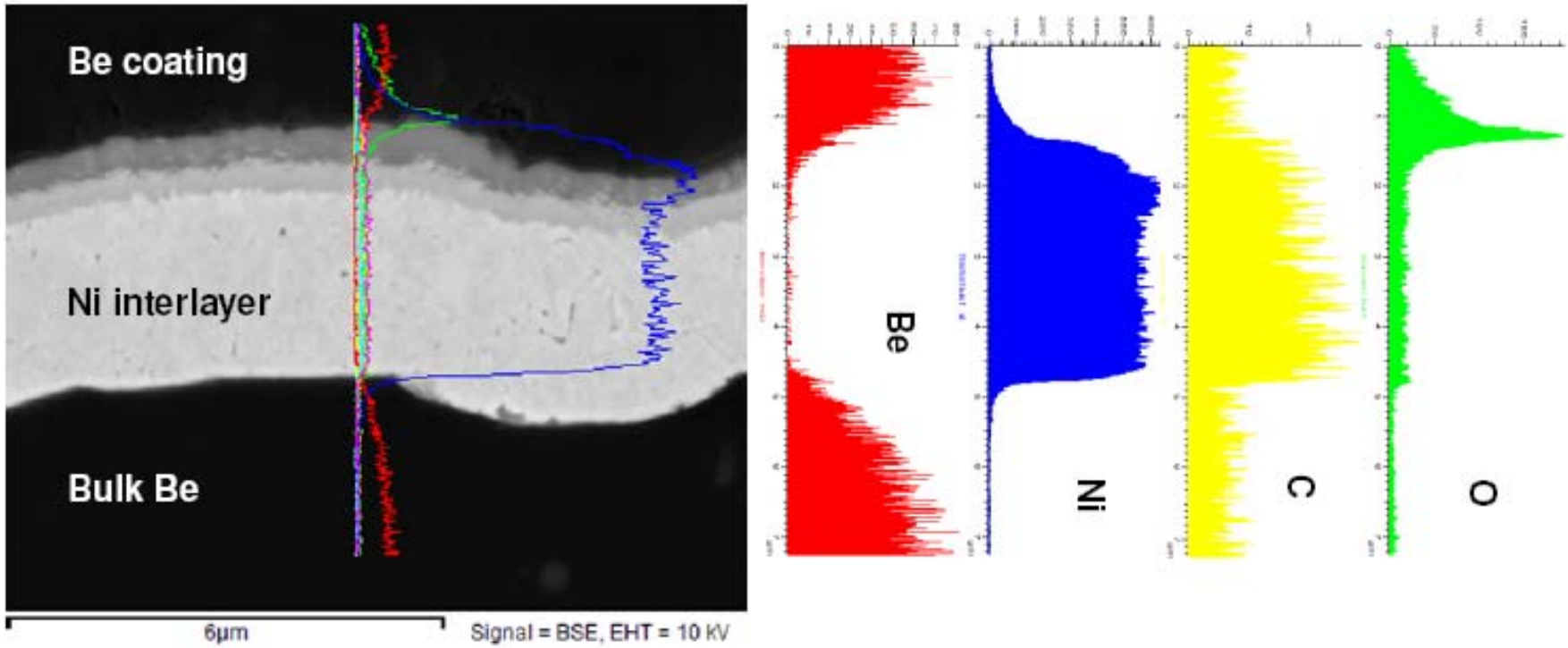

Fig. 25, TC26, 50 cycles of 3.5 MW/m^2 for 10s, BSE image and line scan across the interlayer. O and O background signal at Ni interlayer is caused by artificial effect (high background signal from Ni (high Z) compared with Be (low Z)).

Manufacturing of Be / inconel tiles by thermal evaporation in vacuum

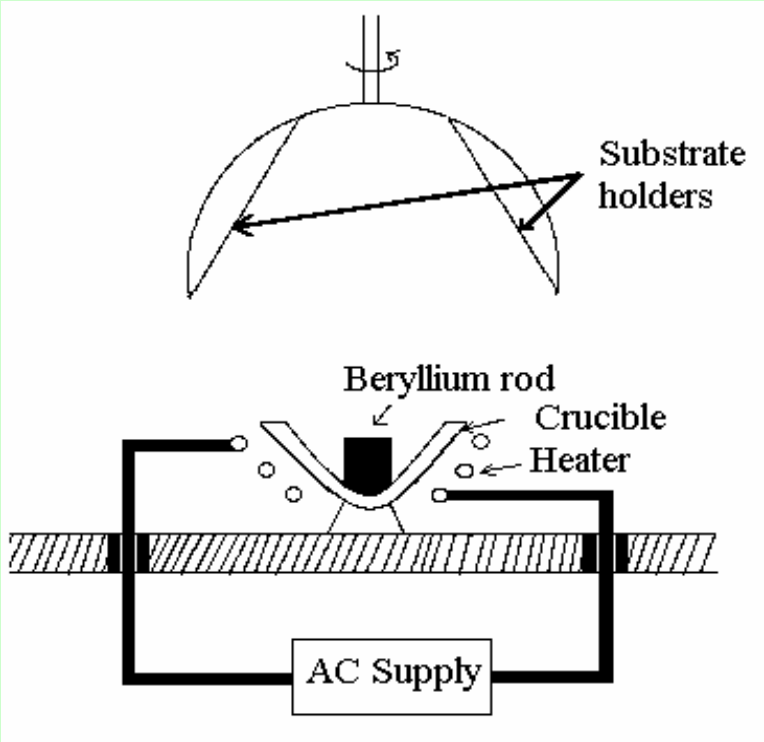

Schematic arrangement for thermal evaporation in vacuum

Photograph of the substrate holder

Inconel coupons and witness Zr substrates

Surface morphology of an inconel tile coated with Be

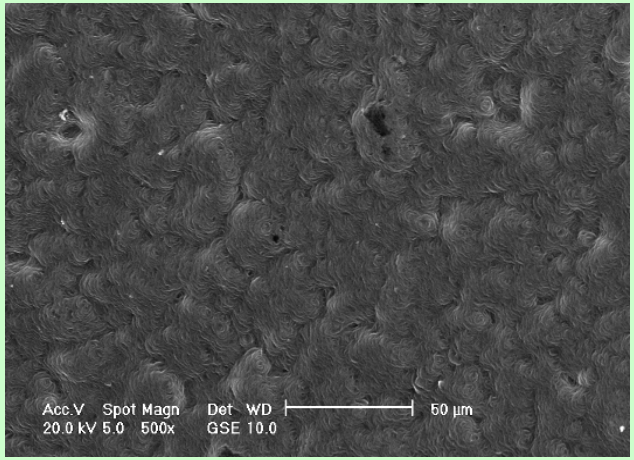

500x

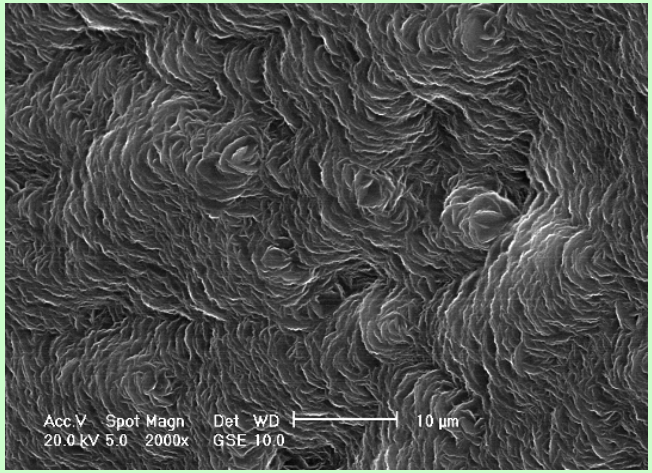

2000x

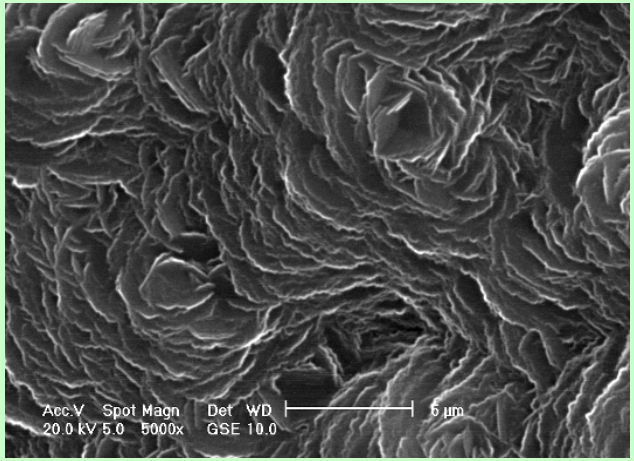

5000x

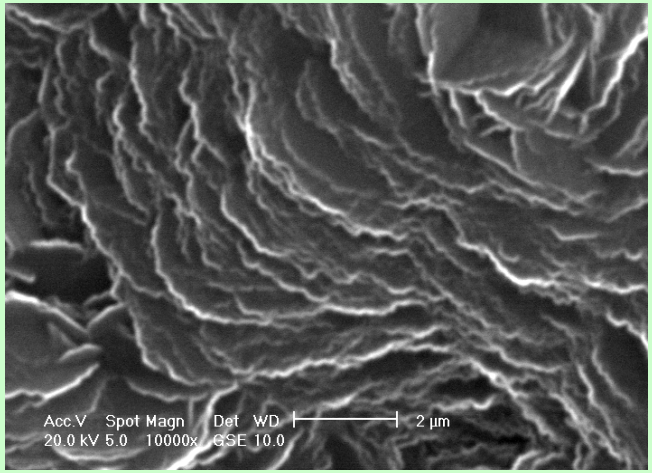

10000x

Comparison of the Surface morphology of an stainless steel substrate coated by thermal evaporation and by TVA method

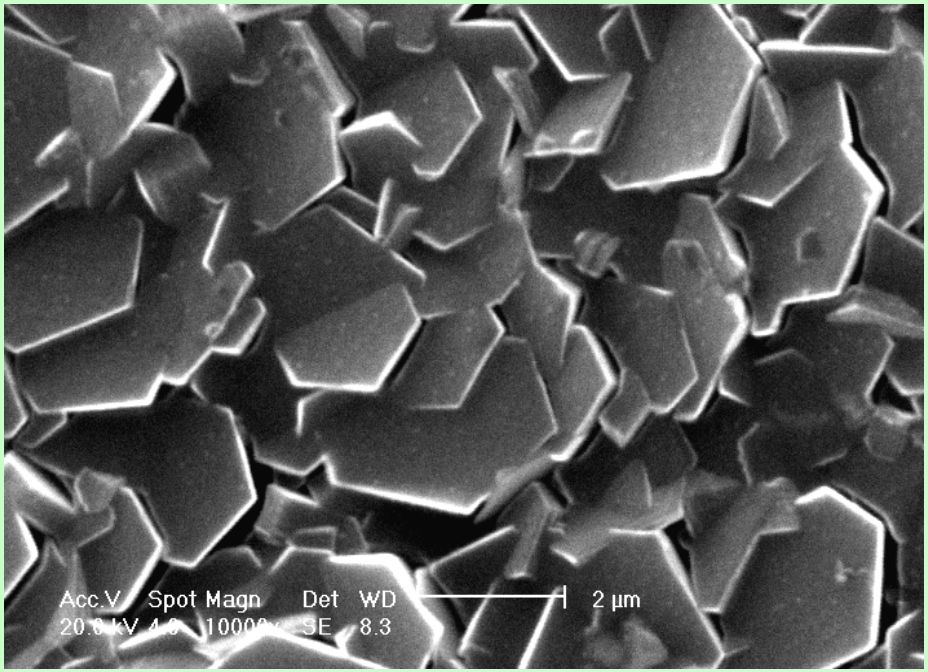

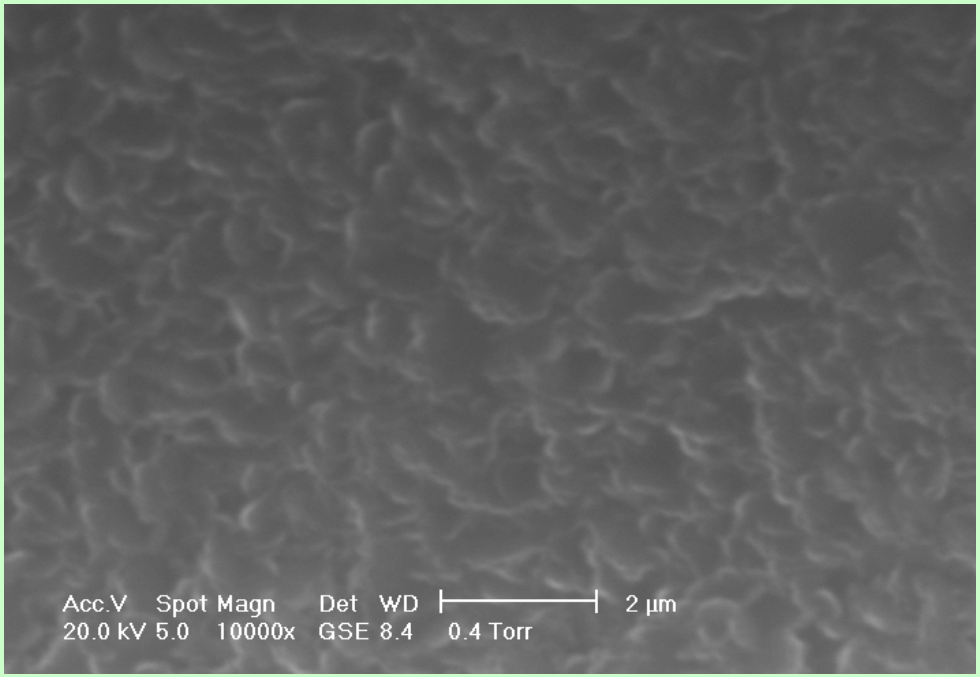

Be coating by **thermal method** on smooth stainless steel (10,000x)

Be coating by **TVA method** on smooth stainless steel (10,000x)

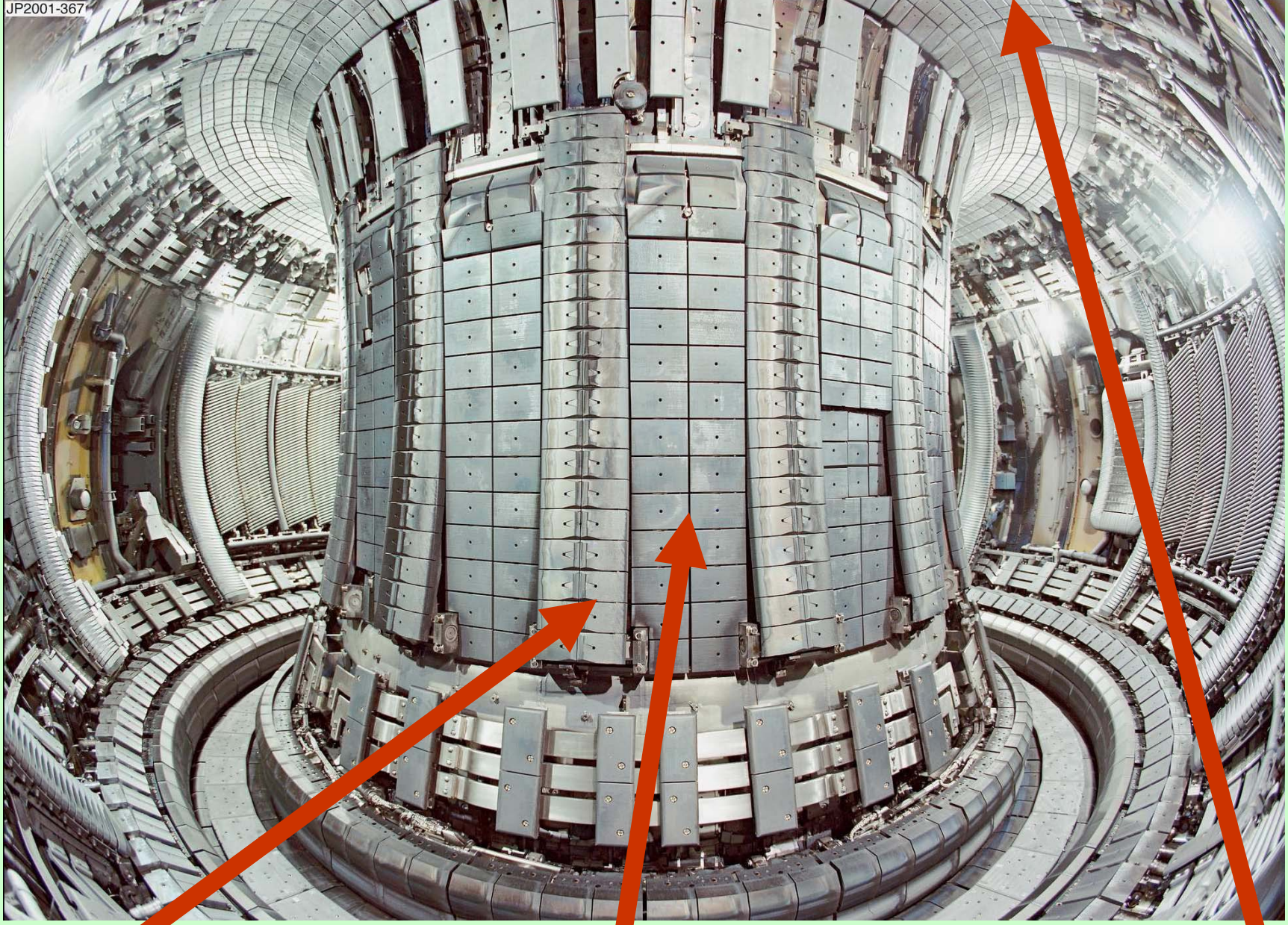

Inner Wall Guard Limiter
112 Be Coated Inconel Tiles

Inner Wall Cladding Tiles
272 Be Coated Inconel Tiles

Dump Plates: 512 Be Coated Inconel Tiles

CONCLUSIONS

- It has been proved that the TVA deposition technology is applicable for Be (also for W, Ni) deposition in high vacuum conditions and in presence of high energy ions of the same material bombarding the growing substrate.

- For tungsten and beryllium there is not necessary to use a crucible because they can be deposited from their rods which are consumed as a burning candle.

- For nickel case there is necessary a crucible (as TiB2 or graphite) but the inclusions of these materials are very low due to the low vapour pressure.

- The results obtained from the film characterisation TVA technique proved that the prepared films present:
  - Smooth surfaces
  - High density
  - High purity
  - Good adhesion of the films to the substrate.